# THE EFFECTS OF SOUND PROPAGATION AND AVOIDANCE BEHAVIOUR ON NAVAL SONAR LEVELS RECEIVED BY CETACEANS

**Paul J. Wensveen**

**A Thesis Submitted for the Degree of MPhil**
**at the**
**University of St. Andrews**

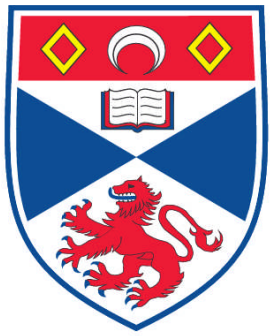

**2012**

# The effects of sound propagation and avoidance behaviour on naval sonar levels received by cetaceans

By Paul J. Wensveen

A thesis submitted to the University of St Andrews for the degree of Master of Philosophy

**School of Biology**

13 March 2012

## Declarations

I, Paul Wensveen, hereby certify that this thesis, which is approximately 22,000 words in length, has been written by me, that it is the record of work carried out by me and that it has not been submitted in any previous application for a higher degree.

I was admitted as a research student in September 2008 and as a candidate for the degree of MPhil in September 2009; the higher study for which this is a record was carried out in the University of St Andrews between 2009 and 2011.

Date: ……  Signature of candidate: ……

I hereby certify that the candidate has fulfilled the conditions of the Resolution and Regulations appropriate for the degree of MPhil in the University of St Andrews and that the candidate is qualified to submit this thesis in application for that degree.

Date: ……  Signature of supervisor: ……

In submitting this thesis to the University of St Andrews I understand that I am giving permission for it to be made available for use in accordance with the regulations of the University Library for the time being in force, subject to any copyright vested in the work not being affected thereby. I also understand that the title and the abstract will be published, and that a copy of the work may be made and supplied to any bona fide library or research worker, that my thesis will be electronically accessible for personal or research use unless exempt by award of an embargo as requested below, and that the library has the right to migrate my thesis into new electronic forms as required to ensure continued access to the thesis. I have obtained any third-party copyright permissions that may be required in order to allow such access and migration, or have requested the appropriate embargo below.

The following is an agreed request by candidate and supervisor regarding the electronic publication of this thesis:

*Access to printed copy and electronic publication of thesis through the University of St Andrews.*

Date: ……  Signature of candidate: ……

Signature of supervisor: ……

## Abstract

The use of active sonar is deemed to be essential for naval operations, but its potential impact on marine life has raised concerns worldwide. In a risk-assessment framework, characterisation of risk of harm is accomplished by combining exposure assessment and dose−response relationships. The overall topic of this thesis is an evaluation of factors that influence exposure assessment, including analysis of how sound levels received by cetaceans are affected by *in-situ* sound propagation and the influence of diving, movement and possible avoidance behaviour of the whales themselves.

Data from an international research programme based on controlled exposure experiments (CEEs) were available for this study. During these experiments, low-frequency active sonar (LFAS: 1-2 kHz band) and mid-frequency active sonar (MFAS: 6-7 kHz band) signals were recorded by suction-cup tags attached to killer whales, long-finned pilot whales and sperm whales, and by a hydrophone array towed near the whales. Chapter two describes how the sonar signals recorded by these systems were quantified, and investigates the influences of range, depth and propagation conditions on the received sound levels. Chapter three focuses upon the effect of simulated vertical and horizontal exposure-avoidance strategies of whales in response to an approaching source on the received sound levels.

A total of 7,091 sonar signals were analysed from the towed-array (2,794) and tag (4,297) recordings. Transmission loss (TL) and excess attenuation (EA) from a simple 20log(range) model were compared among species, signal types and acoustic receivers. TLs followed expected geometric spreading versus range and TL coefficients were 15.5−20.1 for LFAS and 18.8−23.6 for MFAS. One experiment where levels on the animal-attached tag were attenuated due to 'body shielding' (when the animal's body is interposed between the sound recording tag and the sound source) was documented, and other sources of variation in received level dataset were discussed. Variations in EA with depth were consistent with TL patterns predicted using the

acoustic propagation model Bellhop with the highest EAs occurring near the sea surface. The effect of depth on EA was clearest in killer and pilot whale experiments which occurred at locations with stronger gradients in the sound-speed profile, while sperm whale experiments in deeper homogenous offshore waters showed little influence of depth on EA. The results indicate that a simple TL model like 20log(range)+absorption does not accurately predict attenuation levels over the distances (0.1−11.1 km) from a sonar source to a freely-diving animal, but that the overall patterns of TL can be fairly well explained using sound propagation models that take into account local environmental conditions. A consistent different in TL between LFAS and MFAS signals was not explained by the Bellhop model, however, indicating that unidentified sources of variation do influence the sonar signals recorded on freely-diving whales.

To evaluate the potential effect of avoidance strategies of whales on received sound levels, whale positions were simulated with a Monte Carlo method in which a simulated source vessel directly approached the whale. The cumulative sound exposure level ($SEL_{cum}$) received by the whales was estimated using the Bellhop model. Horizontally-stationary animals received the highest levels. The optimal course in terms of reducing $SEL_{cum}$ for animals moving in a straight line was 100° from the heading of the source vessel, while 120−130° was optimal for animals dynamically moving relative to the position of the source. Moving horizontally in the optimal direction away from the vessel path yielded 9−17 dB reduction of $SEL_{cum}$ and vertical avoidance led to reductions of up to 10 dB in certain circumstances. Actual observations of the whales during the sonar experiments indicated that animals often move sideways out of the path of the approaching vessel, close to the optimal angle predicted. The simulation approach is therefore potentially useful to predict how whales react to an approaching sound source. This type of analysis may also be useful to understand the patterns of cetacean strandings relative to the movement of sonar-transmitting military vessels.

## Acknowledgements

The project has been funded with support of Stichting VSBfonds (VSB Foundation; reference number VSB.08/228-E) and the Defensie Onderzoek-beurzenfonds (Defence Research-scholarship fund; project number 032.30370/01.02) owned by The Netherlands Ministry of Defence.

Firstly, I would like to thank my supervisor Patrick Miller for his trust in my abilities and his encouragement throughout the MPhil period. I am very grateful for your all support and the numerous brainstorming sessions we have shared. I also owe a great deal of gratitude to the past and present members of our research lab; in particular to Filipa Samarra, Eva Hartvig, Ana Catarina Alves, Ricardo Antunes, Kagari Aoki, and Marijke Olivierse. Your moral and scientific support throughout the study period has been invaluable.

Many thanks are also due to Frans-Peter Lam and Frank Benders of the Acoustics and Sonar Research Group of TNO for putting me on the acoustic observation team of the 3S-08 research cruise, and for their general guidance over the years. Sincere thanks also go to Michael Ainslie, Sander von Benda-Beckmann and Wim Groen of TNO for their help and advice on acoustic measurements, terminology and analysis, and for the interpretation of some of the findings in this thesis in a broader context.

The participants of the 3S-08 and 3S-09 trials in Norwegian waters have made these cruises very pleasant and successful experiences. There are too many of you to thank by name, but I am particularly grateful to Petter Kvadsheim for his guidance and providing information about the acoustic environment, René Dekeling for making part of funding possible, and to Rob van Bemmelen, Lise Doksæter, Adri Gerk, Rune Roland Hansen, Jeroen Janmaat, Sanna Kuningas, Lars Kleivane, Thomas Sivertsen, Mark van Spellen, Fleur Visser, Paul White, Sander van IJsselmuide and Timo van der Zwan.

Peter Tyack and Stacy DeRuiter of WHOI are thankfully acknowledged for their constructive comments on the received level analysis procedures, and for the fruitful discussions on the subject; René Swift and Clint Blight of SMRU have been very helpful when dealing with a number of GIS-related issues; and Jim Finneran is thanked for providing audiogram data for pilot whales.

The taught modules from the MRes Environmental Biology (with the conversion for Mathematical, Physical and Molecular Sciences) were part of this MPhil programme. The camaraderie among the students of the class of 08-09 made me quickly feel at home in St Andrews.

I am also greatly appreciative for the scientific and mental support by Ron Kastelein and his wife Brigitte Slingerland and all the SEAMARCO affiliates in the Netherlands (in particular Lean Hoek, Jack Terhune, Wim Verboom, and Christ de Jong) which has helped me grow both professionally and as a person.

Last not least, I sincerely thank all my family and friends for their unconditional love. I could not have done it without you.

# Table of Contents

# List of acronyms

| | |
|---|---|
| 3S | Sea mammals and sonar safety |
| AcTUP | Acoustic toolbox user interface and post processor |
| ADC | Analog-to-digital converter |
| ADD | Acoustic deterrence device |
| AHD | Acoustic harassment device |
| AIM | Acoustic integration model |
| APL-UW | Applied Physics Laboratory-University of Washington |
| ATOC | Acoustic thermometry of the ocean climate |
| BRS | Behavioural response study |
| CEE | Controlled-exposure experiment |
| CPA | Closest point of approach |
| EA | Excess attenuation |
| ESME | Effects of sound on the marine environment |
| FFI | Norwegian Defence Research Establishment (Norwegian acronym) |
| GEBCO | General Bathymetric Chart of the Oceans |
| GIS | Geographic information system |
| HFEVA | High-frequency ocean environmental acoustic models handbook |
| IQR | Interquartile range |
| LFAS | Low-frequency active sonar |
| MAREANO | Marine areal database for Norwegian waters |
| MFAS | Mid-frequency active sonar |
| MPD | Marine Primary Data |
| NGU | Geological Survey of Norway (Norwegian acronym) |
| NHS | Norwegian Hydrographic Service |
| RL | Received level |
| RMS | Root mean square |
| SAKAMATA | Sea animal-kind adaptive mitigated active transmission aid |
| SEAMARCO | Sea Mammal Research Company |
| SEL | Sound exposure level |
| SMRU | Sea Mammal Research Unit |
| SNR | Signal-to-noise ratio |
| SONATE | Sonar effects on marine life (Norwegian acronym) |
| SPL | Sound pressure level |
| SURTASS LFA | Surveillance towed array sensor system low frequency active |
| TL | Transmission loss |
| TNO | Netherlands Organisation for Applied Scientific Research (Dutch acron.) |
| TOF | Time of flight |
| WHOI | Woods Hole Oceanographic Institution |
| WMS | Web map service |

# Chapter 1. General introduction

## 1.1 Cetaceans and sonar

In water, light and radio waves are attenuated to a far greater degree than is sound, making sound the most efficient means of transmitting information under water (Urick, 1983). Sound travels almost five times faster in water than in air; and very low-frequency sounds like the calls of some baleen whales can potentially be detected by other whales over distances of many hundreds of miles under optimal propagation conditions (Clark *et al*., 2009). In this environment the hearing system of marine mammals, particularly cetacea, has evolved to be the primary sensory faculty. Hence, sound plays a key role in orientation (Verfuß *et al*., 2005), prey detection and capture (Miller *et al*., 2004) and communication (Tyack, 1981) in cetaceans.

Navies depend upon underwater sound for the same reasons as marine mammals. Worldwide, naval fleets utilise sonar in order to acoustically monitor the environment, navigate, and identify potential incoming threats. Passive sonar systems only 'listen' and do not transmit sound; active sonars transmit pulses and time the return echoes to obtain the distance to a reflector (Hildebrand, 2009). Such active systems are used, for example, to detect, locate, and classify submarines, to navigate torpedoes and to find objects such as mines (Richardson *et al*., 1995). To use sonar effectively, operators must train regularly under different kinds of realistic conditions. Sonar training therefore takes place in both deep-ocean and coastal waters, and may occur within the natural habitat of most cetacean species.

National policies reflect the importance of national security and the navies' need to use active sonar. Over the last two decades, however, concerns have been raised by scientists and regulators as well as the general public about the potential impacts of man-made 'anthropogenic' noise on the environment, in particular on the acoustically-sensitive cetaceans (NRC, 2003, 2005; Cox *et al*., 2006). Concerns specifically regarding high-intensity naval sonar were sparked by a number of mass strandings of primarily

beaked whales that coincided in time and space with multi-ship sonar exercises (Frantzis, 1998; Balcomb and Claridge, 2001; D'Amico *et al*., 2009; Filadelfo *et al*., 2009).

The environmental concerns about active sonar led to a series of legal disputes between the US Navy and several environmental NGOs regarding the risk assessments conducted by the Navy prior to sonar exercises and its mitigation protocols (Reynolds *et al*., 2009; McCarty, 2010). These legal cases emphasise the importance of balancing the need for effective sonar training against the risk of harm that active sonar imposes on marine mammals (Zirbel *et al*., 2011).

Besides stranding events, active sonar may also lead to a range of less overt, but still detrimental impacts on marine mammals. Like all anthropogenic noise sources, active sonar has the potential to mask biological sounds themselves, reducing the distance over which animals can communicate with conspecifics or detect prey and predators (Clark *et al*., 2009; Kastelein *et al*., 2009). Use of active sonar can lead to changes in the vocal behaviour of cetaceans as a disturbance or in an apparent attempt to compensate for acoustic interference (Watkins *et al*., 1985; Rendell and Gordon, 1999; Miller *et al.*, 2000), cause aversive behavioural responses (NMFS, 2005) and induce hearing injury when animals are close to intense sources (Mooney *et al*., 2009). Interpreting the influence of these impacts on vital rates, however, requires detailed knowledge about the environment (*e.g.*, quality of the area to the animals), the duration of the response, the size of the population, and the species' natural behaviour. The magnitude and extent to which many of these potential impacts are significant risks to the animals are largely unknown. Depending on the biological context, both short-term and long-term responses may or may not be of concern (Nowacek *et al*., 2007).

## 1.2 Environmental risk assessment

Risk can be defined as the threat itself or the probability that something hazardous will occur. Risk assessment is the quantification of this probability (Rowe, 1977), and risk management is concerned with minimising risk in the face of uncertainty (Harwood, 2000). To assess what risk active sonar imposes on marine mammals, or any risk for that matter, one can apply the analytical four-step risk-assessment framework developed by the US Environmental Protection Agency (EPA, 1992; Boyd *et al*., 2008). These four steps indicate the phases of: 1) hazard identification, 2) exposure assessment, 3) dose−response assessment, and 4) risk characterisation. When a risk is characterised it can eventually be managed; actions can be taken to reduce risk when thresholds with acceptable levels are exceeded. With regards to marine mammal protection, the implementation of mitigation measures (Barlow and Gisiner, 2006; Dolman *et al*., 2009) are part of risk management.

A number of quantitative risk-assessment frameworks that follow the above four-step process have been developed to determine the risk, in terms of hearing injury and behavioural disturbance, of underwater noise to marine life (*e.g.*, AIM: Frankel *et al*., 2002; ESME: Shyu and Hillson, 2006; SAKAMATA: Benders *et al*., 2004; SONATE: Nordlund and Benders, 2008). These software tools allow the user to conduct exposure assessments (step two in the analytical model) based on information on the signal characteristics and movements of the source, the acoustic environment, and the distribution and movements of the animals. Parameter values can be taken automatically from global databases (sound speed profile, bathymetry, animal distribution, etc.) or inputted manually. During exposure simulations, the locations of the animals are determined by mechanistic movement models that operate according to user-defined sets of rules (Houser, 2006). Dose−response relationships (step three) can be varied but are usually based upon criteria from environmental guidelines for noise exposure (Scholik-Schlomer, 2010; Tasker *et al*., 2010). Eventually, the risk of harm (step four) per species or hearing sensitivity group is obtained by ‘weighting’ the

results of the exposure assessment by the appropriate dose−response relationship, and is expressed in units of animals or area affected.

Due to the importance of dose−response relationships in risk-assessment frameworks, obtaining these empirical relationships for marine mammals has been identified as an important research priority (Southall *et al*., 2007; Boyd *et al*., 2008). Controlled exposure experiments (CEEs) conducted with animals in their natural environment are especially fit to address this research need because these experiments are designed to imitate real-life exposure situations, and provide a significant degree of control over the sound source (Tyack *et al*., 2003; Tyack, 2009). For this reason, CEEs were performed on killer whales (*Orcinus orca*), long-finned pilot whales (*Globicephala melas*) and sperm whales (*Physeter macrocephalus*) during the 3S-06, 3S-08 and 3S-09 research cruises in Norwegian waters (Miller *et al*., 2011a). During the experiments, whales were tagged with sound and movement-recording sensors “Dtags” (Johnson and Tyack, 2003), carefully exposed to low-frequency active sonar (LFAS; 1−2 kHz) and mid-frequency active sonar (MFAS; 6−7 kHz) by means of a towed sound source, and tracked using visual observations and towed array acoustics. A summary of events for each experiment and detailed descriptions of the methods are published in Miller *et al*. (2011a), and current work in this area is focussed on deriving dose−response relationships from the experimental results (Miller *et al*., 2011b).

Robust noise risk assessment requires a level of understanding about the hearing of marine mammals (especially the received level that can cause hearing damage or disturbance), spatial and temporal distributions of species, and the way animals move in relation to a sound source that is far greater than current knowledge permits. Because received sound levels depend strongly on the source range, depth and relative speed between source and receiver (D’Spain *et al.*, 2006), the lack of knowledge about the natural behaviour of marine mammals of and their movements in relation to disturbing sound sources gives rise to much uncertainty in the risk estimates.

## 1.3 Current study

Typically, the sound levels received by simulated whales in risk-assessment tools are calculated from transmission losses that are predicted by geometrical spreading or a sound propagation model. Transmission loss depends greatly on depth, range and environmental characteristics (sound speed, bottom type, etc.), and not every propagation model performs well or is equally valid in every situation (Siderius and Porter, 2009). Transmission loss predictions should therefore be ground-truthed with measurements taken at the location of the actual animal. In the 3S study, acoustic recordings were made with devices near or attached to whale subjects. This provides an ideal setting to explore predictions of whale exposure levels, and the sources of variation in received level in their natural environment.

This MPhil project uses data collected during the 3S research cruises, and seeks to advance our understanding of step two in the analytical risk-assessment framework; the exposure assessment. Chapter two focuses upon using animal-borne sound recorders to evaluate commonly used tools to conduct exposure assessment. The steps in this chapter include 1) measuring and processing sonar signals recorded with animal-attached tags, 2) the influences of range, depth and propagation on the sound field surrounding the animals, and 3) the predictions of common propagation models such as 20log(range)+absorption and the beam-tracing model Bellhop (Porter and Bucker, 1987). Chapter three considers the potential influence or effect on exposure assessment that a behavioural response to the sounds, specifically horizontal and vertical avoidance, can itself alter the exposure level received by the animal. Indeed, marine mammals might specifically respond in order to reduce sound levels (Kastelein *et al*., 2005; 2006a; 2006b, 2008). The effects of simple horizontal and vertical exposure-avoidance strategies of whales on cumulated sound levels are investigated using Monte Carlo movement simulations of source-whale encounters. Animal movement strategies are compared to avoidance responses described in literature and patterns of sonar-related whale strandings.

# Chapter 2. The effects of range, depth and acoustic propagation on sonar levels received by killer, long-finned pilot and sperm whales

## Chapter summary

The use of high-intensity active sonar is deemed to be essential in naval operations, but its impact on marine life has raised concerns worldwide. High intensity sonar can lead to direct physical injury or cause aversive behaviour effects. The relationship between sonar and behavioural response was examined during controlled exposure experiments conducted in the Vestfjorden area of Norway. Low-frequency active sonar (LFAS; 1−2 kHz) and mid-frequency active sonar (MFAS; 6−7 kHz) signals transmitted at realistic source levels were recorded at ranges from the source of 0.1 to 11 km using a hydrophone array and acoustic tags attached to killer whales, pilot whales and sperm whales. In this chapter, the recorded sonar signals were quantified and influences on the sound field surrounding the animals were investigated. Maximum sound pressure levels (200-ms RMS average) and cumulative sound exposure levels ranged from 67 to 180 dB re 1 µPa and from 65 to 186 dB re 1 $\mu Pa^2$ s, respectively. Transmission loss (TL) as function of range and excess attenuation (EA) as function of depth were calculated and compared among species, signal types and acoustic receivers. Measured TLs generally followed basic geometric spreading laws and TL coefficients ranged from 15.5 to 20.1 for LFAS and from 18.8 to 23.6 for MFAS. Generally, TLs for LFAS were lower than for MFAS. Variations in EA with depth in the top 100-m layer were consistent with TL predictions made using the beam-tracing model Bellhop. EAs were highest (thus received levels lowest) near the water surface at 0−10 m depth. An experiment in which levels were attenuated due to the body of the whale between the sound receiving tag and the sonar source was evaluated. This type of 'body shielding' and other sources of variation in received level dataset were discussed.

## 2.1 Introduction

A wide spectrum of sounds is present under water. The world's oceans contain sounds from biotic sources like snapping shrimps, fish and marine mammals and from abiotic sources like raindrops on the surface or geological sources (Wenz, 1962). Besides naturally-occurring sounds, humans increasingly contribute to the background noise in the ocean by employing shipping, seismic surveys, pile driving, echosounders and fisheries sonars, as well as military sonar systems (Hildebrand, 2009). In fact, from early 1960s to around 1980, the deep ocean ambient noise in the low-frequency range (10-400 Hz) increased by 5 dB/decade due to human activities like shipping (Ross, 1976) and has since been increasing with a rate of 3 dB/decade (Chapman and Price, 2011).

In water, light and radio waves are attenuated to a far greater degree than is sound, making sound the most efficient means of transmitting information (Urick, 1983). Also, sound travels almost five times faster in water than in air. In this environment sonar is the most effective way of detecting objects. Passive sonar systems only 'listen' and do not transmit sound. Active sonars transmit pulses 'pings' and time the return echoes to obtain the distance to the reflector. Such systems are used by navies for example to detect, classify and locate submarines, to navigate torpedoes and to locate mines or other obstacles. Sonar frequencies range from a hundred hertz for long-range search sonars to hundreds of kilohertz for sonars used for mine-hunting or mapping of the seafloor (Richardson *et al*., 1995).

The performance range and spatial resolution of sonars are inversely related; low-frequency sonars can be used over hundreds of kilometres but detect only large objects, while high-frequency sonars can detect smaller objects but have narrow operational ranges because of high absorption losses at those frequencies (Ainslie, 2010). Sonars used for detecting submarines operate at low- and mid-frequencies (~0.1−12 kHz) and source levels of up to 235 dB re 1 µPa m or more (*e.g.*, US Navy's SURTASS LFA and AN/SQS-53C sonars; D'Amico and Pittenger, 2009; Hildebrand,

2009). A number of European navies presently use mid-frequency active sonar (MFAS) systems with pulses in the 5−9 kHz band. The pulses are usually of short duration (0.3−1.2 s) and the pulse interval (usually between 10 and 30 s) depends on the expected distance to the target submarines (Funnel, 2009). In the coming 5 to 10 years, surface ships will also make more use of new European low-frequency active sonar (LFAS) systems transmitting pulses in the 1−2 kHz band. Such systems are currently being implemented to detect submarines at greater distances. The sweep duration of these new systems will be up to several seconds; the sweep interval is expected to be around 30 s.

The use of active sonar is deemed to be essential for naval operations, but its impact on marine mammals has raised concerns worldwide. Hearing is the primary sensory faculty of cetacea and they sense their surroundings through passive listening (Barrett-Lennard *et al*., 1996) or actively through echolocation (Au, 1993). Hence, sound plays a key role for cetacea in orientation (Verfuß *et al*., 2005), prey detection and capture (Miller *et al*., 2004) and inter-animal communication (Tyack, 1981). Although exposure to sonar may sometimes have beneficial outcomes for the whale (*e.g.*, avoidance of ship-strikes) and often no effect at all (positive or negative), it may also lead to negative impacts. For example, noise can mask biological-significant sounds, reducing the range over which animals can communicate with conspecifics or detect prey and predators (Clark *et al*., 2009; Kastelein *et al*., 2009). Active sonar can also cause changes in acoustic behaviour (Watkins *et al*., 1985; Rendell and Gordon, 1999), aversive behavioural responses (NMFS, 2005), stranding events (D'Amico *et al*., 2009; Filadelfo *et al*., 2009) and hearing injury when animals are close to the source (Southall *et al*., 2007; Mooney *et al*., 2009). On the population level, sonar may reduce survival, reproductive success and feeding opportunities if marine mammals avoid important areas or have negative responses to sonar over long periods of time.

In addition to determining what types of effects sonar might have on marine mammals, it is important to identify what acoustic levels or other features of the sonar

(the sonar 'dose') trigger behavioural responses. Dose−response relationships of behavioural responses of marine mammals to sonar have been investigated by conducting controlled exposure experiments (CEEs). CEEs were performed on killer whales (*Orcinus orca*), long-finned pilot whales (*Globicephala melas*) and sperm whales (*Physeter macrocephalus*) during the 3S-06, 3S-08 and 3S-09 research trials in Norwegian waters (Kvadsheim *et al*., 2009). During the experiments, whales were tagged with sound- and movement-recording tags and the animals were exposed to LFAS and MFAS sonar using a towed high-intensity sonar source. A summary of each experiment and detailed descriptions of the methods are published in Miller *et al*. (2011a). Observations indicated a large number of changes in behaviour during exposure to sonar that can be considered 'putative effects' of the sonar.

In this chapter, the sonar signals transmitted during the CEEs were quantified and influences of range, depth and propagation on the sound field surrounding the animals were investigated. Quantitative analyses of the effects of the sonar on the whales are currently in progress and will be presented elsewhere. In this analysis of the factors affecting received sonar signals, influences of the environment (*e.g.*, sound propagation conditions), or animal behaviour (*e.g.*, diving, movement) are considered. In addition to describing what occurred during the experiments, themselves, this analysis should improve our ability to predict how marine mammals in their natural environment are exposed to actual navy exercises that use sonar. Madsen *et al.* (2006a) found that signals from an airgun array received by a tag attached to diving sperm whales were strongly affected by their diving depth and distance from the source. The received pattern of airgun sounds was complex, most likely reflecting the sound transmission and propagation characteristics of airgun sounds (DeRuiter *et al*., 2006; Madsen *et al*., 2006a). This study is therefore an opportunity to explore how more tonal and longer duration sonar signals are received by tags attached to freely-diving cetaceans, and how animal depth and distance influence those signals in real-world sound propagation conditions.

## 2.2 Materials and methods

### 2.2.1 Study species and sites

CEEs were performed during the 3S-06, 3S-08 and 3S-09 research cruises in the Vestfjorden area of Norway (Kvadsheim *et al*., 2007; 2009). Experiments were conducted along the coast of Norway between 67° and 70° northern latitude (Figure 1) in the winter of 2006 and the summers of 2008 and 2009. In 2006, the study species was the killer whale within the marine valley and fjords (Thorsnes *et al*., 2009) of the Vestfjord area. In 2008 and 2009, the study area also included the continental shelf plain, the continental slope, and the deep sea plain northwest of Lofoten Islands. Concurrent with this change in field site and timing after 2006, the study species were also expanded to include sperm whales and long-finned pilot whales.

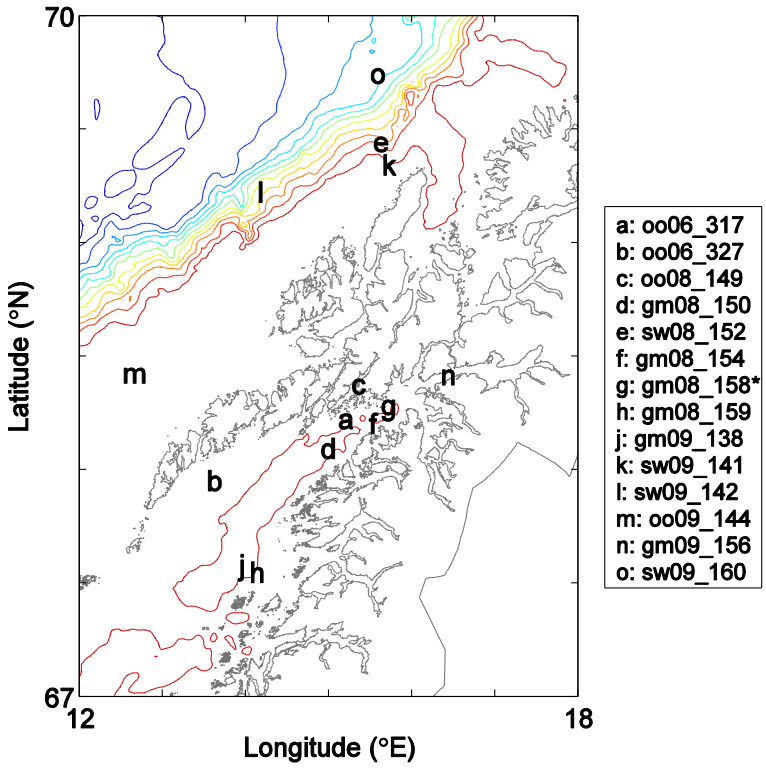


Figure 1: Map of the study area surrounding Lofoten Islands including the locations of the sonar experiments and the 250-m to 3-km depth contours (red to blue; 250-m intervals). The depth data on the map is limited to the offshore and Vestfjorden areas (GEBCO; IOC *et al*., 2003); data for the inner fjord systems is not shown. The experiment ID by which each experiment is labelled consists of a species code ('oo' for killer whale; 'gm' for long-finned pilot whale; 'sw' for sperm whale), the last two digits of the cruise year, and the Julian day of the experiment. *: Tag data was lost for this experiment.

### 2.2.2 Controlled-exposure procedure

CEEs were conducted using the 55-m R/V H.U. Sverdrup II as the source vessel. Concurrently, the 12-m R/V Nøkken (2006) or the 29-m MS Strønstad (2008−2009) served as independent tracking and observation vessel. Both the source vessel and observation vessel had dedicated observer teams on board who located and tracked whales using towed array acoustics and visual observation.

In the tagging phase, movement- and sound-recording sensors "Dtags" (Johnson and Tyack, 2003) were attached to the whales off the Sverdrup's workboats using a long carbon fibre pole or a pneumatic tag launching system "ARTS" (Heide-Jørgensen *et al*., 2001). When one or two whales were tagged, the operation entered the post-tagging phase in which tracking of the whale was established. Thereafter followed consecutively the pre-, during-, and post-exposure phases of the first vessel approach. Once a tag was attached, tracking and behavioural observations were done in a consistent manner throughout all phases of the experiment.

Vessel approaches with active sonar 'sonar runs' or started when the source vessel was positioned 6−8 km away from the focal animal. The source vessel then steadily moved towards the subject, only adjusting course to approach the animal. At one-kilometre distance, the vessel no longer turned, but passed the subject and then ceased transmission five minutes after the closest point of approach (CPA). To minimise the risk of inducing hearing injury in undetected nearby animals, and to increase the range of levels received by the tagged animals, the source level was gradually increased over 10 min according to a ramp-up scheme designed in the risk mitigation tool SAKAMATA (Benders *et al*., 2004). Transmission was also stopped when animals entered the 100-m safety zone around the source. A safety shut-down occurred once during a sonar run with sperm whales and three times during sonar runs with pilot whales (Miller *et al*., 2011a).

One to four vessel approaches were performed within one CEE, with a maximum of three sonar runs per experiment. Besides the active sonar transmissions two controls were also used: 1) a silent vessel approach with the same experimental protocol but where the source transmitted an empty sound file, and 2) killer-whale sound playbacks from one of the workboats with either herring-feeding or mammal-feeding killer whale sounds. Only sound levels received during sonar runs when the source was actively transmitting were considered in this study.

### 2.2.3 Sonar source

Sonar pulses were transmitted using a multi-purpose towed acoustic source (Socrates, developed by TNO). Socrates model I was used in 2006, and model II, identical to the first but with a higher maximum power output, was used in 2008 and 2009. These military experimental sonars both consist of a towed body with two free-floated ring transducers; one low frequency (LF) ring for transmitting 1−2 kHz signals, and one mid frequency (MF) ring for transmitting 6−7 kHz signals. The source also contains a hydrophone, a depth-pitch-roll sensor, and a temperature sensor. The LF transducer is omnidirectional in the horizontal plain and has a 3-dB beamwidth of 74° in the vertical plain (Gerk, 2003). The MF transducer is horizontally-omnidirectional in the free-field and has a vertical 3-dB beamwidth of 90°. Inside the towed body the MF transducer may not be fully omnidirectional because the larger pressure box and LF ring are positioned in front of the MF ring (Figure 2).

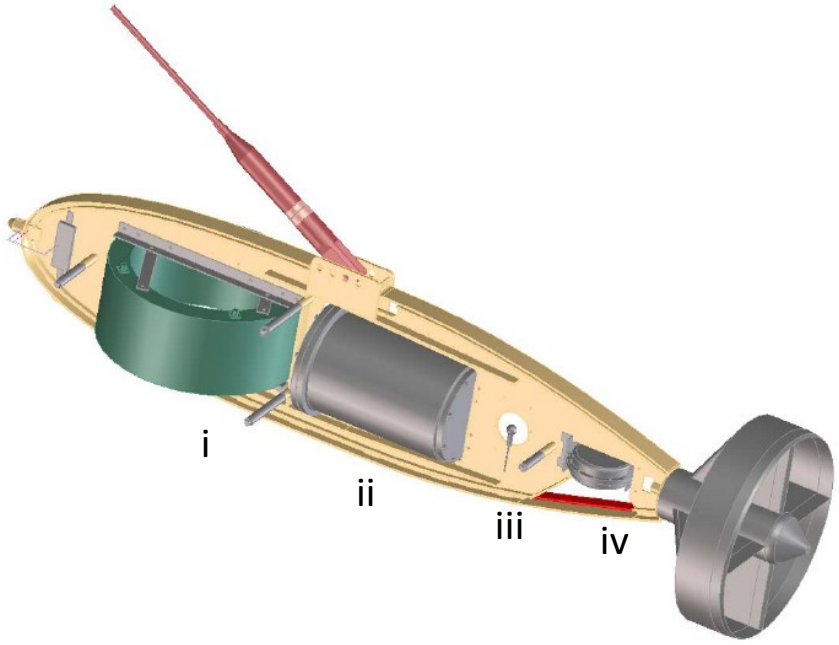


Figure 2: Schematic representation of the towed body of the Socrates source with the: (i) LF ring, (ii) pressure box, (iii) hydrophone, and (iv) MF ring. Figure courtesy of TNO.

The sound source transmitted one of three signal types per sonar run: 1–2 kHz hyperbolic frequency-modulated (HFM) upsweeps (LFAS-UP), 1–2 kHz HFM downsweeps (LFAS-DO), or 6–7 kHz HFM upsweeps (MFAS-UP). The signal duration was always 1 s including two 50-ms cosine-shaped tapers, thus the steady portion of the signal was 900 ms. Initially only 1–2 kHz and 6–7 kHz upsweeps were tested, because of their resemblance to signals from new European LFAS and MFAS systems. In 2008 downsweeps were added as test signal because it was hypothesized that upsweeps may cause an anti-predator response and stronger avoidance in animals (killer whale hypothesis; Zimmer and Tyack, 2007).

The source level started at 152 and 156 dB re 1 µPa m (150 and 138 dB in 2006), and was gradually increased during ramp-up to 214 and 199 dB re 1 µPa m (209 and 197 dB in 2006) for LFAS and MFAS, respectively. The inter-pulse interval (IPI) was 20 s during both ramp-up and full-power transmission, except in 2006 when the IPI was 10 s during ramp-up.

### 2.2.4 Acoustic receivers

Before an experiment began, one or more whales were tagged with a miniature movement- and sound-recording suction-cup tag “Dtag” (version two; Johnson and Tyack, 2003). The tag contains a VHF transmitter for tracking the tagged whale and for finding the tag after release. All sensor data are stored in flash memory, so the tag must be retrieved in order to obtain the data. The tag records stereo sound at a sampling rate of 96 or 192 kHz using a 16-bit resolution sigma-delta analog-to-digital converter (ADC). To increase the recording dynamic range, the internal gain in one of the two channels was set to 12 dB during experiments. The tag also records depth, temperature, three-dimensional acceleration, and three-dimensional magnetometer data that are synchronised with the audio recording. The non-acoustic sensors are sampled at 50 Hz, allowing a fine-scale reconstruction of the movements of the whale.

Figure 3: Dtag version two inside its housing. The hydrophones are located in the front of the tag (left in photo). Figure courtesy of WHOI.

The hydrophones and acoustic processing of five Dtags used during the 3S cruises were calibrated in an anechoic pool at TNO, The Netherlands. From 1−4 kHz, the mean sensitivity (±SD) was −185 (±2) dB re 1 µPa$^{-1}$. All Dtags appeared to be slightly less sensitive between 4 and 25 kHz, with the mean sensitivity being reduced by 6 dB at 10 kHz. However, these tags were calibrated without the housing, floating body and suction cups. Extensive testing of the Dtags with and without housing at the Acoustic Test Facility at the Naval Undersea Warfare Center in Newport, US, resulted in similar frequency responses for tags without housing, but the effect of the housing was not consistent among tags or frequencies and ranged from 1 to 4 dB reduction in

sensitivity. These results combined suggested an overall sensitivity of −188 dB re 1 $\mu Pa^{-1}$ between 1 and 40 kHz for Dtags with housing with an uncertainty range of ±5 dB.

The towed hydrophone array “Beamer” (Miller and Tyack, 1998) was deployed from the observation vessel for monitoring of the sound field near the subject animals and recording the sonar signals during experiments. The array’s 130-m tow cable is a streamer cable (Cortland Cable) with 18 twisted pairs, an outer weave (Kevlar) for towing, and external fairing threads to reduce tow noise. The active section consists of 16 hydrophones (Benthos AQ-2S) with custom 40-dB preamplifiers located next to each hydrophone at 13-cm spacing. Signals from 12 channels of the array were recorded with a digital harddisk recorder (Alesis HD24) that samples at 96 kHz with 24-bit resolution. The sonar signals that were analysed in this study were recorded on channel 11 of the array. The hydrophone and acoustic processing of this channel was calibrated at TNO and had a sensitivity of −171 (±1) dB re 1 $\mu Pa^{-1}$ between 4 and 20 kHz and a low-frequency rolloff over 10 dB between 1 and 4 kHz. The array was located at a depth of 5−10 m at typical tow speeds.

### 2.2.5 Source-to-receiver range

The sound source closely followed the trail of the ship at typical water current, tow speeds and turning angles. The source’s track was therefore similar to the ship’s track but with a time delay caused by the length of the deployed tow cable, the source depth, and speed of the ship. Because all this information was available, the lat/lon positions of the source when pings were transmitted were derived from the track of the ship after correction for the offset in time due to the position of the source behind the vessel.

The lat/lon position of the acoustic array towed by the observation vessel was estimated using the same method. The source-to-array range was then calculated for every received ping from the geographical coordinates of the source and the array.

The one-way travel time, or 'time of flight' of the pings and an assumed underwater sound speed of 1500 m/s were used to estimate the source-to-whale range. Ping transmission times were stored in UTC by the Socrates with high precision, but ping arrival times derived from the tag attachment time often created an offset in the range estimates. Using ordinary-least-squares, this offset was minimised for killer and pilot whale experiments by fitting the time-of-flight range function to the range data derived from the whale sightings (Figure 4). The average (N=23) root-mean-square error (RMSE) of the fits was 80 metres (range: 39−145 m), thus ±100 m is considered to be a conservative estimate of the uncertainty for the range measurements. For sperm whales, the time-of-flight range function was fixed using the nearest sighting of the whale beginning a dive by raising its flukes.

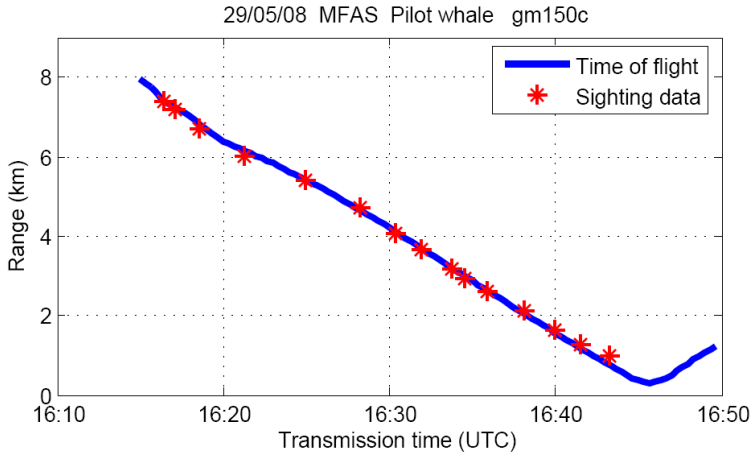


Figure 4: The 'time-of-flight' range function was fitted to the ranges derived from the sightings to determine the distance from source to whale over the entire sonar run.

### 2.2.6 Sound level measurements

#### *2.2.6.1 Ping selection*

Sonar signals recorded with the tags and hydrophone array were processed using a custom-written MATLAB (The Mathworks, 2007) program "CEE_Analyser" (Appendix I for user's guide). Waveform and spectrogram views of the signals guided every step of the analysis, and a strict protocol was followed to address challenges imposed by interfering noises.

A flip-template matched filter (Burdic, 1991) was used to identify the first arrival of the signal, and afterwards a time cue was stored. After visual inspection of the signal a 200-ms window of stationary noise preceding the ping was marked. If a noise overlapped with the beginning of the ping and caused the automatic method to be in error, an alternative start-time cue was manually selected and stored.

#### *2.2.6.2 Metrics and level computation*

Most received sonar signals had time-varying pressure envelopes [Figure 5(b)(e)] as they result from multiple arrivals of different phase and amplitude. To account for this temporal effect the maximum sound pressure level ($SPL_{max}$; in dB re 1 µPa) was calculated; the highest value of SPL that occurred during a specified time interval after a running average was performed on the instantaneous or mean square pressures (Morfey, 2001). The sliding windows had RMS averaging times of 10 and 200 ms, resulting in two time-weighted sound pressure levels, $SPL_{10}$ and $SPL_{200}$, respectively [Figure 5(a)(d)]. The maximum of $SPL_{200}$ is reported here as $SPL_{max}$. The time window of 200 ms was considered relevant in terms of sensation for the frequencies used in this study, because for non-transients sounds the mammalian ear integrates sound intensity over ~200 ms for signal detection (Plomp and Bouman, 1959; Fay, 1988). Comparable integration time constants were reported for the bottlenose dolphin (1-4 kHz, ~200 ms; Johnson, 1968), and the harbour porpoise (1-8 kHz, ~200-600 ms; Kastelein *et al*., 2010).

In some cases clicks from sperm whales interfered with the received sonar signals. Where needed, echolocation clicks of sperm whales were removed from the estimation of ping levels. An algorithm automatically identified these transient signals when the difference between the $SPL_{10}$ (one-way running average) and $SPL_{200}$ (two-way running average, to prevent phase shifts) was more than 6 dB. Clicks were also selected manually. Each click in the $SPL_{10}$ data was replaced through interpolation between the minima on either side of the peak, and the $SPL_{200}$ was recalculated from the 10-ms data.

The signal duration $\tau_{20dB}$ was defined as the time during which the $SPL_{10}$ exceeded a 20 dB threshold below the maximum. Because more than one threshold crossing could occur in each direction, the first crossing with increasing SPL and the last crossing with decreasing SPL that occurred over a 10-s period starting from the first-arrival time cue were selected. Within the 10-s period the reverberation level had always dropped below the threshold, even when late echoes of the transmission contained most of the sound energy. For pings overlapped by noise, the alternative-start time cue was used as the start point and/or the 10-s window was shortened to prevent the noise from influencing the duration measure. The final values reported for $SPL_{max}$ and SEL (next paragraph) were computed using $\tau_{20dB}$ as integration time *T* (Equation 1).

A common measure for calculating received sound levels is the sound exposure level (SEL; in dB re 1 $\mu Pa^2$ s), defined as the level of the cumulative sum-of-square pressures (Morfey, 2001). As it accounts for signal duration, SEL is also useful for quantifying intermittent noise events like sonar:

$$\mathrm{SEL} = 10 \cdot \log_{10} \left( \frac{\sum_{n=1}^{N} \int_{0}^{T} p_n^2(t) \cdot dt}{p_{ref}^2 \cdot t_{ref}} \right) \qquad (1)$$

where *N* is the number of transmitted pings, *T* is the ping duration (in s), and $p_n^2(t)$ is the square pressure of the $n^{th}$ transmission as function of time (in $\mu Pa^2$). Reference pressure $p_{ref}^2$ and reference time $t_{ref}$ are 1 $\mu Pa^2$ and 1 s, respectively.

The single-ping SEL [*N*=1; Figure 5(b)(e)] and the cumulative 'total' SEL (*N*>1) per exposure run were calculated for each ping. As a consequence of the click removal procedure, SELs were computed by cumulative summation of the mean square

pressures $p_{rms}^2(t)$. To eliminate the influence of background noise on the exposure levels, the mean square pressure of the noise segment preceding the ping was subtracted from $p_{rms}^2(t)$ before each SEL was calculated.

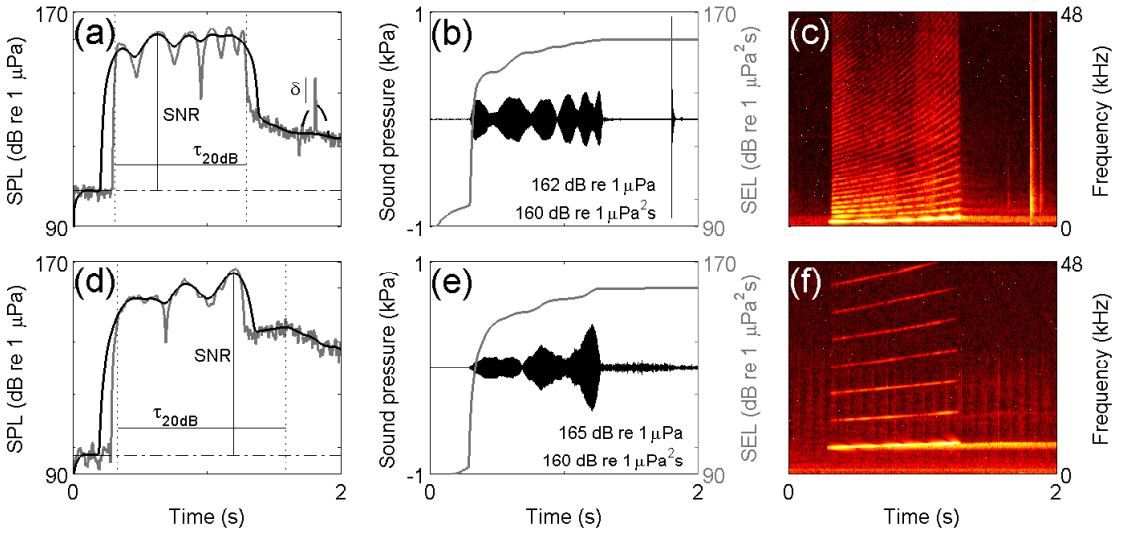


Figure 5: (a)(b)(c) Different representations of a LFAS upsweep signal followed by a sperm whale click, and of (d)(e)(f) a MFAS upsweep signal. (a)(d) The 10-ms average (grey line) and 200-ms average (black dashed/solid line: before/after click removal) time-weighted SPLs, and 3 measures derived from SPL: the signal-to-noise ratio (SNR), signal duration ($\tau_{20dB}$), and SPL ratio ($\delta$) used for click detection. (b)(e) The pressure waveform (black line) and SEL (grey line), with the numerical values for $SPL_{max}$ and SEL. (c)(f) Power spectrogram (Hann window, FFT length 512, 50% overlap) showing the relative power between the fundamental and harmonics.

Occasionally, when pings were intense and flow noise levels low, reverberation had not completely vanished after 20 seconds. In such cases the signal-to-noise ratio (SNR; defined here as the difference between the $SPL_{max}$ and the SPL of the 200-ms noise segment preceding the ping) was in fact a signal-to-reverb ratio. The lowest observed signal-to-reverb ratio was about 40 dB, thus the noise subtraction procedure did not significantly influence the level of such pings.

Sometimes a signal could not be measured but was still likely received by the animal. A ping was scored as 'received at full level' when a tagged sperm whale rested at the surface, or when pilot or killer whale vocalisations or splashing water sounds

coincided with the signal. It is possible that some animals may use their surfacing to reduce sound exposure, by placing their hearing organs in the region of pressure-release just below the sea surface. A ping was scored as 'not received at full level' by the animal when a tag on a killer or pilot whale was completely out of the water over the full duration of the signal. Only for pings marked as 'received at full level' single-ping levels were estimated from the adjacent ping levels by linear interpolation, and the cumulative SEL over the experiment was recalculated. To estimate the received level in the beginning of the ramp-up period, the first measured ping level was extrapolated and levels were corrected for differences in source level. This approach was taken because one group of animals (oo04_144) appeared to respond vocally to the sonar before any ping could be measured using the strict criteria employed here (Miller *et al.*, 2011a).

#### *2.2.6.3 Spectral content and frequency weighting*

The SPL and SEL of each ping were calculated for the 1−40 kHz 1/3-octave frequency bands. To avoid the influence of background noise, levels of frequency bands in which the signal-to-noise ratio (SNR) was 10 dB or higher (Madsen *et al*., 2006a) were integrated to obtain the broadband $SPL_{max}$ and SEL. The filter width of 1/3-octave is in agreement with common practice in underwater acoustics (Madsen *et al*., 2006b) and was considered practical, even though the exact widths of the critical bands and auditory filters of cetaceans are still uncertain (Au and Moore, 1990; Finneran *et al*., 2002). A spectrogram and associated band levels were checked visually for sounds from sources other than the sonar, and 1/3-octaves in which such sounds were found to interfere with the SPL were excluded from the analysis. All bandpass filters were implemented in the time domain using sixth-order Butterworth filters.

The sound source produced harmonic distortion at higher source levels [Figure 5(c)(f)]. The presence of harmonics raised the concern that the animals may have been responding to the harmonics instead of to the fundamental, as the hearing of odontocetes is generally more sensitive to higher frequencies (killer whales: Szymanski

*et al*., 1999; pilot whales: Paucini *et al*., 2010; Schlundt *et al*., 2011). For killer whales, this concern was addressed by applying a frequency weighting based on killer whale hearing threshold data (Figure 6) to emphasize or de-emphasize spectral components in the sound (pilot whale and sperm whale audiograms were not available when the analysis was carried out). Wensveen and Van Roij (2007) created this weighting function for sounds received by killer whales by inverting an idealised audiogram and normalising it at its maximum sensitivity (see also Ainslie, 2010). The idealised hearing threshold (HT) consisted of three separate power functions that were fitted to the raw killer whale threshold data from Hall and Johnson (1972) and Szymanski *et al*. (1999), and is mathematically described as:

$$\mathrm{HT}(f) = \begin{cases} 445.2 \cdot f^{-0.05401} - 344.4 & 0.5 \le f < 11.3 \\ 242.9 \cdot f^{-0.7578} + 0.5643 \cdot f^{1.076} & 11.3 \le f < 46.2 \\ 2.792 \cdot f^{0.7537} - 2.064 & 46.2 \le f \le 80 \end{cases} \quad (2)$$

with $f$ in kHz. The weighting (in dB) is then:

$$\mathrm{W}(f) = \min(\mathrm{HT}) - \mathrm{HT}(f) \quad (3)$$

with min(HT) = 39.0 dB re 1 μPa.

The resulting weighting function was used to obtain weighting correction factors for the 1/3-octave bands between 1 and 40 kHz, and the weighted broadband maximum SPL and weighted broadband SEL were calculated after applying the weightings in the 1/3-octave bands.

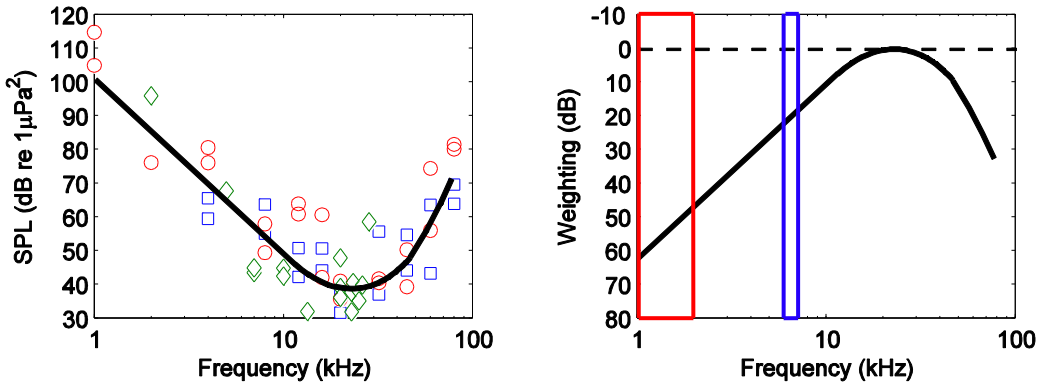


Figure 6: (left) Hearing threshold data for killer whales (green diamonds: behavioural thresholds from Hall and Johnson, 1972; red circles and blue squares: AEP and behavioural thresholds, respectively, from Szymanski *et al*., 1999), and the idealised audiogram (black line; Wensveen and Van Roij, 2007) based on these data. (right) Auditory weighting function derived from the audiogram (black line) with in red and blue the LFAS (1−2 kHz) and MFAS (6−7 kHz) bands, respectively.

### 2.2.7 Bellhop sound propagation model

The beam-tracing model "Bellhop" was used with Gaussian beams to predict the TL in the area around the source. The Gaussian beam-tracing method is based on ray-tracing theory, but does not suffer from particular ray-tracing artefacts such as infinite energy at caustics and perfect shadows (Porter and Bucker, 1987). With Gaussian beam-tracing, the source launches a fan of beams that propagate through the medium according to standard ray equations. The intensity of a beam is defined by a Gaussian distribution centred about that beam. The acoustic field at any given point is then constructed by adding up the contribution from each beam at that point (Baxley *et al*., 2000).

The 3-dB points of the vertical directivity patterns of the LFAS and MFAS transducers were used as the start- and end-angle of the fan. The number of Gaussian beams $N_{beam}$ that were traced was based on the relationship:

$$N_{beam} = \frac{\pi}{2} \cdot \sqrt{\frac{6 \cdot f \cdot r}{c}} \qquad (4)$$

where *f* is the frequency in Hz, *r* is the maximum range in m, and *c* is the sound speed at the source in m $s^{-1}$ (which was taken as 1500 m $s^{-1}$). This equation, part of earlier versions of Bellhop, was preferred over the new version's equation to decrease the runtime of the model. No noticeable differences at 1.4 kHz were observed in pre-tests when $N_{beam}$ was increased above the value suggested by the Equation 4. McCammon (2008) also found no noticeable difference at 1 kHz and above when the number of beams was increased.

For LFAS and MFAS respectively, Bellhop was used to calculate incoherent TLs as a function of range and depth at 1.4 and 6.5 kHz (the logarithmic mid points of the sonar bands). Incoherent TL was preferred over coherent TL, which includes effects of constructive and destructive interferences on the received waveform, because the source and receivers were moving and the sonar signal was a frequency sweep, which both have averaging effects on the received level.

Bellhop and the module "Bounce" for calculating bottom reflection coefficients are part of the Acoustic Toolbox[1] (Porter, 2011). The MATLAB front-end for the toolbox (AcTUP[2]) was used as user interface so that pings could be easily processed in batches. The water surface was modelled in Bellhop as a perfect reflective mirror because the experiments were only conducted in relatively quiet sea-state (SS) conditions (SS0 1x; SS1 5x; SS2 6x; SS3 1x). More information on the sound speed profiles, bathymetry data and acoustic bottom parameters that were used as input to Bellhop is given below.

[1] Downloaded on 23-11-2009 from http://oalib.hlsresearch.com/Modes/AcousticsToolbox/.

[2] V2.2L. Downloaded on 23-11-2009 from http://cmst.curtin.edu.au/products/actoolbox.cfm.

#### *2.2.7.1 Sound speed profiles*

During the 3S cruises, CTD (Conductivity, Temperature, Depth) profiles were taken using a SAIV SD-200 CTD-profiler in the transmission path between the sonar and the tagged animal. In addition, temperature profiles were taken using a Sippican T7 Expendable Bathythermograph (XBT). The XBT-profiles were partly taken during experiments and partly during search phase to estimate the marine mammal detection range of the hydrophone arrays (Kvadsheim *et al*., 2009).

One CTD- or XBT-profile was selected per sonar run. The selected profiles were collected in the field immediately after the entire experiment had ended, at or near the location of CPA. For XBTs, the density anomaly as function of pressure was calculated using the equation of state of seawater from UNESCO (1983) and an estimated salinity of 35 ‰. For both XBTs and CTDs, pressures (in dbar) were converted to depths (in m) using the latitude of the measurement location (UNESCO, 1983). One SSP was selected per sonar run, thus the propagation model assumed this profile was representative for the entire 4D oceanographic field of the site. Because of this simplification, profiles were smoothed to remove insignificant features and subsampled to decrease the run-time of Bellhop (Porter, 2011).

#### *2.2.7.2 Bathymetry data*

For the experiments in Vestfjord, Ofotfjord and Oksfjord, the bathymetry data were obtained from the high-resolution Marine Primary Data (MPD) of the Norwegian Hydrographic Service. The depth-contour intervals of the MPD are at (in m): 0.5, 5, 10, 20, 30, 40, 50, and 100, and then every 50. These depth data in vector format were converted in Manifold 8.0 to ASCII gridded XYZ format with a grid size of 3.6 arc-seconds. The offshore area was not fully covered by the MPD, therefore the bathymetries of the offshore experiments were reproduced from the GEBCO One Minute Grid (IOC *et al*., 2003).

The selected grid was read in MATLAB to obtain the bathymetry along a transect line between the transmitting source and a receiver. Depths were evaluated at a large number of positions on the transect line, which resulted in a data vector consisting of distinct constant-depth segments. Thereafter, gradually-changing bathymetry was created by linear interpolation between the mid points of the segments.

#### *2.2.7.3 Bottom properties*

The surficial sediments off the coast of Lofoten were recently mapped in high detail by the MAREANO group (Knies, 2009). Sediments were characterised according to a ternary classification scheme (SOSI; Bøe *et al*., 2010) which is similar to the Folk scheme (Folk, 1980). Ternary schemes base sediment names on the proportions of three component size classes (gravel-sand-mud in this case), rather than on the bulk mean grain size ($M_z$; in ϕ). The parameter $M_z$ however is useful for estimating other geo-acoustic bottom parameters, therefore the sediment types of the MAREANO were linked to values of $M_z$ based on HFEVA (APL-UW, 1994).

For offshore sonar runs, area maps (Figure 7; others in Appendix II) were created to determine which sediment type was most abundant in the source−receiver path. The maps were created in MANIFOLD (CDA International, 2007) by importing combined sediment−hillshade image titles from the NGU WMS server[3] and overlaying this image layer with the source vessel and whale tracks. Sediment types were selected visually and ranged from hard deposits like gravel, pebbles and boulders to soft deposits like sandy mud (with mud: clay and silt). The surficial sediment types in the offshore area were predominantly sandy gravel and gravel, coddles and boulders (Appendix II).

[3] Accessed online at:
http://www.ngu.no/wmsconnector/com.esri.wms.Esrimap?VERSION=1.1.1&SERVICE=WMS&REQUEST=GetMap&SRS=EPSG:32633&TRANSPARENT=true&SERVICENAME=MareanoBunnsedimenterWMS&FORMAT=image/png&LAYERS=Kornstørrelse_regional,Kornstørrelse_detaljert

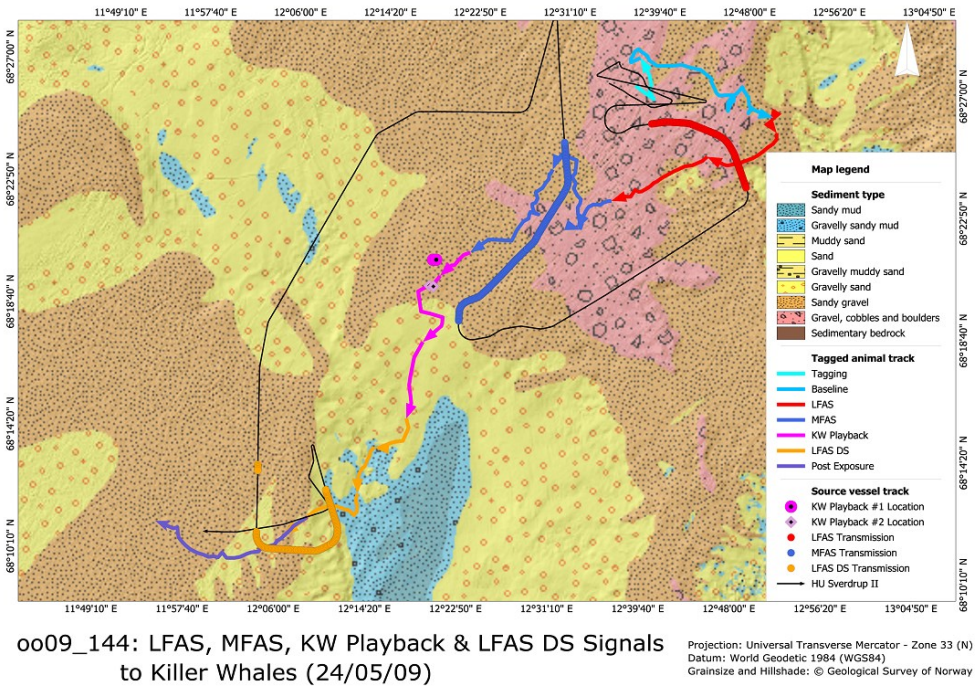


Figure 7: Map of the study site of experiment oo09_144 with the seafloor sediment types, the vessel track of Sverdrup, and the track of one of the tagged killer whales reconstructed from the sighting data.

Sediment data for the inshore experiments were not available from MAREANO, although their data showed that the Vagsfjord (bordering on Ofotfjord) consisted primarily of sandy mud. Bottom samples and historical surface sediment data (Jenserud, 2002; Jenserud and Ottesen, 2002) suggested that sandy mud was also appropriate for most of the experiments conducted in the fjords. Gravelly sand was selected only for experiment oo06_327, which was conducted in the western, shallower part of Vestfjord (Figure 1).

The bottom was modelled as a homogeneous layer with constant acoustic properties. The geo-acoustic bottom parameters used in the TL modelling work were the compressional sound speed ($V_p$), the bulk density of the sediment ($\rho$), and the compressional wave attenuation ($\alpha$). Values for bottom surface roughness and the shear wave parameters were kept at zero. The $V_p$ in the sediment was estimated from the $V_p$ in the pore water using the relationship between $M_z$ and the sediment−water sound speed ratio ($V_pR$; Richardson and Briggs, 2004; in Jackson and Richardson, 2007):

$$V_pR = 1.184 - 0.0307 \cdot M_z + 0.001 \cdot M_z^2 \qquad 0 < M_z < 12 \tag{5}$$

where $V_pR$ is unitless. The bulk density of the sediment was then estimated from $M_z$ using the equation of Hamilton and Bachman (1982):

$$\rho = 2.374 - 0.175 \cdot M_z + 0.008 \cdot M_z^2 \qquad 1 \le M_z \le 9 \tag{6}$$

where $\rho$ is in g cm$^{-3}$. Next, the compressional wave attenuation $\alpha$ was derived from $M_z$ through attenuation factor $k$ using the formulas of Hamilton (1972):

$$k = \begin{cases} 0.4556 - 0.0245 \cdot M_z & 0 \le M_z \le 2.6 \\ 0.1978 + 0.1245 \cdot M_z & 2.6 < M_z \le 4.5 \\ 8.0399 - 2.5228 \cdot M_z + 0.20098 \cdot M_z^2 & 4.5 < M_z \le 6 \end{cases} \tag{7}$$

with $k$ in dB m$^{-1}$ kHz$^{-1}$, and $\alpha = kf$ with $\alpha$ in dB/m and frequency $f$ in kHz. Finally, $\alpha$ was converted to $\alpha_p$ in dB/λ by the standard relationship between sound speed, frequency and wavelength.

No such empirical relationships exist for grain sizes smaller than zero. Therefore, for the three sonar runs with sediment type 'sandy gravel' or 'gravel, cobbles and boulders' $V_p$ was based on HFEVA's $V_pR$, $\rho$ was based on HFEVA's sediment−water density ratio, and $\alpha_p$ was assumed to be 0.8 dB/λ.

A table with the seafloor sediment types, and the related SOSI definitions and selected grain sizes for all the sonar runs can be found in Appendix III.

### 2.2.8 Analysis of range- and depth effects

One or two acoustic tags recorded sonar signals during 13 experiments (30 sonar runs in total). For two sonar runs conducted during one experiment (gm08_158) the tag did not record due to a battery failure. The hydrophone array was towed from the observation vessel nearby the tagged animal during 10 experiments and recorded sonar signals during 23 out of 32 sonar runs. This unique dataset of sonar sounds recorded at or near the location of the whales was analysed to investigate the sources of variation in the sound levels such as from source range, whale depth, whale orientation and underwater propagation conditions.

The measured transmission loss (TL; in dB) of each ping was calculated as the difference between the source level (SL) and the received $SPL_{max}$ of the ping:

$$\mathrm{TL} = \mathrm{SL} - \mathrm{SPL}_{\max} \qquad (8)$$

where TL includes attenuation from geometrical spreading, losses due to absorption, and other non-geometrical effects such as scattering. Using least-squares regression, a basic spreading loss model was then fitted to the TL data from the Dtags and towed array to examine for range-dependent effects in the dataset:

$$\mathrm{TL} = X \cdot \log_{10}(r) + \alpha \cdot r \qquad [\text{with } \alpha = 3.6 \cdot 10^{-5} \cdot f^{1.5}] \qquad (9)$$

where *X* is the geometric TL coefficient, *r* the source-to-receiver range in m, *α* the absorption coefficient in dB/m, and *f* the centre of the sonar frequency band in kHz. Parameter *X* equals 20 in the case of perfect spherical spreading of sound energy; *X* equals 10 when the acoustic spreading is cylindrical. The value for *α* was estimated *a priori* using the numerical relationship with frequency reported in Richardson *et al*. (1995) for absorption in seawater, which is given above in square brackets. Because of the shallow depth of the hydrophone array, the geometric spreading law was fitted only to the data of the nine sonar runs in which the tagged animal had only made

shallow surface dives. Equation 9 was also fitted to the TL data predicted by Bellhop to compare between measured and predicted values.

The portion of the total attenuation that is not accounted for by spherical spreading is called excess attenuation (EA; in dB; Brenowitz, 1982). Absorption was added to the standard equation for EA to correct as much as possible for any range-dependencies in the dataset:

$$\mathrm{EA} = \mathrm{TL}_{\mathrm{meas}} - 20 \cdot \log_{10}(r) + \alpha \cdot r \qquad (10)$$

where absorption coefficient $\alpha$ was calculated again using the Richardson *et al*. formula. After calculating the EA for every received sonar signal, the EA data was binned by species and sonar frequency in 10-m bins. Pings that were likely to have been shielded by the body of the whale, pings for which the source-to-whale range was unknown and pings for which the sound levels were estimated by interpolation and extrapolation of neighbouring pings (section 2.2.6.2) were excluded from the analysis.

## 2.3 Results and discussion

### 2.3.1 Quantifying sonar signals using acoustic tags

Sound-recording tags sample the acoustic field at the animal and so provide insight into the input of a key sensory faculty of cetaceans (Johnson *et al*., 2009). During controlled sonar exposure experiments the sounds at the whale consists not only of the transmitted test signals, but also of potentially interfering sounds such as echolocation clicks and whale vocalisations. In addition to real-occurring sounds, flow noise is present in the acoustic data that depends in magnitude on the size and placement of the tag, as well as on the speed of the tagged animal. Silences occur when the tag comes out of the water during surfacings of the whale, even though the animal's hearing pathways may still have been submerged. These types of interference can cause high rejection rates during the analysis of the acoustic data recorded with tags.

In the current study, a total of 7,091 pings were recorded with the acoustic tags (4,297) and/or the towed hydrophone array (2,794). For pings that were masked or not recorded but assumed to be 'received at full power' (section 2.2.6.2), sound levels were estimated by interpolation (279 pings; 4%) or extrapolation (369 pings; 5%) and, if necessary, corrected for source level differences between pings. A high percentage (90%) of pings was thus extracted and quantified directly from the tag recordings, mostly due to the relatively long duration (1 s) of the transmissions and the removal of sperm whale clicks from the data. The inter- and extrapolations were included to be able to find the received levels for any given time in the sonar run, so that all moments of behavioural change could be related to the correct levels (Miller *et al*., 2011a). Only the 113 pings (1%) scored as 'not received at full level' were left out of the analysis completely.

The main objective of the 3S cruises in Vestfjorden, Norway, was to study the effects of sonar on the behavioural responses of free-swimming cetaceans using a dose–response paradigm. CEEs were designed in a way that the received levels, part of

the sonar dose, at the study animals escalated throughout the vessel approach so that potential behavioural responses could occur over a range of received levels. Figure 8 illustrates how the received unweighted $SPL_{max}$ and SEL levels of the sonar increased during the 10-min ramp-up and 50-min full-power period of the MFAS run in experiment oo09_144, and kept increasing with decreasing source-to-whale distance until the animal was passed by the source. Note that the sound levels of the pings received in the first five minutes of the sonar run are extrapolations of the first measured ping that had a SNR above 10 dB.

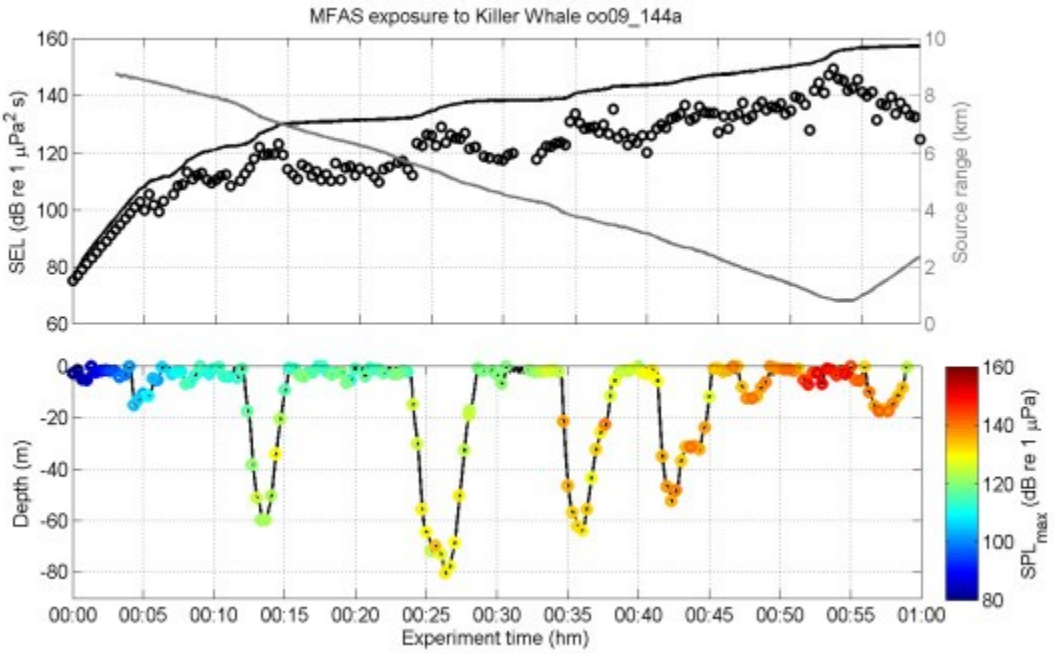


Figure 8: (top panel) Unweighted broadband single-ping SEL (black circles) and cumulative SEL (black line) received by a killer whale with tag oo09_144a during a controlled MFAS exposure, as well as the corresponding source-to-whale range (grey line). (bottom panel) The dive profile of the same animal overlaid with the unweighted broadband $SPL_{max}$ (RMS averaging time: 200 ms) of the same signals.

The responses of the whales were closely monitored throughout each sonar run, and mitigation protocols stopped the exposure if any animal came within 100 m of the source or if behavioural effects occurred that appeared to present a risk of harm. A more conservative approach was taken during the first experiments to gain experience on the responses of the species, while in later experiments subjects were exposed to

higher levels as the sonar did not appear to be severely harmful. This general trend is reflected in the highest unweighted $SPL_{max}$ and $SEL_{cum}$ levels as well as in the minimum range to the source, in particular for experiments with killer whales and pilot whales (Table 1 and 2). Sperm whales were under water for most of the exposure time and thus often more difficult to approach closely than the other two species.

Although behavioural responses are not the focus here, the minimum range to the source and highest received level per sonar run also give indications of the degree of responsiveness of the whales. Note that the source no longer turned towards the animal at 1 km distance. The minimum range to the source for killer whales and pilot whales averaged 1.0 and 0.3 km for LFAS runs, respectively, and 0.8 and 0.3 km for MFAS runs, respectively (Table 1 and 2). The highest unweighted $SPL_{max}$ received by killer whales and pilot whales averaged 166 and 173 dB re 1 µPa for LFAS runs, respectively, and 151 and 158 dB re 1 µPa for MFAS runs, respectively (Table 1 and 2). Generally, pilot whales thus allowed the source to come closer and this species received higher levels from the sonar than the killer whales.

Table 1: The range of unweighted broadband $SPL_{max}$ and $SEL_{cum}$ levels received by killer whales, pilot whales and sperm whales during controlled exposures to LFAS upsweep (LFAS-UP) and downsweep (LFAS-DO) signals, including the range of whale depths and source-to-whale distances. Data of second tagged animals are shown in parentheses. *: no range data for sw08_152a because the animal was not sighted during the exposure.

| **Tag ID** | **CEE start (UTC)** | **CEE stop (UTC)** | **Signal type** | **Whale depth (m)** | **Source range (km)** | **Unweighted $SPL_{max}$ (dB re µPa)** | **Unweighted $SEL_{cum}$ (dB re µPa$^2$s)** |
|---|---|---|---|---|---|---|---|
| Killer whale | | | | | | | |
| oo06_317s | 14:10 | 14:43 | LFAS-UP | 0–28 | 2.5–7.0 | 90–155 | 87–162 |
| oo08_149a | 14:56 | 15:46 | LFAS-UP | 0–29 | 1.2–6.3 | 82–166 | 79–176 |
| oo09_144a (oo09_144b) | 14:13 | 14:47 | LFAS-UP | 0–53 (0–56) | 0.5–7.6 (0.4–7.9) | 91–174 (78–169) | 89–181 (75–173) |
| | 21:13 | 21:51 | LFAS-DO | 0–63 (0–69) | 0.8–7.2 (0.7–7.4) | 92–168 (80–166) | 88–179 (77–176) |
| Long-finned pilot whale | | | | | | | |
| gm08_150c | 18:05 | 18:36 | LFAS-UP | 0–16 | 0.3–6.8 | 91–170 | 87–177 |
| gm08_154d | 01:15 | 02:35 | LFAS-UP | 0–64 | 0.6–11.1 | 79–163 | 76–169 |
| gm08_159a | 00:33 | 01:08 | LFAS-UP | 0–15 | 0.4–8.0 | 75–175 | 73–176 |
| gm09_138a (gm09_138b) | 14:42 | 15:14 | LFAS-UP | 0–14 (0–13) | 0.4–6.7 (0.4–6.7) | 83–172 (73–167) | 77–175 (70–173) |
| | 20:32 | 21:05 | LFAS-DO | 0–11 (0–14) | 0.1–6.6 (0.2–6.5) | 72–175 (75–175) | 66–176 (72–176) |
| gm09_156b | 01:36 | 02:09 | LFAS-UP | 0–19 | 0.3–6.2 | 68–180 | 65–186 |
| | 04:55 | 05:25 | LFAS-DO | 0–533 | 0.1–5.5 | 91–177 | 89–181 |
| Sperm whale | | | | | | | |
| sw08_152a | 04:10 | 05:10 | LFAS-UP | 0–306 | * | 84–159 | 75–173 |
| sw09_141a | 12:18 | 12:58 | LFAS-UP | 0–188 | 0.6–6.0 | 91–169 | 88–178 |
| sw09_142a | 21:46 | 22:30 | LFAS-UP | 0–266 | 1.3–7.2 | 84–165 | 77–178 |
| | 04:03 | 04:53 | LFAS-DO | 0–319 | 0.7–9.2 | 95–154 | 92–166 |
| sw09_160a | 14:45 | 15:28 | LFAS-UP | 0–274 | 0.7–7.8 | 81–170 | 77–176 |
| | 20:13 | 21:12 | LFAS-DO | 0–769 | 0.5–8.1 | 79–166 | 79–176 |

Table 2: The range of unweighted broadband $SPL_{max}$ and $SEL_{cum}$ levels received by killer whales, pilot whales and sperm whales during controlled exposures to MFAS upsweep signals, including the range of whale depths and source-to-whale distances. Data of second tagged animals are shown in parentheses.

| **Tag ID** | **CEE start (UTC)** | **CEE stop (UTC)** | **Signal type** | **Whale depth (m)** | **Source range (km)** | **Unweighted $SPL_{max}$ (dB re µPa)** | **Unweighted $SEL_{cum}$ (dB re µPa$^2$s)** |
|---|---|---|---|---|---|---|---|
| Killer whale | | | | | | | |
| oo06_327s (oo06_327t) | 13:36 | 14:10 | MFAS-UP | 0–65 (0–65) | 0.7–6.0 (0.7–6.0) | 71–154 (67–152) | 68–159 (65–159) |
| oo08_149a | 12:48 | 13:40 | MFAS-UP | 0–5 | 1.5–7.0 | 75–142 | 71–149 |
| | 22:38 | 23:08 | MFAS-UP | 0–20 | 0.4–1.2 | 111–155 | 109–162 |
| oo09_144a (oo09_144b) | 16:15 | 17:14 | MFAS-UP | 0–81 (0–81) | 0.8–8.7 (0.6–9.0) | 78–151 (77–150) | 75–157 (74–158) |
| Long-finned pilot whale | | | | | | | |
| gm08_150c | 16:12 | 16:50 | MFAS-UP | 0–24 | 0.3–8.0 | 84–150 | 79–153 |
| gm08_154d | 03:35 | 04:00 | MFAS-UP | 0–8 | 0.2–4.8 | 70–152 | 67–153 |
| gm08_159a | 02:10 | 02:46 | MFAS-UP | 0–429 | 0.3–6.3 | 74–159 | 70–163 |
| gm09_138a (gm09_138b) | 16:40 | 17:15 | MFAS-UP | 0–10 (0–9) | 0.2–6.3 (0.2–6.6) | 77–167 (76–161) | 74–166 (72–159) |
| gm09_156b | 03:10 | 03:37 | MFAS-UP | 0–542 | 0.3–5.3 | 83–156 | 82–162 |
| Sperm whale | | | | | | | |
| sw08_152a | 01:35 | 03:10 | MFAS-UP | 0–663 | 19–9.2 | 82–146 | 77–155 |
| sw09_141a | 14:00 | 14:52 | MFAS-UP | 0–474 | 0.7–7.2 | 79–150 | 75–158 |
| sw09_142a | 23:27 | 00:00 | MFAS-UP | 21–575 | 1.8–5.2 | 82–146 | 80–156 |
| sw09_160a | 12:20 | 13:02 | MFAS-UP | 0–996 | 1.5–10.0 | 73–151 | 69–156 |

Experiments oo09_327, gm09_138 and oo09_144 were conducted with not one but two tagged whales. In all three of these two-tag experiments both animals were part of the same group and had comparable diving behaviour, often diving simultaneously (Miller *et al*., 2011a). During these three experiments the same sonar transmissions were thus recorded twice at roughly the same depth and distance from the source.

The levels received on the two tags were mostly similar, except for experiment oo09_144 during the entire LFAS-UP run and in the early phase of the LFAS-DO run. During these periods the group of killer whales moved perpendicular to the heading of the source ship (Figure 7). Tag oo09_144a was located on the right side below the dorsal fin of a female-sized animal. Tag oo09_144b was located at the left side of the body of a large male (Figure 9) but the tag slid slightly downwards on the whale's body as the LFAS-UP run progressed. In Figure 9 the difference in broadband $SPL_{max}$ between each tag and the towed array for every ping received during the experiment is plotted as function of the horizontal angle of arrival of the sound. At horizontal angles of arrival of about 80°−140° the levels received on tag oo09_144b were about 15 dB lower than the levels received on the towed array, while for other angles most data fell within a range of ±10 dB, similar as for the data from tag oo09_144a.

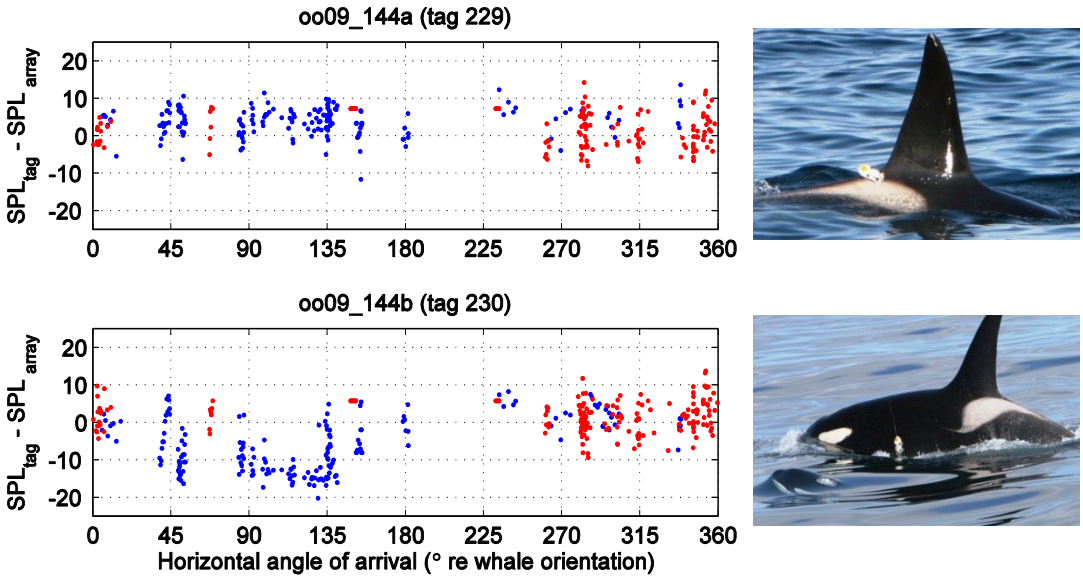


Figure 9: (left) The tag−array difference in broadband $SPL_{max}$ per ping received during the killer whale CEE in 2009 as function of the horizontal angle of arrival of the signals at the animal. Blue markers represent the pings from the LFAS sonar and red markers indicate MFAS pings. (right) Location of the Dtag sensor on the killer whale (top panel: tag oo09_144a; bottom panel: tag oo09_144b).

The body of the large killer whale male with its air-filled lung apparently shielded, or blocked, the signals arriving on tag oo09_144b when the source was located at the opposite side of the whale, thereby attenuating the levels received on the tag. Body

shielding occurs due to a mismatch in acoustic impedance between the sea water and the tissue, bone and airways in the body of the whale (Madsen *et al*., 2006a). The degree of attenuation due to shielding depends on the interaction between frequency and the size of the body parts of the whale; the effect is more severe at small wavelengths and for large obstacles. It is likely that some of the pings received during other experiments were affected by body shielding, although this hypothesis has not been tested at the time. The described case is possibly the most extreme example of body shielding in the dataset because of the animal's size, position of the tag (lower on the body than usual and behind the lung) and constant geometry between the source and the whale.

### 2.3.2 Effects of range, depth and sound propagation

Cetaceans can be found in the same shallow-water coastal areas as naval sonar exercises. In these environments the sound field is site-specific and highly variable as it is affected by the acoustic properties of the sea surface and bottom as well as by variations in sound speed with depth and range (Urick, 1983). When assessing the influence of sonar on cetaceans it is particularly important to understand at which ranges active sonar poses a risk of harm to the animals and at which ranges behavioural disturbance and masking of biologically-important sounds can occur (Nowacek *et al*., 2007). Transmission loss during underwater propagation is a key element for calculating such impact ranges for sonar exposure. The transmission loss at an animal is often predicted using basic geometrical spreading laws or sound propagation models but is only sporadically validated empirically (*e.g.*, Miksis-Olds and Miller, 2006; DeRuiter *et al*., 2009). The question here was therefore how animal depth and distance influence the sonar signals received by tags attached to freely-diving cetaceans in real-world sound propagation conditions.

Transmission losses of the sonar signals were recorded with the acoustic tags and towed hydrophone array and plotted as function of range (Figure 10). For all but one

experiment (oo06_327) the measured TLs generally increased with distance to the source following the pattern of geometrical spreading, but deviations of ±10 dB from the TL predicted by the spreading loss model were common in the dataset. The increase in TL at 4–6 km for oo06_327 can be explained by the fact that both tagged whales received higher levels during two deep dives and then started travelling when the source came closer. Both oo06_317 and oo06_327 were conducted in winter when a positive sound speed gradient in the upper layer of the water causes upwards refraction of sound rays that then bounce off the sea surface (Appendix IV), so the animals were probably in a convergence zone during the dives.

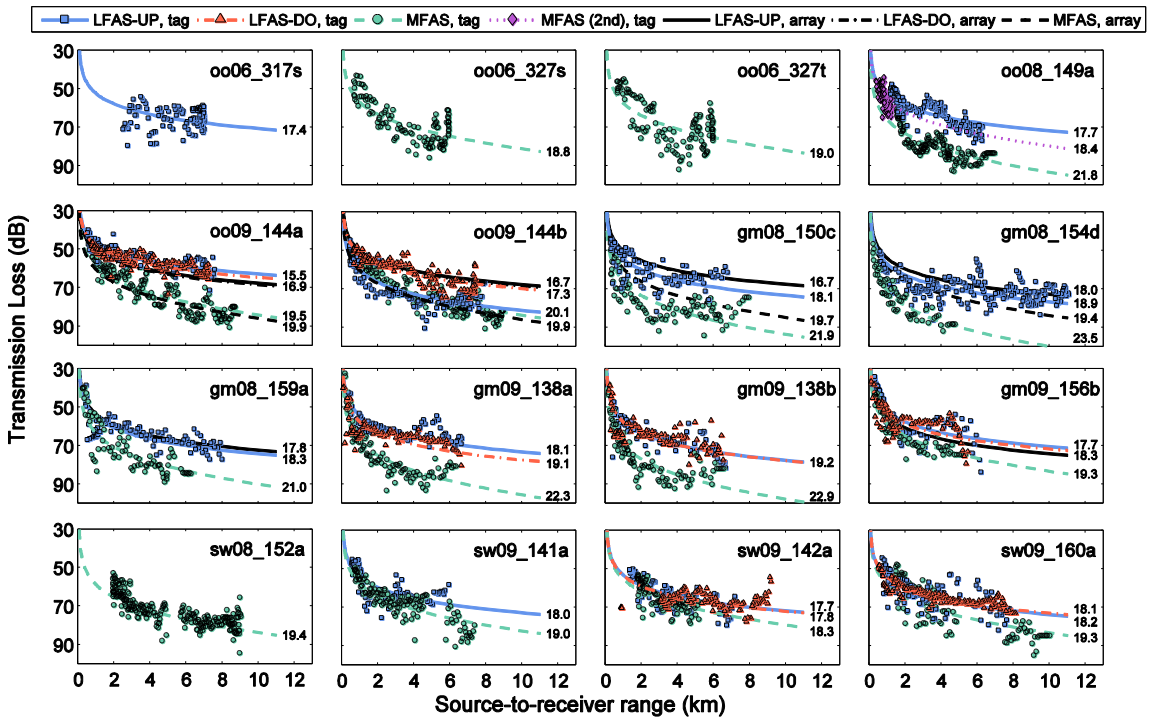


Figure 10: Transmission loss of sonar signals (markers) as function of range per tag deployment, the corresponding geometrical spreading loss model fits (colour lines) and the spreading loss coefficient *X* of the curve fits. Spreading loss models fitted to the towed array data for the sonar runs when the animal was shallow diving are indicated with black lines. Only the highest and lowest *X* values are shown where the lines of the models laid very close to one another. Data for the LFAS run during sperm whale experiment sw08_152 are not plotted as the animal was not seen at the surface and thus no range data was available.

For sperm whales, the TLs measured during sonar runs were similar within signal frequencies; the geometric TL coefficient *X* ranged from 17.7 to 18.2 for LFAS signals

and from 18.3 to 19.4 for MFAS signals. The RMSEs of the model fits averaged 5 dB and ranged from 2 to 7 dB. Experiments with sperm whales were conducted inside canyons at the shelf break and in the deep waters off the coast of Lofoten Islands, where the water column was less stratified than in inshore areas (Appendix IV). TL coefficients close to 20 (spherical spreading) are not unusual in these moderate to deep environments. The animals spent relatively more time at shallow depths during LFAS than MFAS exposure (Table 1 and 2) possibly in response to the low-frequency sonar sounds (Miller *et al*., 2011a).

Compared to sperm whales, transmission losses of the sonar signals calculated from the tag data were much more variable for killer and pilot whales. For both species combined, the TL coefficients calculated from the tag recordings (excluding of the LFAS-UP run on shielded tag oo09_144b) ranged from 15.5 to 19.2 for LFAS signals and from 18.5 to 23.6 for MFAS signals. The RMSEs of the model fits averaged 5 dB and ranged from 3 to 8 dB. During the experiments in summer, a sound channel centred within ~100-m from the surface was present due to the thermocline in the water (Appendix IV). Part of the variation in TL coefficients was thus due to the location of this sound channel relative to the vertical behaviour of the whale. TLs were similar between LFAS-UP and LFAS-DO runs within experiments, thus the sound propagation conditions did not hugely change within hours at nearby experiment locations.

Surprisingly, the difference between LFAS and MFAS was consistent among species and sonar runs; even though the sonar runs were conducted close to each other in time and space. The difference possibly resulted from one (or a combination) of the following factors: 1) Source directivity. The acoustic power radiating from the MFAS transducer in the forward direction may have been less than expected as the horizontal beam pattern of the transducer plus towed body was unknown (section 2.2.3). The source vessel moved towards the whales and changed course to approach more closely if needed, therefore animals were often located directly in front of the transducer. 2) Receiver directivity. Calibrations of the Dtags with housing showed only

a minor difference in sensitivity between 1–2 kHz and 6–7 kHz, but the frequency responses were not measured for different angles. Considering the size of the tag and positioning of the hydrophones, it is imaginable that the tag was acoustically directional, especially at MFAS frequencies. 3) Body shielding. The level of attenuation due to body shielding increases with frequency (section 2.3.1), thus MFAS pings are more likely to be affected than LFAS pings. Not only the horizontal plain but also the vertical plain should be considered, for example in the cases when the tag is on top of the animal and the source passes underneath. 4) Behavioural response. Animals may have received different levels if they consistently responded differently to LFAS than MFAS, especially if the animal altered their diving behaviour.

To further investigate the effect of signal frequency, the Bellhop propagation model was used to predict the TL of every ping received by a tagged whale. The geometrical spreading law was fitted per signal type to the measured and predicted TLs for comparison (Figure 11). The TL coefficients of the fits to the measured and predicted TL data for LFAS were 17.9 and 18.9, respectively. The TL coefficients of the fits to the measured and predicted TL data for MFAS were 20.1 and 18.1, respectively. Overall the Bellhop model thus predicted slightly higher TLs for LFAS signals than that were derived from the tag data. Conversely, the TLs during MFAS runs were predicted by Bellhop to be lower than the TLs derived from the tag data. The difference in TL between LFAS and MFAS was thus not explained by standard propagation effects.

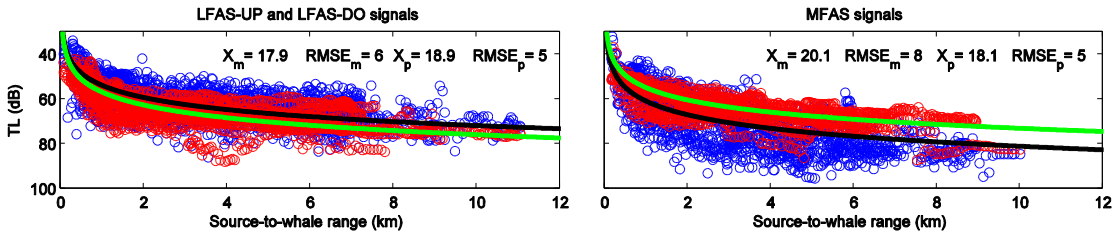


Figure 11: Measured and predicted TLs (blue and red markers, respectively) of the sonar signals as function of range per sonar frequency band. The geometrical spreading loss models that were fitted to the measured and predicted TL data are indicated with black and green lines, respectively.

Geometric spreading loss models were also fitted to the towed hydrophone array data, for sonar runs in which the tagged animal was not deep diving. For the LFAS-UP run during experiment oo09_144, in which the body of one tagged whale shielded many pings, the *X* value corresponded poorly between tag and towed array (absolute difference of 3.4) (Figure 10). For other LFAS runs the *X* values corresponded quite well when comparing between receivers (absolute differences between 0.4 and 1.4). Therefore, the effects of tag directivity and body shielding were likely limited in these LFAS recordings. For MFAS runs for which tag and array recordings were compared the absolute difference in *X* was quite small in one case (0.4), but larger in the two other cases (2.2 and 4.2). Whether these larger differences were due to measurement errors or differences in vertical position cannot be determined. It is, however, quite common that researchers estimate the received sound levels of whales using nearby hydrophone measurements (*e.g.*, Madsen and Møhl, 2000; Miller *et al*., 2000; Buckstaff, 2004). The data here suggest that this practise can work reasonably well, but the depth of the whales and hydrophones should always be considered, especially in areas where the water column is heavily stratified.

Much of the variation in received level unexplained by range is because of the changing depth of the whale (for example in Figure 8). The effect of whale depth in the first 100 m of the water column was investigated by calculating the excess attenuation (Brenowitz, 1982) from spherical spreading with absorption of each ping in the tag recordings and plotting them as function of depth. Figure 12 summarises the results of this analysis. For killer and pilot whales, by far most of the pings were received when the whale was at a depth of 0−10 m. The median EA in this top layer was always higher than at greater depths, indicating that the received levels of the sonar signals were lowest near the surface. The gradients in the sound speed profiles plotted in Figure 12 explain part of this depth-dependency in EA. The C-shaped profiles for killer and pilot whales indicate the presence of a sound channel that acts as a waveguide around the depth of the sound speed minimum. Therefore, received sonar levels were often higher when these species were diving at depths between 20 to 70 m than between 0

to 10 m. For sperm whale experiments the dependency on depth of EA was less pronounced and median EAs were more constant throughout the first 100 m of the water column because of the nearly iso-velocity environments where the sperm whale experiments were performed.

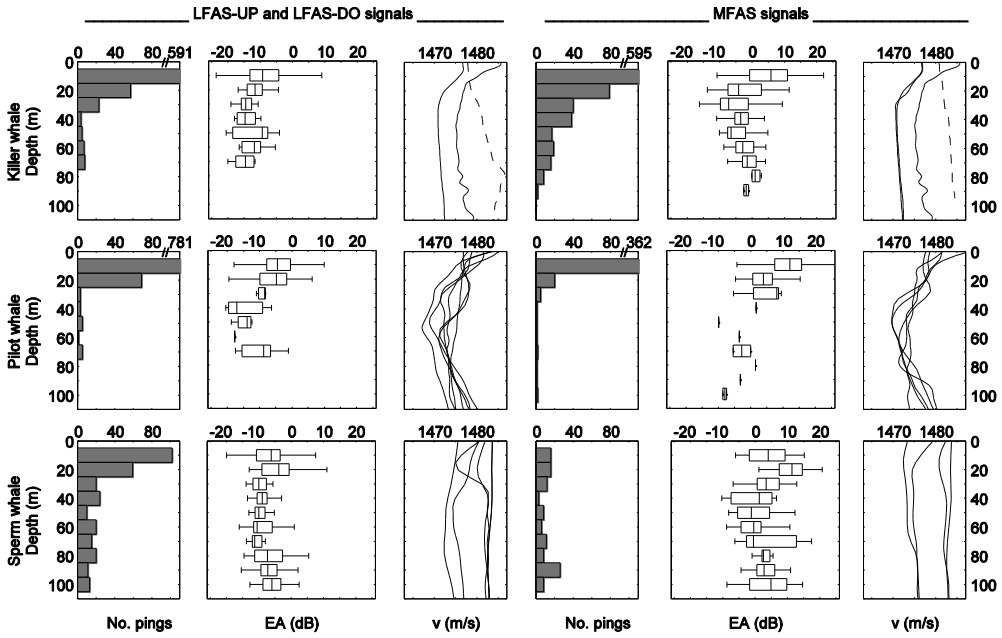


Figure 12: Histograms of the pings that were included in the EA analysis (grey bars), boxplots of the EA data and the SSPs that were collected at the location of the sonar runs (solid and dashed lines: summer and winter profiles, respectively). Data were analysed per species and sonar frequency.

### 2.3.3 Frequency weighting

Numeric thresholds of acoustic risk criteria for behavioural effects of marine mammals should be expressed in weighted levels so that they are applicable to sounds of various frequencies (Finneran and Schlundt, 2011). Weighted levels are normally calculated using auditory weighting functions which emphasize or de-emphasize the spectral components in sound according the perception of the listener. The most common auditory weighting functions for humans (A-, and C-weighting; Kinsler *et al.*, 1982) were derived from equal-loudness contours obtained from subjective loudness tests (Suzuki and Takeshima, 2004). These weighting functions currently exist only for one marine mammal species, the bottlenose dolphin, and were validated for this

species by the frequency-dependent difference in temporary threshold shift onset (Finneran and Schlundt, 2011). Due to the lack of loudness level data, two other weighting techniques are also available for marine mammals; 'M-weighting' (Southall *et al*., 2007) that is similar to C-weighting for humans, or the use of hearing threshold data for weighting sounds (*e.g.*, Verboom and Kastelein, 2005).

In this study, M-weighting was not applied because the response of the M-weighting filter for 'mid-frequency cetaceans', the hearing sensitivity group that includes killer, pilot and sperm whales, is effectively flat (<0.5 dB) in the frequency band of interest (1−40 kHz) (Southall *et al*., 2007). However, a weighting function based on a mean killer whale audiogram (section 2.2.6.3) was applied to the sound levels that were received by the killer whales in the experiments. Table 3 presents the range of weighted broadband $SPL_{max}$ and $SEL_{cum}$ levels, as well as the difference between the unweighted and weighted broadband $SEL_{cum}$ level at the end of the sonar run. The weighting function suggests that killer whales are about 30 dB more sensitive at 6−7 kHz than at 1−2 kHz for very faint sounds, with weighting levels of approximately 20 and 50 dB in the LFAS and MFAS bands, respectively (Figure 6). The actually-measured weightings for MFAS signals were 18−19 dB, indicating that only sound energy in the 6−7 kHz sonar band contributed to the weighted broadband level. In contrast, the measured weightings for LFAS signals ranged from 38 to 52 dB. The sound energy of the harmonic distortion [Figure 5(c)] did contribute significantly to the broadband weighted level for LFAS, particularly during the LFAS-UP and LFAS-DO runs in experiment oo09_144. Due to the rise in absorption loss with frequency, the number and level of harmonics received by the whale increased with decreasing distance to the source. This suggests that when the source-to-whale distance decreased, the LFAS sonar was more and more perceived as a broadband signal by the whale. The mean number of 1/3-octave bands that were analysed per sonar run (Table 3) also indicate an inverse relationship exists between the number of bands (presence of harmonics) and the weighted level, although this relationship was not completely

straightforward because only bands with a SNR > 10 dB were included and the noise level depended on the speed of the animals.

Table 3: The range of received broadband weighted $SPL_{max}$ and $SEL_{cum}$ levels during controlled exposures of killer whales to LFAS upsweep (LFAS-UP), LFAS downsweep (LFAS-DO) and MFAS upsweep (MFAS-UP) signals. Also shown is the difference between the unweighted and weighted $SEL_{cum}$ when the sonar transmission ended, and the mean number of 1/3-octave bands over which levels where integrated (averaged over all pings in the sonar run). Data for the second tagged animal is shown in parentheses.

| **Tag ID** | **Signal type** | **Weighted $SPL_{max}$ (dB re µPa)** | **Weighted $SEL_{cum}$ (dB re µPa$^2$s)** | **Unweighted – weighted $SEL_{cum}$** | **Mean no. of 1/3-octave bands** |
|---|---|---|---|---|---|
| oo06_317s | LFAS-UP | 41–105 | 36–110 | 52 | 5 |
| oo08_149a | LFAS-UP | 34–119 | 28–126 | 50 | 9 |
| oo09_144a | LFAS-UP | 38–130 | 35–135 | 46 | 9 |
| (oo09_144b) | | (29–125) | (24–130) | 43 | 6 |
| | LFAS-DO | 40–131 | 36–138 | 41 | 13 |
| | | (32–131) | (27–138) | 38 | 12 |
| oo06_327s | MFAS-UP | 51–136 | 48–141 | 18 | 2 |
| (oo06_327t) | | (47–134) | (45–141) | 18 | 2 |
| oo08_149a | MFAS-UP | 55–123 | 52–130 | 19 | 3 |
| | MFAS-UP | 92–137 | 90–144 | 18 | 3 |
| oo09_144a | MFAS-UP | 59–133 | 56–138 | 19 | 2 |
| (oo09_144b) | | (57–131) | (54–139) | 19 | 2 |

A weighting function based on the audiogram likely underestimates (overweighs) the influence of low frequencies on the perception of high-intensity sound, therefore the effect of the harmonic energy observed here may have been less that the weighted levels predicted. However, it is important to be aware of the fact that high-intensity low- and mid-frequency active sonar sources can produce significant harmonic energy at frequencies where marine mammal hearing is more sensitive. When the source was close to the receiver, the LFAS signal could contain harmonic energy all the way up to 100 kHz. The possibility that other signals are masked by such broadband signals is

much higher than if the sonar would only transmit in the 1−2 kHz band. The zones of impact for audibility, responsiveness and hearing injury (Richardson *et al*., 1995) may also increase when harmonics are taken into account.

# Chapter 3. Simulating exposure-avoidance strategies of killer and long-finned pilot whales using data from controlled sonar experiments

## Chapter summary

Avoidance of the sound source is a commonly documented response to noise, but most studies have evaluated responses to stationary sources. Behaviour of killer and pilot whales exposed to sonar during the 3S-08 and 3S-09 research trials in the Vestfjorden area of Norway suggested that cetaceans may use diverse avoidance strategies in response to an approaching sound source. To evaluate possible explanations for the types of movement responses observed, the potential of simple vertical and horizontal avoidance strategies to reduce the total sound exposure received by an animal from an approaching sound source was investigated using simulations. Vertical movements were either deep diving representative of foraging for the species or surface shallow diving. Horizontal movements were either stationary, straight-line relative to the heading of the source, or relative to the source position. Whale positions were simulated using a Monte Carlo method, and the cumulative sound exposure level ($SEL_{cum}$) received by the whales was estimated from transmission loss (TL) predicted using the beam-tracing model Bellhop. The sound source was modelled after a realistic naval source transmitting 1−2 kHz and 6−7 kHz signals with a maximum source level of 214 and 199 dB re 1 µPa m, respectively. Sound propagation conditions were based on environmental profiling conducted during experiments. The simulations showed that horizontally-stationary animals received the highest SELs. The optimal course in terms of sound exposure (resulting in the lowest $SEL_{cum}$) for animals moving in a straight line was 100° relative to the course of the source, while 120−130° was optimal for animals moving relative to the position of the source. Moving horizontally in the optimal direction yielded 9−17 dB reduction of $SEL_{cum}$ and vertical avoidance led to reductions of up to 10 dB. This simulation approach is useful to predict how whales might react to an approaching disturbance source, aiding study of behavioural reactions and spatial patterns of strandings relative to naval operations.

## 3.1 Introduction

Some of the most severe and well publicised impacts of high-intensity active sonar on marine wildlife over the last two decades are the mass strandings of cetaceans. These events with often lethal consequences have caused much debate in the scientific community (e.g., Evans and Miller, 2004), for example about which mass strandings were sonar-related, how to prevent them from happening in the future and what mechanisms caused the whales to strand (Cox *et al*., 2006).

Recently, a large dataset of historical beaked whale strandings and naval activity was compiled and statistically analysed (D'Amico *et al*., 2009; Filadelfo *et al*., 2009). Out of 127 reported mass stranding events two events were directly related to naval sonar use, 14 events coincided in place and time with major (multi-ship) naval exercises that may have used sonar, and another 24 events occurred in the vicinity of a naval base or ship but without evidence of the use of sonar. Although the majority of stranded animals were beaked whales, sonar has also been suggested to have caused strandings of minke whales, short-finned pilot whales, dwarf sperm whales, striped dolphins and a pantropic spotted dolphin (Balcomb and Claridge, 2001; Hohn *et al*., 2006; Yang *et al*., 2008). So far the exact mechanisms behind sonar-related mass strandings are unknown, but many hypotheses assume that the events are triggered by a behavioural response of the animals (e.g., Tyack *et al*., 2006).

Anthropogenic noise sources like active sonar can also cause non-lethal behavioural responses, ranging from mild to severe responses like long-term area avoidance (Southall *et al*., 2007). For instance, area avoidance by beaked whales over a period of two to three days was observed after a multi-ship sonar exercise at the Atlantic Undersea Test and Evaluation Center (AUTEC) in the Bahamas, by counting echolocation clicks received on a bottom-mounted hydrophone array (Moretti *et al*., 2010; Tyack *et al*., 2011). Long-term horizontal displacement of marine mammals can also be induced by other anthropogenic disturbance sources like pile driving (Tougaard *et al*., 2009), whale-watching boats (Bejder *et al*., 2006; Lusseau and Bejder, 2007) and

acoustic harassment devices (AHDs; Morton and Symonds, 2002). Interpreting the significance of these responses, however, requires detailed knowledge about the environment (*e.g.*, quality of the area to the animals) and the natural behaviour of the species. Depending on the biological context, both short-term and long-term displacement may or may not be of concern (Nowacek *et al*., 2007).

The importance of biological context can be exemplified using reports of change in the acoustic behaviour of marine mammals. Call rates of pilot whales increased up to two seconds after sonar signals were heard (Rendell and Gordon, 1999), but as these whales are often very vocal (Nemiroff, 2009) the biological significance of these responses is uncertain. Humpback whales increased their song lengths in response to sonar transmissions (Miller *et al*., 2000; Fristrup *et al*., 2003). As singing in humpback whales is thought to be a sexual display, this type of acoustic masking by sonar can potentially lead to more detrimental effects for long exposure durations. Clearer evidence for a significant behavioural change is found when deep-diving species stop transmitting echolocation clicks, which indicates the cessation of foraging (Johnson *et al*., 2004; Miller *et al*., 2004). Silencing in response to sonar was observed in sperm whales in their natural habitat (Watkins *et al*., 1985), and in Blainville's beaked whales during controlled playback experiments of simulated sonar and control sounds at the AUTEC range (Tyack *et al*., 2011). The latter study also showed that when a whale stopped clicking in response to a playback the animal abandoned its foraging dive and initiated an unusually long and slow ascent. The behavioural response of these beaked whales thus consisted of a change in acoustic behaviour related to foraging as well as horizontal and vertical avoidance.

Marine mammals sometimes respond vertically to anthropogenic noise. For example northern right whales in the Bay of Fundy exhibited a vertical response to signals designed to alert animals about the presence of ships (Nowacek *et al*., 2004). Five out of six whales stopped their foraging dive, ascended quickly to subsurface depths (1−10 m) and stayed there for an abnormally long time, thereby in fact

increasing the risk of vessel collision. During CEEs in the Gulf of Mexico the sperm whale that ended up closest to the firing airgun array was resting at the surface until short after the 2-hour exposure, while sperm whales further away from the source kept diving (Miller *et al*., 2009). Animals may also respond to noise by diving. Migrating bowhead whales in Alaska dived abruptly and decreased their surfacing times in response to helicopter activity (Patenaude *et al*., 2002). More subtle changes such as increased descent velocity were reported for juvenile northern elephant seals responding to the acoustic thermometry of the ocean climate (ATOC) signal (Costa *et al*., 2003).

Besides changes in vertical position, many species also respond to anthropogenic noise by moving horizontally. Migrating grey whales and bowhead whales in Alaska and humpback whales in Australia showed horizontal avoidance around industrial or seismic noise sources (Malme *et al*., 1983, 1984; Richardson *et al*., 1985, 1990; McCauley *et al*., 2000). Horizontal displacement around the source was also observed during studies with captive and free-ranging harbour porpoises and harbour seals that were responding to acoustic deterrence devices (ADDs; Culik *et al*., 2001), AHDs (Johnston *et al*., 2002; Olesiuk *et al*., 2002; Kastelein *et al*., 2006b) and underwater communication signals (Kastelein *et al*., 2005, 2006a). Studies on the effects of boat noise have found comparable changes in behaviour, including increases in speed and decreases of track linearity (*e.g.*, Nowacek *et al*., 2001; Williams *et al*., 2002; Constantine *et al*., 2004).

Avoidance responses can often be explained by one of two reasons; 1) the sound will trigger an anti-predator response, for example a deep diver like the elephant seal may dive to depths where predators cannot follow (even when this will bring the animal closer to the source; Costa *et al*., 2003), or 2) animals will move to a location where the received level is lower due to, for instance, increased distance from the source , positioning relative to the directivity of the sound source (Kastelein *et al*., 2005; 2006a; 2006b, 2008), the presence of a shadow zone, or the pressure-release

below the water surface (Jensen, 1981). Some marine mammals, pinnipeds especially, may also keep their head out of the water to reduce sound exposure (Kastak *et al*., 1999).

During the 3S-06, 3S-08 and 3S-09 research cruises in Norwegian waters, CEEs were conducted to quantify the dose−response relationships of responses of killer whales, long-finned pilot whales and sperm whales to active sonar signals (Kvadsheim *et al*., 2009). During these CEEs free-ranging whales were tagged with sound- and movement-recording sensors “Dtags” (Johnson and Tyack, 2003) and tracked using visual observations and towed array acoustics. Animals were carefully exposed to LFAS (1−2 kHz) or MFAS (6−7 kHz) signals in order to investigate the effect of signal frequency on the behavioural responses of the whales. Experiments started when the source was positioned 6−8 km away from the focal animal. The source vessel then steadily moved towards the subject, only adjusting course to approach the animal. At one kilometre distance, the vessel no longer turned, but passed the subject and then ceased transmission five minutes after CPA. To minimise the risk of inducing hearing injury in undetected nearby animals, the source level was gradually increased according to a ramp-up ‘soft start’ scheme. Transmission was stopped if animals entered the 100-m safety zone around the source. Results suggest that the animals used diverse avoidance strategies in response to the approaching sound source (Miller *et al*., 2011a).

A number of risk-assessment and mitigation tools for underwater noise include ramp-up schemes to allow animals time to move away from a sound source (Dolman *et al*., 2009). Such tools include mechanistic models of how animals might move in relation to the sound source, but there is little information on what strategies marine mammals might actually use to avoid a sound source (which may often be moving), and what consequences such strategies might have for the received level of the sound. Better knowledge on avoidance of marine mammals to sounds is necessary to

interpret the responses observed during CEEs and is essential for judging the success of using ramp-up schemes in risk mitigation protocols (Benders *et al.*, 2004).

The objectives of this part of the research were 1) to define simple horizontal and vertical avoidance strategies that whales might use in response to the sonar source, 2) to simulate how the animals' behaviour under such strategies would affect the total sound exposure, and 3) to determine which of the observed movement patterns of free-ranging whales might indicate that the whales used an avoidance strategy in response to the sonar.

This work aims at improving the understanding of cetacean avoidance responses to sonar, aiding study of behavioural reactions to noise and spatial patterns of stranding events relative to naval operations.

## 3.2 Materials and methods

### 3.2.1 Study species and sites

The model organisms used in the avoidance simulations were the killer whale and long-finned pilot whale. Simulations with the killer whale model were based on experiment oo09_144 conducted on a group of herring-feeding killer whales on 25 May 2009. Simulations with the pilot whale model were based on experiment gm09_156 conducted on a group of long-finned pilot whales on 6 June 2009. Both experiments were performed during the 3S-09 research trial in the Vestfjorden area of Norway (Kvadsheim *et al*., 2009). The experiment with killer whales was conducted off the coast of Lofoten Islands on the continental shelf plain (Thorsnes *et al*., 2009) and the pilot whale experiment was conducted in the middle of Ofotfjord (Figure 13). The characteristics of the environment (sound speed profile, water depth and bottom type), signal properties of the sonar (source level, frequency, duration and IPI), and several aspects of the source and whale movements during the simulations were based on the actual experiments.

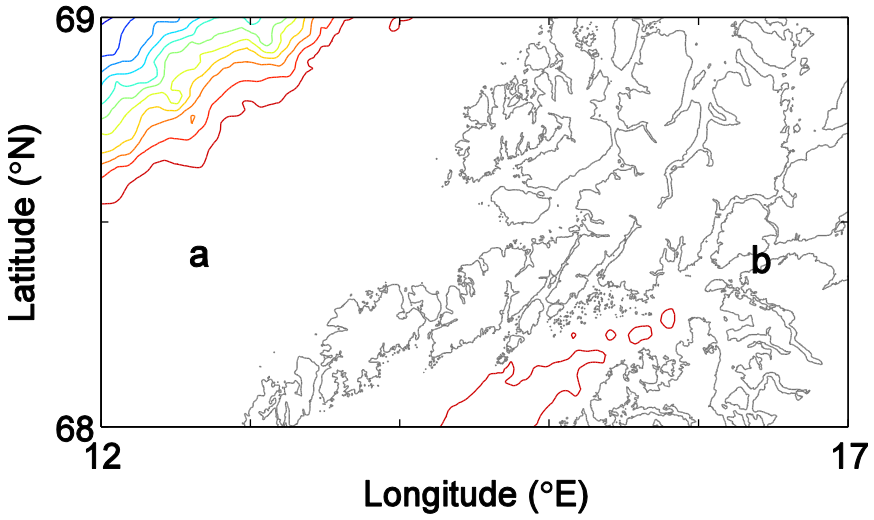


Figure 13: Map of the study area surrounding Lofoten Islands including the locations of the two sonar experiments that were selected for the simulations: the killer whale experiment (location a) and the long-finned pilot whale experiment (location b). The 250-m to 3-km depth contours (red to blue; 250-m interval) were plotted to show the continental shelf break. The depth data on the map was limited to the offshore and Vestfjorden areas (GEBCO; IOC *et al*., 2003).

### 3.2.2 Sound source and receivers

The simulated acoustic source was modelled after the real military experimental sonar (Socrates II, TNO) that was used during the 3S-09 trial in Norway. The real sonar source transmitted 1−2 kHz HFM upsweeps during the killer whale experiment and 6−7 kHz HFM upsweeps during the pilot whale experiment, but to reduce computational power these signal were simulated as 1.4 kHz and 6.5 kHz continuous wave signals. Other properties of the transmitted signals were the same in the simulations as during the actual experiments. The source level started at 152 and 156 dB re 1 µPa m and was gradually increased over a 10-min ramp-up period to 214 and 199 dB re 1 µPa m for LFAS and MFAS, respectively. The signal duration of the transmitted sonar pulses was always one second. The IPI was 20 s during both ramp-up and full-power transmission.

Before an experiment began, at least one whale was tagged with a movement- and sound-recording suction-cup tag (Dtag, version two; Johnson and Tyack, 2003). The tag contained a VHF transmitter for tracking the whale and finding the tag after release. The tag recorded sounds in stereo at a sampling rate of 96 or 192 kHz using a 16-bit resolution sigma-delta ADC. The tag also recorded depth, temperature, three-dimensional acceleration, and three-dimensional magnetometer data that were synchronised with the audio recording. All sensor data were stored in flash memory, meaning the tag had to be retrieved in order to obtain the data.

More information on the sound source and the acoustic sensors can be found in sections 2.2.3 and 2.2.4, respectively.

### 3.2.3 Avoidance scenarios

Four exposure-avoidance scenarios were evaluated: 1) simulated shallow diving vs. deep diving for both species with the same horizontal track of the source and whale as during the real experiments, 2) simulated shallow diving vs. deep diving for both species with a simulation of the whale being horizontally stationary, 3) the simulated

whale moving in a straight line relative to the course of the source, and 4) the simulated whale adjusting its course continuously relative to the position of the source (Figure 14).

Avoidance scenarios 1 and 2 were used to investigate the effect of vertical responses on the total sound exposure to the whale, and scenarios 2, 3 and 4 were used to investigate the effect of horizontal responses on the total sound exposure to the whale. In scenarios 2, 3 and 4 the course of the source was fixed to straight towards the location of the whale at the start of the simulated behaviour change so that the sound exposure could be compared between horizontal strategies (Figure 14). For scenarios 3 and 4 only one type of diving was modelled per species (shallow diving for the killer whale; deep diving for the pilot whale) as these scenarios focused purely upon horizontal avoidance.

For scenario 1 the horizontal positions of the source and whale were kept the same, therefore short summaries of the two experiments are given below. More extensive summaries of the experiments can be found in Miller *et al*. (2011a).

Killer whale experiment

After a period of deep diving, the killer whales started high-speed travelling southwards at the point of behavioural change and changed their direction of movement gradually to westwards throughout the experiment. The source vessel with transmitting sonar approached the group from the west and turned towards the last sighting of the group a number of times. Both tagged whales were shallow diving throughout the exposure and made one deep dive to ~60-m depth when the group passed in front of the source vessel. The average depth and speed of the source was 44 m and 8 kts, respectively. The source-to-whale distance ranged from 8 km at the start of transmission to 520 m at the CPA (Figure 15; section 2.2.5 explains how these ranges were derived).

Pilot whale experiment

The group of pilot whales was approached from the northeast by the source vessel. After being at or near the surface for 1.5 h the tagged animal started deep diving at the time of the behavioural change, early on in the experiment. The animal completed two deep dives while the source was transmitting. The source vessel only made small course changes as the animal was resighted after the first deep dive nearby its previous location. The average source depth and speed was 43 m and 8 kts, respectively. The source-to-whale distance ranged from 6 km at the start of transmission to 280 m at CPA (Figure 15).

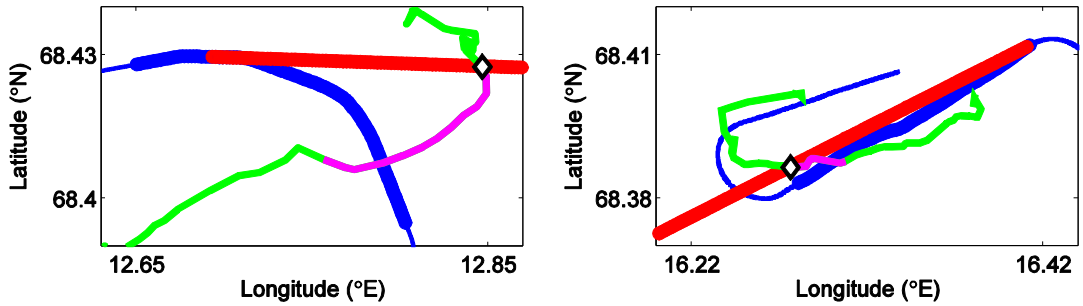


Figure 14: Maps of the sonar experiments with the (left) killer whale and (right) pilot whale model that formed the basis of the avoidance strategy analyses. The thin blue line shows the track of the source vessel (killer whale: approaching from W; pilot whale; approaching from NE) and the thick blue line indicates where the source was transmitting originally. The track of the focal whale is shown in green (pre and post exposure) and purple (during exposure), and the diamond indicates the location of the whale at the behavioural change point. The thick red line represents the simulated track of the source that was altered to compare the sound exposure under the different horizontal avoidance strategies.

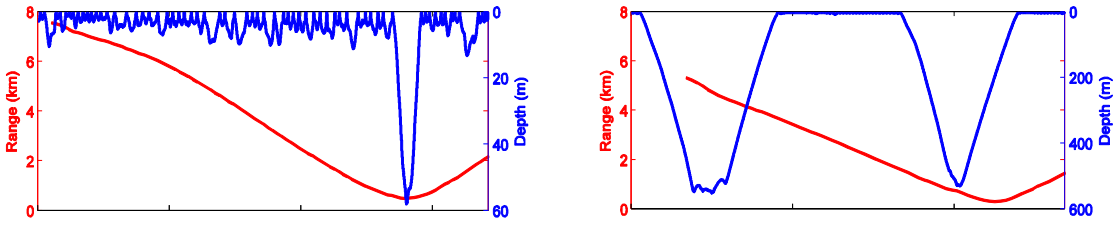


Figure 15: The source-to-whale range in red and the depth of the tagged whale in blue during the real (left) LFAS upsweep exposure to killer whales and (right) MFAS upsweep exposure to pilot whales. Note the order-of-magnitude difference between the depth scales.

### 3.2.4 Sound level predictions

The sonar pulses recorded on the Dtags were processed using a custom-written MATLAB (The Mathworks, 2007) program (CEE_Analyser; see Appendix I for the user's guide). Waveform and spectrogram views of the signals guided every step of the analysis, and a strict protocol was followed to address challenges imposed by interfering noises. For both the killer whale and pilot whale experiment the SPL and $SEL_{cum}$ levels received by the whale were calculated from the audio recordings made with the Dtags. Section 2.2.6 describes in more detail the method that was used for extracting, processing and quantifying the sonar signals.

TL as function of depth and range from the source was predicted using the beam-tracing model Bellhop in Gaussian beam mode (Porter and Bucker, 1987). Bellhop and its module for calculating bottom reflection coefficients were run using the MATLAB user interface AcTUP[4]. As the effective duration of a sonar signal was about one second the received SEL of a ping equalled the received SPL, and thus equalled SL−TL. Hence, the single-ping SELs for any simulated whale trajectory were obtained from the TL(range, depth)-function (Figure 16 and Figure 17) and the energy was power-summed to obtain the corresponding $SEL_{cum}$ level. To validate the TL model, the broadband $SEL_{cum}$ levels of the sonar measured with the calibrated Dtag sensor were compared to the $SEL_{cum}$ levels predicted by Bellhop using the dive profile of the tagged whale. The difference between the two methods was expressed in the absolute difference in $SEL_{cum}$ at the end of the exposure and in RMSE between the two types of $SEL_{cum}$ levels.

[4] V2.2L. Downloaded on 23-11-2009 from http://cmst.curtin.edu.au/products/actoolbox.cfm.

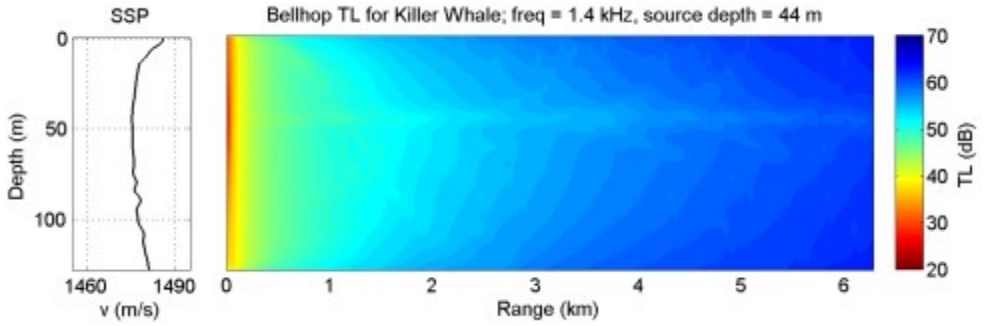


Figure 16: (left) Sound speed profile measured straight after the killer whale sonar experiment and (right) predicted TL as function of range and depth used for the simulations.

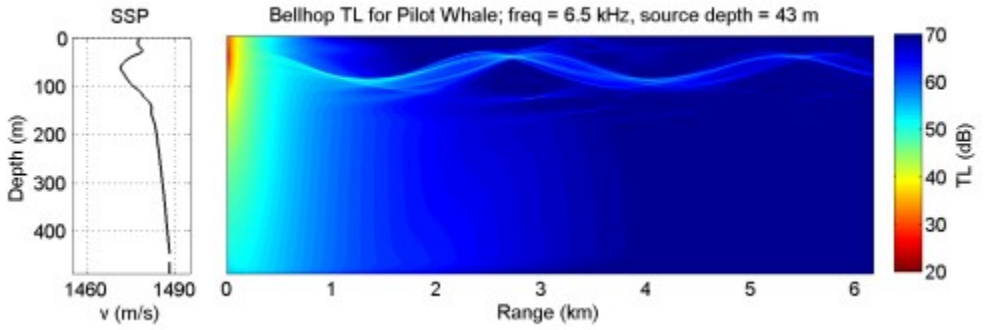


Figure 17: (left) Sound speed profile measured straight after the pilot whale sonar experiment and (right) predicted TL as function of range and depth used for the simulations.

The environmental parameters used for TL modelling were based on data collected during the actual experiments. CTD-profiles were taken from the source vessel using a SAIV SD-200 CTD-profiler in the transmission path between the sonar and the tagged animal (Kvadsheim *et al*., 2009). The profiles were collected straight after the entire experiment had ended, at or near the location of CPA. One SSP was collected per experiment, thus it is assumed this profile was representative for the entire four-dimentional oceanographic field of the site. SSPs were smoothed to remove insignificant features and subsampled to increase the run-time of Bellhop (Porter, 2011).

Bathymetry data for the killer whale experiment were obtained from the GEBCO One Minute Grid (IOC *et al*., 2003) and for the pilot whale experiment from the

Norwegian Hydrographic Service's MPD. After inspection of the data it was found that both experimental areas had a relatively flat bottom (killer whale: 130-m depth; pilot whale: 500-m depth). The bottom layer was modelled as a flat, homogeneous fluid layer with constant acoustic properties. The geo-acoustic parameters (compressional sound speed, bulk density of the sediment and compressional wave attenuation) needed for calculating bottom reflection coefficients were estimated using their numerical relationships with bulk mean grain size described by Hamilton (1972), Hamilton and Bachman (1982) and Richardson and Briggs (2004). More information on the acoustic propagation model and the derivation of the environmental parameters can be found in section 2.2.7.

### 3.2.5 Iterative process to develop simulations

For each species two composite dive profiles were created; one representative of deep diving and one representative of shallow diving (Figure 18). For both species the deep dives were in reality likely foraging dives. Killer whales were in reality mostly travelling when shallow diving and pilot whales were also resting or socialising when shallow diving. A few of the deepest pilot whale dives were shortened so that TLs could be estimated for every depth in the dive profile. The horizontal swim speeds related to the composite dive profiles were obtained from the dead-reckoning tracks of the Dtags.

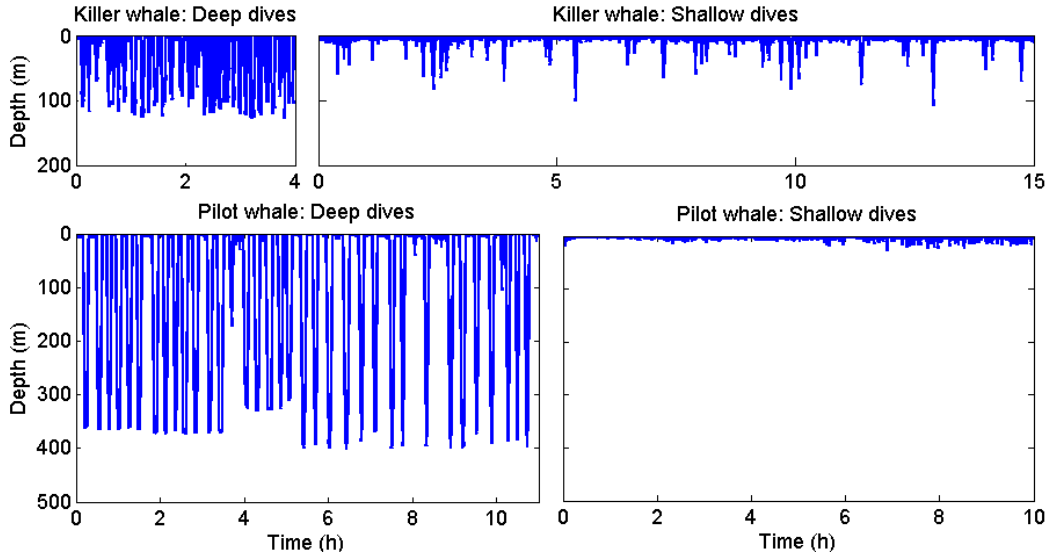


Figure 18: (upper panels) The composite dive profiles of the killer whale model for when the animal is (left) deep diving or (right) shallow diving. (lower panels) The composite dive profiles of the pilot whale model for (left) deep diving and (right) shallow diving.

When a transmitting source moves straight towards a whale the received level depends strongly on the horizontal and vertical range to the source at the time of the closest sonar transmission. For example, if the IPI is 20 s and the sound source moves at 8 kts, the closest ping can be theoretically transmitted at the whale position, or as much as 80 m away from the animal, which corresponds to a maximum difference in SPL of 38 dB under spherical spreading conditions. Here, this arbitrary timing effect was accounted for by applying an iterative Monte Carlo method on the whale positions.

A new $SEL_{cum}$ datapoint per vertical-horizontal movement combination was calculated with every iteration, and in the process a distribution of $SEL_{cum}$ levels was built that was characterised using median and inter-quartile range (IQR). More specifically, the start of a new segment in the composite dive profile was randomly selected to obtain a new set of whale depths with every iteration. In avoidance scenario 1 and 2 the locations of the source and whale, and thus the range between them, were known *a priori*. This made it easy to extract the TLs corresponding to the new depths and ranges, and to calculate the $SEL_{cum}$ for that iteration. Hence, 1,000,000 iterations were to used construct the $SEL_{cum}$ distributions for avoidance scenario 1 and 2.

During scenario 3 and 4 the source-to-whale ranges varied not only per ping but also per iteration, which made these scenarios much more computationally intensive. Here it was necessary to calculate a new source-to-whale range for every ping because the horizontal speed of the animal varied simultaneously with the dive profile. Also, 19 directions of movement (0–180°, 10° steps) were calculated to find the optimal direction of movement in terms of sound exposure (resulting in the lowest $SEL_{cum}$). Because the source vessel had a fixed course towards the animal in these avoidance scenarios, only angles from 0° to 180° were investigated. The $SEL_{cum}$ distributions for scenario 3 and 4 were constructed using 1,000 iterations per direction of movement.

## 3.3 Results

### 3.3.1 Received levels and model validation

The maximum received broadband SPL (RMS averaging time: 200 ms) throughout the killer whale LFAS experiment ranged from 91 to 174 dB re 1 µPa. The maximum received broadband SPL (RMS averaging time: 200 ms) throughout the pilot whale MFAS experiment ranged from 82 to 156 dB re 1 µPa. The cumulative broadband SEL throughout the killer whale LFAS experiment ranged from 89 to 181 dB re 1 $\mu Pa^2$ s. The cumulative broadband SEL throughout the MFAS experiment with pilot whales ranged from 82 to 162 dB re 1 $\mu Pa^2$ s (Figure 19).

Modelling the $SEL_{cum}$ levels yielded similar results as the measured levels. The maximum difference between the $SEL_{cum}$ predicted by Bellhop and $SEL_{cum}$ measured with the Dtag at any time during the experiment was 4 dB (RMSE: 3 dB) and 3 dB (RMSE: 2 dB) for killer whale and pilot whale experiments, respectively. At the end of the experiment the absolute difference in level (calculated as measured minus predicted) was +3 dB for the killer whale and 0 dB for the pilot whale.

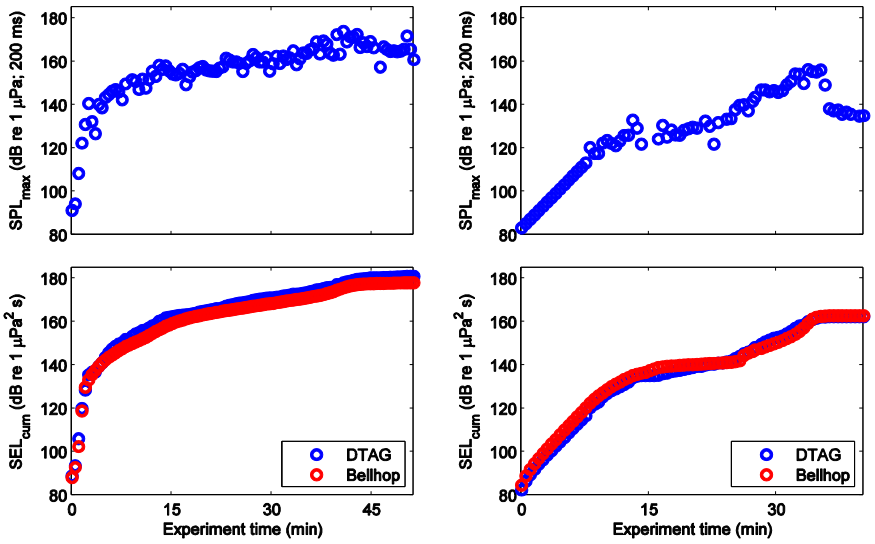


Figure 19: (upper panels) Broadband $SPL_{max}$ (RMS averaging time: 200 ms) measured using the Dtag for every sonar transmission received by the (left) killer whale and (right) long-finned pilot whale. (lower panels) Broadband $SEL_{cum}$ measured using the Dtag and broadband $SEL_{cum}$ predicted by Bellhop for every sonar transmission received by the two species.

### 3.3.2 Vertical avoidance

In the first avoidance scenario (Scenario 1) only the dive pattern of the whale model was changed and the horizontal track of the source and whale were the same as during the real experiments. For the shallow-diving killer whale model the median $SEL_{cum}$ was 178 dB re 1 $\mu Pa^2$ s, which is the same level Bellhop predicted was received by the killer whale in the real LFAS experiment (Figure 20). The median $SEL_{cum}$ for the deep-diving killer whale model was 1 dB higher. The IQR for both shallow and deep diving was small; 0.5 and 0.2 dB, respectively.

For the shallow-diving pilot whale the median $SEL_{cum}$ was 166 dB re 1 $\mu Pa^2$ s (IQR = 0.8 dB), while for deep diving the median $SEL_{cum}$ was 165 dB re 1 $\mu Pa^2$ s (IQR = 4.5 dB) (Figure 20). The small difference between the median values can be explained by the fact that the pilot whale model still spent a significant amount of time in the upper layer of the water column while in deep diving mode. The histogram revealed that the $SEL_{cum}$ levels for deep diving are in fact bimodally distributed, with a second lower maximum at around 160 dB re 1 $\mu Pa^2$ s. This second maximum reflects the relatively high probability that the animal was at the bottom of a deep dive (300−400 m) while the source passed overhead. The animal thus received 6 dB less sound exposure when deep under water compared to when it stayed closer to the surface.

The $SEL_{cum}$ to the pilot whale during the real MFAS experiment predicted using Bellhop was an intermediate 163 dB re 1 $\mu Pa^2$ s. This level is consistent with the above results as the animal was deep diving throughout most of the experiment, but was ascending when the source was nearest (Figure 15).

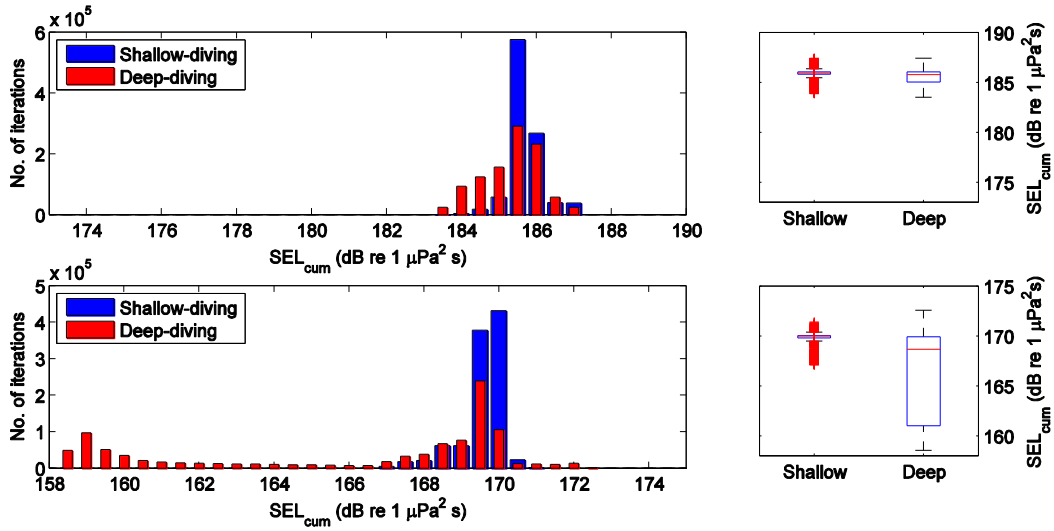


Figure 20: Histogram and boxplot representations of the $SEL_{cum}$ distributions for vertical avoidance by the killer whale (upper panels) and pilot whale (lower panels). Vertical movements were either shallow diving or deep diving for both species. The dotted horizontal line in the boxplot indicates the level that was received by the tagged whale in the actual sonar experiment.

To investigate the effect of horizontal avoidance strategies the source track was altered so that the course of the source was fixed straight towards the location where the avoidance response began. The second avoidance scenario (Scenario 2) consisted of the whale model shallow diving or deep diving while stationary at the avoidance response location, and can be considered part of both the horizontal and vertical avoidance analyses.

For the stationary killer whale model the median $SEL_{cum}$ was 186 dB re 1 $\mu Pa^2$ s for both shallow diving and deep diving. The IQR for both dive modes was small; 0.2 and 1.1 dB, respectively (Figure 21).

For the pilot whale the stationary response resulted in a median $SEL_{cum}$ of 170 dB re 1 $\mu Pa^2$ s (IQR: 0.2 dB) for shallow diving, and a median $SEL_{cum}$ of 169 dB re 1 $\mu Pa^2$ s (IQR: 8.9 dB) for deep diving (Figure 21). Like in the vertical avoidance analysis of scenario 1 the distribution of $SEL_{cum}$ levels for the deep-diving pilot whale was bimodal in shape, now with the second maximum at 159 dB re 1 $\mu Pa^2$ s. Thus, when the source

passed directly overhead, the sound exposure of a whale deep under water was approximately 10 dB less than the sound exposure of more shallow animals.

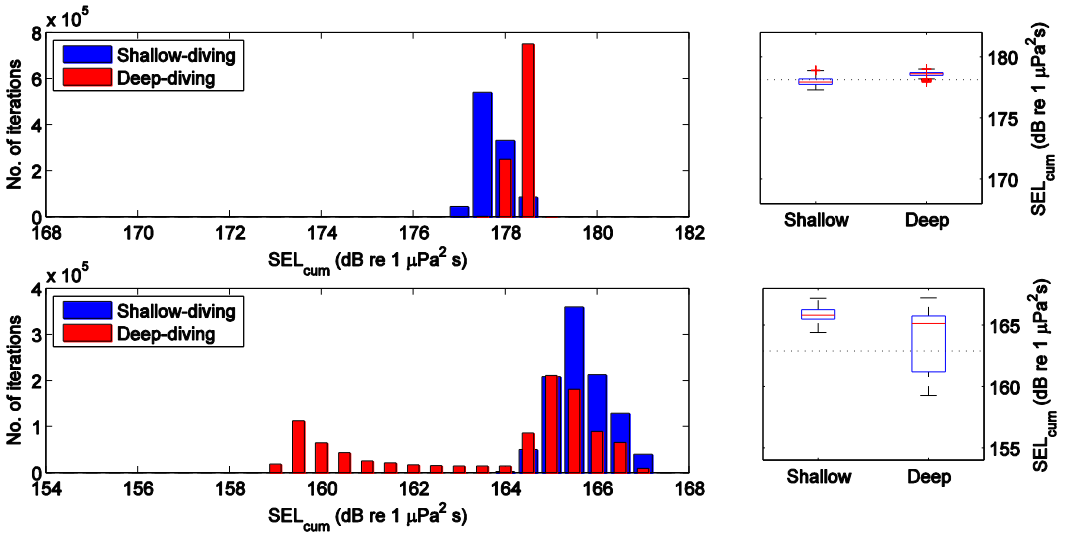


Figure 21: Histogram and boxplot representations of the $SEL_{cum}$ distributions for the stationary killer whale (upper panels) or pilot whale (lower panels) scenarios. There was no horizontal movement of the whale, and vertical movements were either shallow diving or deep diving for both species.

### 3.3.3 Horizontal avoidance

For avoidance scenarios 3 and 4 only shallow diving was simulated for the killer whale, and only deep diving for the pilot whale.

For the killer whale responding to the sound source by moving horizontally in a straight line, the direction of movement in terms of sound exposure resulting in the lowest $SEL_{cum}$ was nearly perpendicular to the course of the source. The optimal course was 100° relative to the heading of the source, and the corresponding median $SEL_{cum}$ was 177 dB re 1 $\mu Pa^2$ s (IQR: 0.8 dB). The 1-dB and 3-dB fans, defined as the range of directions where the median $SEL_{cum}$ deviated by less than 1 and 3 dB from the level of optimal course, were 50°–140° and 20°–160°, respectively (Figure 22).

The result for the pilot whale moving horizontally in a straight line was similar as for the killer whale despite the pilot whale's different dive mode and lower horizontal speed. The direction of movement optimal for avoiding sound exposure was also 100°

for the pilot whale, the 1-dB fan was 60°–130°, and the 3-dB fan was 40°–150°. The median $SEL_{cum}$ for the optimal course was 152 dB re 1 $\mu Pa^2$ s (IQR: 2.3 dB) (Figure 22).

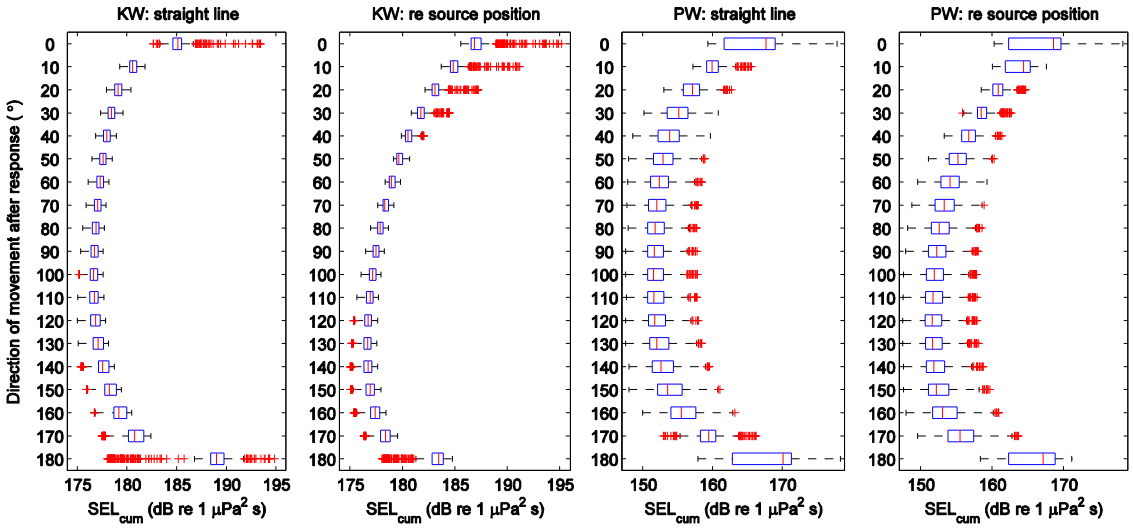


Figure 22: Boxplot representations of the $SEL_{cum}$ distributions for 4 different horizontal avoidance scenarios (from left to right): the killer whale moving in a straight line throughout the approach, the killer whale moving on a course relative to the source position, the pilot whale moving in a straight line throughout the approach, and the pilot whale moving on a course relative to the source position. Vertical movements were shallow diving for the killer whale and deep diving for the pilot whale.

The fourth and last avoidance strategy that was investigated was movement relative to the source position, as opposed to source heading in the previous strategy simulation. Under the strategy of movement relative to the position of the source, the animal adjusted its course continuously during the time the source was transmitting.

The optimal direction of movement of the killer whale model for this strategy was 130° relative to the direction of the source; slightly more away from the approaching source than for straight-line avoidance based upon direction of movement of the source (Figure 23). The 1-dB and 3-dB fans measured 90°–160° and 40°–170°, respectively. The median $SEL_{cum}$ of the optimal direction of movement was the same as for straight-line avoidance, namely 177 dB re 1 $\mu Pa^2$ s (IQR: 0.7 dB). For the pilot whale moving relative to the position of the source the median $SEL_{cum}$ was also the same as

for straight-line avoidance; 152 dB re 1 µPa$^2$ s (IQR: 2.4 dB). The optimal course for the whale to avoid exposure was 120°, and the 1-dB and 3-dB fans were 80°−150° and 60°−160°, respectively.

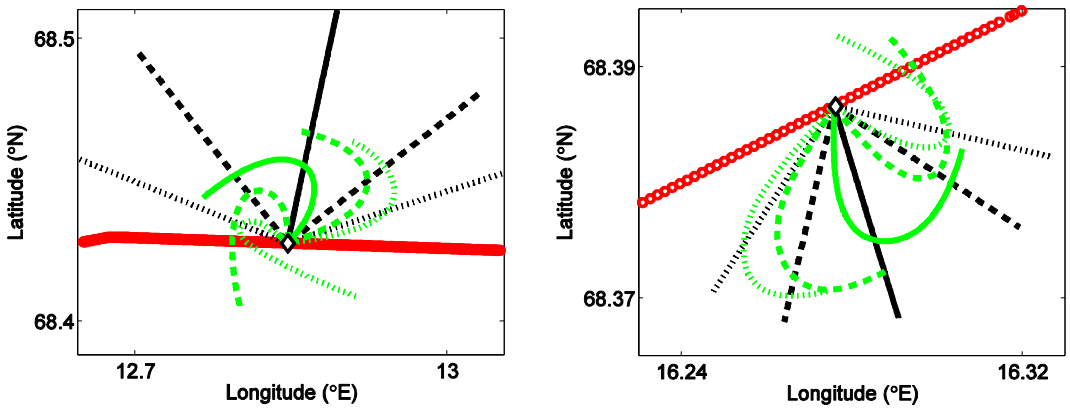


Figure 23: Horizontal avoidance of the killer whale (left) and pilot whale (right) visualised. The location of the whale at the start of the response (and thus the location of the stationary animal) is indicated by the white diamond. The transmission path of the source which approached the killer whale from W and the pilot whale from NE is shown in red. The optimal direction of movement in terms of sound exposure, the 1-dB fan and the 3-dB fan are shown with the solid, dashed and dotted lines (black: straight-line avoidance; green: avoidance relative to source position). Note the pilot whale map is zoomed in further as the horizontal speed of this deep diving animal was lower than of the shallow-diving killer whale.

## 3.4 Discussion

### 3.4.1 Evaluation of the data

The results of the vertical avoidance analyses indicate that the dive mode of the whale was relatively unimportant for the killer whale in the actual acoustic environment. The sonar pings that were received at close range from the source determined for the most part the total sound exposure. Transmission loss did not vary with depth much because there were no rapid changes in sound speed, because the area had a reflective bottom, and because the source was towed halfway of the water column. Therefore the killer whale model could not reduce sound exposure significantly by swimming deeper within the normal bounds of its recorded dive depths.

The sound exposure to the deep-diving pilot whale model was usually not lower than to the shallow-diving animal, however close inspection of the histograms showed that being at the bottom of a deep dive (300−400 m) when the source passed at its closest point yielded a reduction of 6−10 dB (depending on horizontal range at CPA). If the animal is able to estimate the distance to and speed of the source, the animal may use its normal deep-diving behaviour to reduce sound exposure. The effectiveness of vertical exposure-avoidance thus depends on the diving capability of the species. Here, species-typical behaviour was used to simulate the movements of the whales, but one might predict that animals would extend their diving limits, possibly by diving deeper and longer than normally, in order to avoid high received levels.

By moving away horizontally, either with a fixed course or relative to the source position, the killer whale model optimally achieved a reduction in $SEL_{cum}$ of 9 dB compared to when it stayed at the same location. Similarly, the pilot whale model achieved an average reduction in $SEL_{cum}$ of 17 dB. The range to the nearest transmission was not equal for the two species (killer whale: 31 m; pilot whale: 21 m) as the source transmitted a ping every 20 seconds, which influenced the level in the stationary-animal analysis. This difference in range accounts for 3 dB =

[$20*\log_{10}(31/21)$] of the difference in sound reduction. The rest of the difference is possibly explained by the differences in dive mode and propagation conditions.

To avoid high sound exposure from the approaching sound source it was always best for the whale to move away from the expected track of the source. The most optimal direction of movement was between 100° and 130° (depending on the species and strategy) but is influenced by the speed of the animal relative to the speed of the source. Surprisingly, the range of directions of movement where the animals achieved nearly-optimal results was quite wide. The 1-dB fans around the optimal angle were between 70° and 90° wide, and the 3-dB fans around the optimal angle were between 100° and 140° wide (Figure 23). Thus, as long as animals move roughly away from the predicted trajectory of the source this tactic can achieve substantial reductions of sound exposure.

### 3.4.2 Comparison with responses in the field

Some species respond to threats by trying to outrun them (*e.g.*, minke whales; Ford *et al*., 2005). If the threat is faster than the whale, however, moving sideways to the incoming disturbance would be a good solution for the animal. During the CEE with killer whales exposed to LFAS upsweeps in 2009 on which the simulations were based here, the animals responded to the sonar by speeding up and moving perpendicular to the heading of the source vessel. Perpendicular movement relative to the heading of a source was also observed in short-finned pilot whales during exposure to airguns during seismic exploration (Weir, 2008) and during CEEs with killer whales during in 2006 and long-finned pilot whales in 2008 (Miller *et al*., 2011a).

Movement relative to the source heading suggests that whales are not only able to estimate the angle from which the sound is coming, but also to track the precise location and course of the source. During two killer whale CEEs conducted in Norway horizontal avoidance started straight after one or more animals made a deep dive into

the sound channel (Miller *et al*., 2011a). Possibly these dives are orientation dives by the whales to monitor the source and its movement more precisely. This would imply that the animals are aware of the propagation conditions under water and that they respond vertically not only to reduce sound exposure immediately but also in anticipation on future events.

The water surface, bottom and coastline can limit the physical space in which the whales can respond. The water surface however also provides the animal an opportunity for a special type of vertical avoidance; to come out of the water when the sound is otherwise received. For example, seals increase their time at the surface and hauled out in response to exposure to underwater fatiguing noise (Kastak *et al*., 1999; R.A. Kastelein, pers. comm.) and long-finned pilot whales were observed to synchronise their surfacings with sonar transmissions (Miller *et al*., 2011a). This special type of avoidance was not accounted for in the simulations, but can be incorporated in similar future research.

The directivity of the source can have a significant impact on the sound field, as was seen during CEEs of sperm whales to airguns (Madsen *et al*., 2006). Sonars are also often directional in the vertical plain (Hildebrand, 2009), which make vertical exposure-avoidance strategies in response to such source more effective, especially at close range. On the receiver side directivity may also play a role, as the hearing of cetaceans is directional, especially at higher frequencies (Au and Moore, 1984). It is recommended for future studies in which responses of cetaceans to sonar are simulated that the hearing sensitivity and receiving beam patterns of the whales are taken into account, particularly when the source transmits high-frequency sounds.

The simulation approach is potentially useful to predict how whales might react to an approaching sound source, and may also be useful to understand the patterns of cetacean strandings relative to the movement of sonar-transmitting military vessels. One well-documented mass-stranding event related to sonar use is the stranding of

predominantly Cuvier's and Blainville's beaked whales in the Bahamas on 15−16 March 2000 (Evans and England, 2001). During that event, multiple US Navy ships including five ships using tactical MFAS transited through the Northeast and Northwest Providence Channels. The four ships transmitting sonar for which the movement tracks were reported moved through the Province Channels in two loosely affiliated groups approximately 4−6 hours apart, in generally the same pattern as the beached whales were discovered. Strandings occurred along the northeast side of the channels which is known for its steep-sloping bathymetry, a property also seen during other sonar-related strandings (Cox *et al*., 2006; D'Spain *et al*., 2006). Although the initial location of the whales is unknown, the spatial pattern of the strandings suggests that the whales had responded by moving more or less perpendicularly to the track of the vessels.

# Chapter 4. Conclusions and recommendations

## 4.1 Study goals

In the risk-assessment framework, the characterisation of risk is accomplished by combining exposure assessment and dose−response relationships (EPA, 1992; Boyd *et al.*, 2008). In the previous chapters of this thesis, a number of factors that influence exposure assessment have been evaluated, including analysis of how sound levels received by cetaceans are affected by *in-situ* sound propagation and the influence of diving, horizontal movement and possible avoidance behaviour of the whales themselves.

Chapter two described a systematic analysis approach for processing acoustic recordings of sonar signals made at or near the location of the whales during controlled exposure experiments, and investigated the influences of source range, depth and propagation conditions on the sound field surrounding the animals. The chapter indicated that in Norwegian high-latitude waters TLs generally follow geometric spreading predictions, but that these levels can vary substantially, especially with receiver depth, in shallow coastal waters where the acoustic environment is more variable in time and space.

In chapter three, effects of simple exposure-avoidance strategies on the total sound exposure level received by simulated whales were predicted for four movement scenarios based on data from real controlled exposure experiments. This chapter showed that whales moving under simple horizontal and vertical avoidance strategies can substantially reduce received sound levels from an approaching source, but that the degree of reduction depends on factors such as the horizontal and diving behaviour of the whale relative to the location of the source, physical limitations of the location, and acoustic propagation conditions.

## 4.2 Implications for exposure assessment in the risk-assessment framework

The outcomes of this thesis research have several important implications for the procedure of assessing acoustic exposure to marine mammals. Most importantly, realistic prediction of the sound levels to which animals will be exposed needs to take into account both the local sound propagation conditions and the movement behaviour of the animals within the sound field. While a simple spherical spreading model seemed to approximate the data in deep-water experiments, this is likely to only be the case under certain specific sound propagation conditions. The fjord and continental shelf waters had more complex bathymetries, and site-specific acoustic conditions with quicker changes in sound speed with depth (Appendix IV). For these environments in particular, measurements should be used to validate the propagation models and their input data (sound speed profiles, geo-acoustic parameters, and bathymetries) that are used in exposure assessments. Such measurements could be taken during real sonar exercises, for example as part of observational studies that monitor also the surface behaviour of marine mammals.

The diving behaviour of the whales was a large contributor to the observed variation in received sound levels. In depth-dependent conditions sound propagation models like Bellhop should outperform simple geometrical spreading models, although the quality of the environmental data will determine to a large extend the accuracy of the predictions. Beside depth, the source-to-whale range during the sonar experiments had a substantial effect on the received levels. Therefore, when mechanistic 3D movement models of whales are used in quantitative risk assessments the total exposure to the whales (and thus also the estimated risk) will depend strongly on the modelled behaviour in relation to the movements of the sound source. The optimal horizontal exposure-avoidance strategy of whales predicted in chapter three, movement perpendicular to the anticipated track of the source, has been observed in the field for pilot and killer whales (section 3.4.2), and thus may provide a more realistic type of movement model for these species. However, some caution is needed

when applying such a concept within the exposure assessment framework. First, while there is evidence that cetaceans can change their movement in response to intense sources, it is not well understood if these changes are necessarily designed to reduce sound exposure, or to simply decrease the proximity to a potential threat. Second, the scenarios modelled in this study were fairly simple, using only a signal sonar source. Real-world sonar exercises may have much more complicated geometries with multiple distributed sources. In such case, avoidance strategies may not be able to effectively reduce sound exposure, but observation studies during real multi-ship exercises should be conducted to answer this question.

## 4.3 Suggestions for future work

As detailed above, the results of this thesis may have implications for environmental risk assessment and management of anthropogenic noise impacts on marine mammals. Results may also help future behavioural response studies (BRSs) with the interpretation of observed avoidance responses of cetaceans and acoustic analysis of sound signals recorded on the animals themselves. Although suggestions for future work can be found throughout this document, some of the primary recommendations are summarised and given below.

### 4.3.1 Acoustic measurements and analysis

Body shielding, the blocking of sound waves when the animal's body is interposed between the acoustic-recording tag and the sound source, led to attenuation of about 15 dB in measured SPLs when the tag was located on the opposite side of the LFAS source (section 2.3.1). Caution is thus advised when sound levels are measured with animal-borne tags, especially with regards to high-frequency sounds (the degree of shielding is determined in part by wavelength; Madsen *et al*., 2006a). Placing the tags on different sides of the animal provides one possible solution. Also, advanced numerical techniques such as Finite Element modelling can provide estimates of the expected attenuation levels that could give insight into the variability in sound levels caused by body shielding.

Given the scarcity of CEEs with free-ranging marine mammals and the financial cost that is involved in conducting these experiments, it is recommended that the acoustic recordings are analysed in a systematic manner to retrieve as much information from the data as possible. The MATLAB tool "CEE_Analyser"(Appendix I) was developed for this purpose as part of the present study, and can also be used in future BRSs in which exposure stimuli consist of intermitted tonal sounds, similar as the signals here. To further improve between-studies comparisons of results, exposure signals should be quantified by the same acoustic measures. For example, it could be falsely concluded that one species is more sensitive to noise impacts than another

when studies use different RMS averaging window lengths during the calculation of SPL. Like in a BRS project with beaked whales (Tyack *et al*., 2011), a 200-ms averaging was used here because this duration is generally considered to be relevant in terms of hearing sensation for marine mammals (section 2.2.6.2).

### 4.3.2 Risk assessment for noise exposure

Since unweighted sound levels do not reflect how sounds of different frequencies are perceived by a listener, there is a need for the development of frequency weighting functions based on equal-loudness contours of marine mammal species (Southall *et al*., 2007). Such frequency weighting functions should make empirical dose-response relationships for marine mammals and noise more accurate, and thus should improve the predictability of behavioural responses. To date, this type of weighting function is only available for the bottlenose dolphin (Finneran and Schlundt, 2011), although alternative, more cost-effective techniques based on reaction times may lead to comparable results (Kastelein *et al.*, 2011). The use of a weighting function based on hearing thresholds can be a good starting point when data on loudness perception is unavailable (although there might be a tendency to overweight low-frequency sounds).

The weighting function used in this study (section 2.3.3) illustrates the effect harmonic energy in sonar signals has on the hearing perception of killer whales. Possibilities for reducing harmonics in active sonar signals should be explored as this can be an effective method to mitigate behavioural disturbance with small effects on sonar operations. For example, transmission of sonar signals at slightly lower source levels may lead to relatively large reductions of harmonic distortion because they are a non-linear phenomenon. Sonar systems that produce fewer harmonics could be less disruptive to marine mammals while they can operate at source levels that are similar or higher.

In the future, the simulation approach described in chapter three for whale movements in response to approaching sources could be extended to include the effects of absolute speed and relative speed between the source and whale, different species-specific behaviours, and different acoustic propagation conditions. Such simulations could provide new insights into the underlying mechanisms involved in avoidance behaviour of marine mammals, and into the species-dependency of the avoidance responses. One of the existing risk-assessment software tools (AIM: Frankel *et al*., 2002; ESME: Shyu and Hillson, 2006; SAKAMATA: Benders *et al*., 2004; SONATE: Nordlund and Benders, 2008) could potentially be used for this kind of analyses.

Experiments at sea are notoriously difficult to conduct with cetaceans, but it might be possible to re-analyse existing data using the hypothesized responses presented in this thesis. Alternatively, controlled experiments during BRSs can be designed specifically to test the probability that animals will use one of the predicted avoidance strategies.

# References


Ainslie, M.A. **2010**. *Principles of sonar performance modeling* (Springer-Praxis, Chichester, UK).

APL–UW. **1994**. *High-Frequency Ocean Environmental Acoustic Models Handbook*. APL-UW TR 9407, Applied Physics Laboratory, University of Washington, Seattle.

Au, W.W.L. **1993**. *The Sonar of Dolphins* (Springer-Verlag, New York, USA), pp. 277.

Au, W.W., and Moore P.W. **1984**. Receiving beam patterns and directivity indices of the Atlantic bottlenose dolphin *Tursiops truncatus*. *Journal of the Acoustical Society of America*, **75**, 255–262.

Au, W.W.L. and Moore, P.W. **1990**. Critical ratio and critical bandwidth for the Atlantic bottlenose dolphin. *Journal of the Acoustical Society of America,* **88**, 1635–1638.

Balcomb, K.C., and Claridge, D.E. **2001**. A mass stranding of cetaceans caused by naval sonar in the Bahamas. *Bahamas Journal of Science*, **8**, 1–12.

Barlow, J., and Gisiner, R. **2006**. Mitigating, monitoring and assessing the effects of anthopogenic sound on beaked whales. *Journal of Cetacean Research and Management*, **7**, 239–249.

Barrett-Lennard, L.G., Ford, J.K.B., and Heise, K.A. **1996**. The mixed blessing of echolocation: differences in sonar use by fish-eating and mammal-eating killer whales. *Animal Behaviour*, **51**, 553–565.

Baxley, P.A., Bucker, H., and Porter, M.B. **2000**. Comparison of beam tracing algorithms. *Proceedings of the 5$^{th}$ European Conference on Underwater Acoustics, ECUA 2000.* Lyon, France.

Bejder, L., Samuels, A., Whitehead, H., and Gales, N. **2006**. Interpreting short-term behavioural responses to disturbance within a longitudinal perspective. *Animal Behaviour*, **72**, 1149–1158.

Benders, F.P.A., Beerens, S.P., and Verboom, W.C. **2004**. SAKAMATA A tool to avoid whale strandings. *Proceedings of Undersea Defense Technology Europe,* Nice, France.

Bøe, R., Dolan, M., Thorsnes, T., Lepland, A., Olsen, H., Totland, O., and Elvenes, S. **2010**. *Standard for geological seabed mapping offshore*. NGU Report 2010.033.

Boyd, I.L., Brownell, R., Cato, D., Clarke, C., Costa, D., Evans, P., Gedamke, J., Gentry, R., Gisiner, Gordon, J., Jepson, P., Miller, P., Rendell, L., Tasker, M., Tyack, P., Vos, E., Whitehead, H., Wartzog, D., and Zimmer, W. **2008**. *The effects of anthropogenic sound on marine mammals: A draft research strategy*. European Science Foundation–Marine Board, position paper 13.

Brenowitz, E.A. **1982**. The active space of red-winged blackbird song. *Journal of Comparative Physiology A*, **147**, 511–522.

Buckstaff, K.C. **2004**. Effects of watercraft noise on the acoustic behavior of bottlenose dolphins, Tursiops truncatus, in Sarasota Bay, Florida. *Marine Mammal Science,* **20**, 709–725.

Burdic, W.S. **1991**. *Underwater acoustic system analysis*, 2nd edition (Prentice-Hall, Englewood Cliffs, USA).

Chapman, N.R., and Price, A. **2011**. Low frequency deep ocean ambient noise trend in the Northeast Pacific Ocean. *Journal of the Acoustical Society of America,* **129**, EL161.

Clark, C.W., Ellison, W.T., Southall, B.L., Hatch, L., Van Parijs, S.M., Frankel, A., and Ponirakis, D. **2009**. Acoustic masking in marine ecosystems: intuitions, analysis, and implication. *Marine Ecology Progress Series*, **395**, 201–222.

Constantine, R., Brunton, D.H., and Dennis, T. **2004**. Dolphin-watching tour boats change bottlenose dolphin (*Tursiops truncatus*) behaviour. *Biological Conservation*, **11**, 299–307.

Costa, D.P., Crocker, D.E., Gedamke, J., Webb, P.M., Houser, D.S., Blackwell, S.B., Waples, D., Hayes, S.A., and Le Boeuf, B.J. **2003**. The effect of a low-frequency sound source (acoustic thermometry of the ocean climate) on the diving behavior of juvenile northern elephant seals, *Mirounga angustirostris*. *Journal of the Acoustical Society of America*, **113**, 1155–1165.

Cox, T.M., Ragen, T.J., Read, A.J., Vos, E., Baird, R.W., Balcomb, K., Barlow, J., Caldwell, J., Cranford, T., Crum, L., D'Amico, A., D'Spain, G., Fernandez, A., Finneran, J., Gentry, R., Gerth, W., Gulland, F., Hildebrand, J., Houser, D., Hullar, T., Jepson, P.D., Ketten, D., MacLeod, C.D., Miller, P., Moore, S., Mountain, D.C., Palka, D., Ponganis, P., Rommel, S., Rowles, T., Taylor, B., Tyack, P., Wartzok, D., Gisiner, R., Mead, J., and Benner, L. **2006**. Understanding the impacts of acoustic sound on beaked whales. *Journal of Cetacean Research and Management*, **7**, 177–187.

Culik, B.M., Koschinski, S., Tregenza, N., and Ellis, G.M. **2001**. Reactions of harbor porpoises *Phocoena phocoena* and herring *Clupea harengus* to acoustic alarms. *Marine Ecology Progress Series*, **211**, 255–260.

D'Amico, A., and Pittenger, R. **2009**. A brief history of active sonar. *Aquatic Mammals*, **35**, 426–434.

D'Amico, A.D., Gisiner, R.C., Ketten, D.R., Hammock, J.A., Johnson, C., Tyack, P.L., and Mead, J. **2009**. Beaked whale strandings and naval exercises. *Aquatic Mammals*, **35**, 452–472.

D'Spain, G.L., D'Amico, A., and Fromm, D.M. **2006**. Properties of the underwater sound fields diring some well documented beaked whale mass stranding events. *Journal of Cetacean Research and Management*, **7**, 223–238.

DeRuiter, S.L., Tyack, P.L., Lin, Y-T, Newhall, A.E., Lynch, J.F., and Miller, P.J.O. **2006**. Modeling acoustic propagation of airgun array pulses recorded on tagged sperm whales (*Physeter macrocephalus*). *Journal of the Acoustical Society of America*, **120**, 4100–4114.

DeRuiter, S.L., Hansen, M., Koopman, H.N., Westgate, A.J., Tyack, P.L., and Madsen, P.T. **2009**. Propagation of narrow-band-high-frequency clicks: Measured and modelled transmission loss of porpoise-like clicks in porpoise habitats. *Journal of the Acoustical Society of America*, **127**, 560–567.

Doksæter, L., Rune Godø, O., Olav Handegard, N., Kvadsheim, P.H., Lam, F-P.A., Donovan, C., and Miller, P.J.O. **2009**. Behavioral responses of herring (*Clupea harengus*) to 1–2 and 6–7 kHz sonar signals and killer whale feeding sounds. *Journal of the Acoustical Society of America*, **125**, 554–564.

Dolman, S.J., Weir, C.R., and Jasny, M. **2009**. Comparative review of marine mammal guidance implemented during naval exercises. *Marine Pollution Bulletin,* **58**, 465–477.

Evans, P.G.H., and Miller, L.A. (Eds.) **2004**. *Proceedings of the workshop on active sonar and cetaceans*. Held at the European Cetacean Society's 17th Annual Conference, Las Palmas, Gran Canaria, 8 March 2003.

EPA, **1992**. *Framework for ecological risk assessment*. U.S. Environmental Protection Agency, Risk Assessment Forum, EPA/630/R-92/001.

Evans, D.L., and England, G.R. **2001**. *Joint interim report Bahamas marine mammal stranding event of 15-16 March 2000*. Unpublished report of the U.S. Department of Commerce and Secretary of the Navy. Washington, DC.

Fay, R.R. **1988**. *Hearing in vertebrates: a psychophysics databook* (Hill-Fay Associates, Winnetka, USA).

Filadelfo, R., Mintz, J., Michlovich, E., D'Amico, A.D., Tyack, P.L., and Ketten, D.R. **2009**. Correlating military sonar use with beaked whale strandings: what do the historical data show? *Aquatic Mammals,* **35**, 435–444.

Finneran, J.J., Schlundt, C.E., Carder, D.A., and Ridgway, S.H. **2002**. Auditory filter shapes for the bottlenose dolphin (*Tursiops truncatus*) and the white whale (*Delphinapterus leucas*) derived with notched noise. *Journal of the Acoustical Society of America*, **112**, 322–328.

Finneran, J.J., and Schlundt, C.E. **2011**. Subjective loudness level measurements and equal loudness contours in a bottlenose dolphin (*Tursiops truncatus*). *Journal of the Acoustical Society of America*, **130**, 3124–3136.

Frankel, A.S., Ellison, W.T., and Buchanan, J. **2002**. Application of the Acoustic Integration Model (AIM) to predict and minimize environmental impacts. *Proceedings of MTS/IEEE Oceans 2002*, **3**, 1438–1443.

Frantzis, A. **1998**. Does acoustic testing strand whales? *Nature*, **392**, 29.

Fristrup, K.M., Hatch, L.T., and Clark, C.W. **2003**. Variation in humpback whale (*Megaptera novaeangliae*) song length in relation to low-frequency sound broadcasts. *Journal of the Acoustical Society of America*, **113**, 3411–3424.

Funnell, C. **2009**. *Underwater Warfare Systems 2008-2009*. Coulsdon, Jane's Information group, pp. 171.

Gerk, A. **2003**. *Calibration of the Socrates source*. Unpublished TNO Report.

Hall, J.D., and Johnson, C.S. **1972**. Auditory thresholds of a killer whale, Orcinus orca, Linnaeus. *Journal of the Acoustical Society of America*, **51**, 515–517.

Hamilton, E.L. **1972**. Compressional-wave attenuation in marine sediments. *Geophysics*, **37**, 620–646.

Hamilton, E.L., and Bachman, R.T. **1982**. Sound velocity and related properties of marine sediment. *Journal of the Acoustical Society of America,* **72**, 1891–1904.

Harwood, J. **2000**. Risk assessment and decision analysis in conservation. *Biological Conservation*, **95**, 219–226.

Heide-Jørgensen, M.-P., Kleivane, L., Øien, N., Laidre, K.L. and Jensen, M.V. **2001**. A new technique for deploying satellite transmitters on baleen whales: Tracking a blue whale (*Balaenoptera musculus*) in the North Atlantic. *Marine Mammal Science,* **17**, 949–954.

Hildebrand, J.A. **2009**. Anthropogenic and natural sources of ambient noise in the ocean. *Marine Ecological Progress Series*, **395**, 5–10.

Hohn, A.A., Rotstien, D.S., Harms, C.A., and Southall, B.L. **2006**. *Report on marine mammal unusual mortality event UMESE0501Sp: multispecies mass stranding of pilot whales (Globicephala macrorhynchus), minke whale (Balaenoptera acutorostrata), and dwarf sperm whales (Kogia sima) in North Carolina on 15–16 January 2005*. NOAA Technical Memorandum NMFS-SEFSC-537.

Houser, D. S. **2006**. A method for modeling marine mammal movement and behavior for environmental impact assessment. *IEEE Journal of Oceanic Engineering*, **31**, 76–81.

IOC, IHO, and BODC. **2003**. *Centenary Edition of the GEBCO Digital Atlas*. Published on CD-ROM on behalf of the Intergovernmental Oceanographic Commission and the International Hydrographic Organization as part of the General Bathymetric Chart of the Oceans. British Oceanographic Data Centre, Liverpool.

Jackson, D.R., and Richardson, M.D. **2007**. *High-frequency seafloor acoustics* (Springer, New York, USA).

Jensen, E.B. **1981**. Sound propagation in shallow water: A detailed description of the acoustic field close to surface and bottom. *Journal of the Acoustical Society of America,* **70**, 1397–1406.

Jenserud, T. **2002**. *A collection of oceanographic and geoacoustic data in Vestfjorden – obtained from the MILOC Survey Rocky Road*. FFI-rapport 2002/00304.

Jenserud, T., and Ottesen, D. **2002**. *Analysis of bottom samples from Vestfjorden collected during RUMBLE first sea trial.* FFI-rapport 2002/05018.

Johnson, C.S. **1968**. Relation between absolute threshold and duration-of-tone pulses in the bottlenosed dolphin. *Journal of the Acoustical Society of America*, **43**, 757–763.

Johnson, M.P., and Tyack, P.L. **2003**. A digital acoustic recording tag for measuring the response of wild marine mammals to sound. *IEEE Journal of Oceanic Engineering,* **28**, 3–12.

Johnson, M., Madsen, P.T., Zimmer, W.M.X., Aguilar de Soto, N., and Tyack, P.L. **2004**. Beaked whales echolocate on prey. *Proceedings of the Royal Society of London Series B: Biological Sciences Supplement,* **271**, S383–S386.

Johnson, M., Aguilar de Soto, N., and Madsen, P.T. **2009**. Studying the behaviour and sensory ecology of marine mammals using acoustic recording tags: a review. *Marine Ecology Progress Series*, **395**, 55–73.

Johnston, D.W. **2002**. The effect of acoustic harassment devices on harbour porpoises (*Phocoena phocoena*) in the Bay of Fundy, Canada. *Biological Conservation*, **108**, 113–118.

Kastak, D., Schusterman, R.J., Southall, B.L., Reichmuth, C.R. **1999**. Underwater temporary threshold shift induced by octave-band noise in three species of pinniped. *Journal of the Acoustical Society of America*, **106**, 1142–1148.

Kastelein, R.A., Verboom, W.C., Muijsers, M., Jennings, N.V., and van der Heul, S. **2005**. The influence of acoustic emissions for underwater data transmission on the behaviour of harbour porpoises (*Phocoena phocoena*) in a floating pen. *Marine Environmental Research*, **59**, 287–307.

Kastelein, R.A., van der Heul, S., Verboom, W.C., Triesscheijn, R.J.V., and Jennings, N.V. **2006a**. The influence of underwater data transmission sounds on the displacement behaviour of captive harbour seals (*Phoca vitulina*). *Marine Environmental Research,* **61**, 19–39.

Kastelein, R.A., van der Heul, S., Terhune, J.M., Verboom, W.C., and Treisscheijn, R.J.V. **2006b**. Deterring effects of 8-45 kHz tone pulses on harbour seals (*Phoca vitulina*) in a large pool. *Marine Environmental Research,* **62**, 356–373.

Kastelein, R. A., Verboom, W.C., Jennings, N., de Haan, D., and van der Heul, S. **2008**. The influence of 70 and 120 kHz tonal signals on the behavior of harbor porpoises (*Phocoena phocoena*) in a floating pen. *Marine Environmental Research*, **66**, 319–326.

Kastelein, R.A., Wensveen, P.J., Hoek, L., Au, W.W.L., Terhune, J.M., de Jong, C.A.F. **2009**. Critical ratios in harbor porpoises (*Phocoena phocoena*) for tonal signals between 0.315 and 150 kHz in random Gaussian white noise. *Journal of the Acoustical Society of America*, **126**, 1588–1597.

Kastelein, R.A., Hoek, L., de Jong, C.A.F, and Wensveen, P.J. **2010**. The effect of signal duration on the underwater detection thresholds of a harbor porpoise (*Phocoena phocoena*) for single frequency-modulated tonal signals between 0.25 and 160 kHz. *Journal of the Acoustical Society of America*, **128**, 3211–3222.

Kastelein, R.A., Wensveen, P.J., Terhune, J.M., and de Jong, C.A.F. **2011**. Near-threshold equal-loudness contours for harbor seals (*Phoca vitulina*) derived from reaction times during underwater audiometry: a preliminary study. *Journal of the Acoustical Society of America*, **129,** 488–495.

Kinsler, L.E., Frey, A.R., Coppens, A.B., and Sanders, J.V. **1982**. *Fundamentals of Acoustics* (John Wiley and Sons, New York, USA).

Knies, J. (Ed.) **2009**. MAREANO thematic issue: Sediment characteristics and environmental implications in the Lofoten - Barents Sea region. *Norwegian Journal of Geology*, **89**.

Kvadsheim, P., Benders, F., Miller, P., Doksæter, L., Knudsen, F., Tyack, P., Nordlund, N., Lam, F-P., Samarra, F., Kleivane, L., and Godø, O.R. **2007**. *Herring (sild), killer whales (spekkhogger) and sonar – The 3S-2006 cruise report with preliminary results*. FFI-rapport 2007/01189.

Kvadsheim, P., Lam, F.P., Miller, P., Alves, A. C., Antunes, R., Bocconcelli, A., van Ijsselmuide, S., Kleivane, Olivierse, M., and Visser, F. **2009**. *Cetaceans and naval sonar – the 3S-2009 cruise report*. FFI-rapport 2009/01140.

Lusseau, D. and Bejder, L. **2007**. The long-term consequences of short-term responses to disturbance experiences from whalewatching impact assessment. *International Journal of Comparative Psychology,* 20, 228–236.

Madsen, P.T. **2005**. Marine mammals and noise: problems with root mean square sound pressure levels for transients. *Journal of the Acoustical Society of America*, **117**, 3952–3957.

Madsen, P.T., and Møhl, B. **2000**. Sperm whales (*Physeter catodon L.* 1758) do not react to sounds from detonators. *Journal of the Acoustical Society of America*, **107**, 668–671.

Madsen, P.T., Johnson, M., Miller, P.J.O., Aguilar Soto, N., Lynch, J., and Tyack, P. **2006a**. Quantitative measures of air-gun pulses recorded on sperm whales (*Physeter macrophalus*) using acoustic tags during controlled exposure experiments. *Journal of the Acoustical Society of America*, **120**, 2366–2379.

Madsen, P.T., Wahlberg, M., Tougaard, J., Lucke, K., and Tyack, P. **2006b**. Wind turbine underwater noise and marine mammals: implications of current knowledge and data needs. *Marine Ecology Progress Series*, **309**, 279–295.

Malme, C.I., Miles, P.R., Clark, C.W., Tyack, P., and Bird, J.E. **1983**. *Investigations of the potential effects of underwater noise from petroleum industry activities on migrating gray whale behaviour.* BBN Report No. 5366; NTIS PB86-174174.

Report from Bolt Beranek and Newman Inc. for U.S. Minerals Management Service, Anchorage, AK.

Malme, C.I., Miles, P.R., Clark, C.W., Tyack, P., and Bird, J.E. **1984**. *Investigations of the potential effects of underwater noise from petroleum industry activities on migrating gray whale behavior. Phase II: January 1984 migration*. BBN Report No. 5586; NTIS PB86-218377. Report from Bolt Beranek and Newman Inc. for U.S. Minerals Management Service, Anchorage, AK.

McCammon, D. **2008**. *Investigation of the transmission loss issue in Bellhop.* Defence R&D Canada – Atlantic, Contract Report, DRDC Atlantic CR 2008–054.

McCarty, R.T. **2010**. Winter v. NRDC: The Navy, submarines, active sonar, and whales—an analysis of the Ninth Circuit Review and the Roberts Court Extension of the Military Deference Doctrine. *Houston Law Review*, **47**, 489–527.

McCauley, R.D., Fewtrell, J., Duncan, A.J., Jenner, C., Jenner, M-N., Penrose, J.D., Prince, R.I.T., Adhitya, A., Murdock, J., and McCabe, K. **2000**. Marine seismic surveys - a study of environmental implications. *Australian Petroleum Production and Exploration Association*, **40**, 692–708.

Miksis-Olds, J.L., and Miller, J.H. **2006**. Transmission loss in manatee habitats. *Journal of the Acoustical Society of America*, **120**, 2320–2327.

Miller, P.J., and Tyack, P.L. **1998**. A small towed beamforming array to identify vocalizing resident killer whales (*Orcinus orca*) concurrent with focal behavioral observations. *Deep-Sea Research Part II*, **45**, 1389–1405.

Miller, P.J., Biassoni, N., Samuels, A., and Tyack, P.L. **2000**. Whale songs lengthen in response to sonar. *Nature,* **405**, 903.

Miller, P.J., Johnson, M.P., and Tyack, P.L. **2004**. Sperm whale behaviour indicates the use of echolocation click buzzes “creaks” in prey capture. *Proceedings of the Royal Society of London Series B: Biological Sciences*, **271**, 2239–2247.

Miller, P.J.O., Johnson, M.P., Madsen, P.T., Biassoni, N., Quero, M., and Tyack, P.L. **2009**. Using at-sea experiments to study the effects of airguns on the foraging behavior of sperm whales in the Gulf of Mexico. *Deep-Sea Research Part I*, **57**, 1168–1181.

Miller, P., Antunes, R., Alves, A.C., Wensveen, P., Kvadsheim, P., Kleivane, L., Nordlund, N., Lam, F-P., van IJselmuide, S., Visser, F., and Tyack, P. **2011a**. *The 3S experiments: studying the behavioural effects of naval sonar on killer whales (Orcinus orca), sperm whales (Physeter macrocephalus), and long-finned pilot*

*whales (Globicephala melas) in Norwegian waters*. Scottish Oceans Institute Technical Report: SOI-2011-001.

Miller, P.J.O., Kvadsheim, P., Lam, F.-P.A., Tyack , P.L., Kuningas, S., Wensveen, P.J., Antunes, R.N., Alves, A.C., Kleivane, L., Ainslie, M.A., Thomas, L. **2011b**. Developing dose-response relationships for the onset of avoidance of sonar by free-ranging killer whales (*Orcinus orca*). *Proceedings of the 19th Biennial Conference on the Biology of Marine Mammals*, Tampa, FL, USA.

Mooney, T.A., Nachtigall, P.E., and Vlachos, S. **2009**. Sonar-induced temporary hearing loss in dolphins. *Biology Letters*, **5**, 565–567.

Moretti, D., Marques, T.A., Thomas, L., DiMarzio, N., Dilley, A., Morrissey, R., McCarthy, E., Ward, J., and Jarvis, S. **2010**. A dive counting density estimation method for Blainville's beaked whale (*Mesoplodon densirostris*) using a bottom-mounted hydrophone field as applied to a Mid-Frequency Active (MFA) sonar operation. *Applied Acoustics*, **71**, 1036–1042.

Morton, A.B. and Symonds, H.K. **2002**. Displacement of *Orcinus orca* (L.) by high amplitude sound in British Columbia, Canada. *ICES Journal of Marine Science*, **59**, 71–80.

NMFS. **2005**. *Assessment of acoustic exposure on marine mammals in conjunction with USS SHOUP active sonar transmissions in the eastern Strait of Juan de Fuca and Haro Strait*, *Washington, 5 May, 2003.* National Marine Fisheries Service, Office of Protected Resources. NOAA Report.

Nemiroff, L. **2009**. *Structural variation and communicative functions of long-finned pilot whale (Globicephala melas) pulsed calls and complex whistles*. Biology. Halifax, Nova Scotia, Dalhousie University. Master's thesis.

Nordlund, N., and Benders, F. **2008**. *SONATE 3.0 - A decision aid system to mitigate the impact of sonar operations in Norwegian waters on marine life*. FFI-rapport 2008/01414.

Nowacek, D.P., Johnson, M.P., and Tyack, P.L. **2004**. North Atlantic right whales (*Eubalaena glacialis*) ignore ships but respond to alerting stimuli. *Proceedings of the Royal Society of London Series B: Biological Sciences*, **271**, 227–231.

Nowacek, D.P., Thorne, L.H., Johnston, D.W., Tyack, P.L. **2007**. Responses of cetaceans to anthropogenic noise. *Mammal Review*, **37**, 81–115.

Nowacek, S.M., Wells, R.S., and Solow, A.R. **2001**. Short-term effects of boat traffic on bottlenose dolphins, *Tursiops truncatus*, in Sarasota Bay, Florida. *Marine Mammal Science*, **17**, 673–688.

NRC. **2003**. *Ocean noise and marine mammals* (National Academies, Washington DC, USA). National Research Council Report.

NRC. **2005**. *Marine mammal populations and ocean noise: determining when noise causes biologically significant effects* (National Academies, Washington DC, USA). National Research Council Report.

Olesiuk, P.F., Nichol, L.M., Sowden, M.J., and Ford, J.K.B. **2002**. Effect of the sound generated by an acoustic harassment device on the relative abundance and distribution of harbor porpoises (*Phocoena phocoena*) in Retreat Passage, British Columbia. *Marine Mammal Science*, **18**, 843–862.

Patenaude, N.J., Richardson, W.J., Smultea, M.A., Koski, W.R., Miller, G.W., Wuersig, B. and Greene, C.R. **2002**. Aircraft sound and disturbance to bowhead and beluga whales during spring migration in the Alaskan Beaufort Sea. *Marine Mammal Science*, **18**, 309–355.

Paucini, A.F., Nachtigall, P.E., Kloepper, L.N., Linnenschmidt, M., Sogorb, A., and Matias, S. **2010**. Audiogram of a formerly stranded long-finned pilot whale (*Globicephala melas*) measured using auditory evoked potentials. *The Journal of Experimental Biology*, **213**, 3138–3143.

Plomp, R., and Bouman, M.A. **1959**. Relation between hearing threshold and duration for tone pulses. *Journal of the Acoustical Society of America,* **31**, 749–758.

Porter, M.B. **2011**. *The Bellhop Manual and User's Guide: Preliminary Draft*. Report from Heat, Light, and Sound Research, Inc. La Jolla, CA, USA.

Porter, M.B., and Bucker, H.P. **1987**. Gaussian beam tracing for computing ocean acoustic fields. *Journal of the Acoustical Society of America,* **82**, 1249–1359.

Rendell, L.E., and Gordon, J. **1999**. Vocal response of long-finned pilot whales (*Globicephala melas*) to military sonar in the Ligurian Sea. *Marine Mammal Science*, **15**, 198–204.

Reynolds, J.R., Kiekow, T.G., and Smith, S.Z. **2009**. No whale of a tale: Legal implications of Winter v. NRDC. *Ecology Law Quarterly*, **36**, 753-774.

Richardson, M.D., and Briggs, K.B. **2004**. Relationship among sediment physical and acoustic properties in siliciclastic and carbonate sediments. *Proceedings of the 7$^{th}$ European Conference on Underwater Acoustics, ECUA 2004.* Delft, The Netherlands.

Richardson, W.J., Greene, C.R., Malme, C.I., and Thomson, D.H. **1995**. *Marine Mammals and Noise* (Academic, San Diego, USA).

Richardson, W.J., Fraker, M.A., Würsig, B., and Wells, R.S. **1985**. Behaviour of bowhead whales *Balaena mysticetus* summering in the Beaufort Sea: reactions to industrial activities. *Biological Conservation*, **32**, 195–230.

Richardson, W.J., Würsig, B., and Greene, C.R. Jr. **1990**. Reactions of bowhead whales, *Balaena mysticetus*, to drilling and dredging noise in the Canadian Beaufort Sea. *Marine Environmental Research,* **29**, 135–160.

Ross, D. **1976**. *Mechanics of Underwater Noise* (Pergamon, New York, USA).

Schlundt, C.E., Dear, R.L., Houser, D.S., Bowles, A.E., Reidarson, T., and Finneran, J.J. **2011**. Auditory evoked potentials in two short-finned pilot whales (*Globicephala macrorhynchus*). *Journal of the Acoustical Society of America*, **129**, 1111–1116.

Scholik-Schlomer, A.R. **2010**. Status of NOAA's guidelines for assessing impacts of anthropogenic sound on marine mammals. *Proceedings of the 2nd International Conference on The Effects of Noise on Aquatic Life*, Cork, Ireland.

Shyu, H.-J., and Hillson, R. **2006**. A software workbench for estimating the effects of cumulative sound exposure in marine mammals. *IEEE Journal of Oceanic Engineering*, **31**, 8–21.

Siderius, M., and Porter, M.B. **2006**. Modeling techniques for marine-mammal risk assessment. *IEEE Journal of Oceanographic Engineering*, 31, 49–60.

Southall, B.L., Bowles, A.E., Ellison, W.T., Finneran, J.J., Gentry, R.L., Greene Jr., C.R., Kastak, D., Ketten, D.R., Miller, J.H., Nachtigall, P.E., Richardson, W.J., Thomas, J.A., and Tyack, P.L. **2007**. Marine mammal noise exposure criteria: initial scientific recommendations. *Aquatic Mammals,* **33**, 411–521.

Suzuki, Y., and Takeshima, H. **2004**. Equal-loudness-level contours for pure tones. *Journal of the Acoustical Society of America,* **116**, 918–933.

Szymanski, M.D., Bain, D.E., Kiehl, K., Pennington, S., Wong, S., and Henry, K.R. **1999**. Killer whale (*Orcinus orca*) hearing: Auditory brainstem response and behavioral audiograms. *Journal of the Acoustical Society of America,* **106**, 1134–1141.

Tasker, M., Amundin, M., Andre, M., Hawkins, A.D., Lang, W., Merck, T., Scholik-Schlomer, A., Teilmann, J., Thomsen, F., Werner, S., and Zakharia, M. **2010**. Managing underwater noise in European waters – implementing the Marine

Strategy Framework Directive. *Proceedings of the 2nd International Conference on The Effects of Noise on Aquatic Life*, Cork, Ireland.

Thorsnes, T., Erikstad, L., Doland, M.F.J., and Bellec, V.K. **2009**. Submarine landscapes along the Lofoten-Vesterålen-Senja margin, northern Norway. *Norwegian Journal of Geology*, **89**, 5−16.

Tougaard, J., Carstensen, J., Teilmann, J., Skov, H., and Rasmussen, P. **2009**. Pile driving zone of responsiveness extends beyond 20 km for harbor porpoises (*Phocoena phocoena* (L.)). *Journal of the Acoustical Society of America*, **126**, 11–14.

Tyack, P. **1981**. Interactions between singing Hawaiian humpback whales and conspecifics nearby. *Behavioral Ecology and Sociobiology*, **8**, 105–116.

Tyack, P. **2009**. Acoustic playback experiments to study behavioural responses of free-ranging marine animals to anthropogenic noise. *Marine Ecological Progress Series*, 395, 187–200.

Tyack, P., Gordon, J., and Thompson, D. **2003**. Controlled-exposure experiments to determine the effects of noise on marine mammals. *Marine Technology Society Journal*, **37**, 39–51.

Tyack, P.L., Johnson, M., Aguilar Soto, N., Sturlese, A., and Madsen, P.T. **2006**. Extreme diving of beaked whales. *Journal of Experimental Biology,* **209**, 4238–4253.

Tyack, P.L., Zimmer, W.M.X., Moretti, D., Southall, B.L., Claridhe, D.E., Durban, J.W., Clark, C.W., D'Amico, A., DiMarzio, N., Jarvis, S., McCarthy, E., Morrissey, R., Ward, J., and Boyd, I.L. **2011**. Beaked whales respond to simulated and actual navy sonar. *PLoS ONE*, **6**, e17009.

UNESCO. **1983**. *Algorithms for computations of fundamental properties of seawater*. UNESCO Technical Papers in Marine Science No. 44.

Urick, R.J. **1983**. *Principles of underwater sound*, 3rd edition (McGraw-Hill, New York, USA).

Verboom, W.C., and Kastelein, R.A. **2005**. Some examples of marine mammal discomfort thresholds in relation to man-made noise. *Proceedings of Undersea Defence Technology Conference*, Amsterdam, The Netherlands.

Verfuss, U.K., Miller, L.A., and Schnitzler, H-U. **2005**. Spatial orientation in echolocating harbour porpoises (*Phocoena phocoena*). *The Journal of Experimental Biology*, **208**, 3385–3394.

Watkins, W.A., Moore, K., and Tyack, P.L. **1985**. Sperm whale acoustic behaviors in the southeast Caribbean. *Cetology*, **49**, 1–15.

Weir, C. R. **2008**. Short-finned pilot whales (*Globicephala macrorhynchus*) respond to an airgun ramp-up procedure off Gabon. *Aquatic Mammals*, **34**, 349–354.

Wensveen, P.J., and van Roij, Y.A.L. **2007**. *Exposure Data Analysis: 3S-2006 trial*. TNO Internship Report, TNO-DV 2007 SV291.

Wenz, G.M. **1962**. Acoustic ambient noise in the ocean: Spectra and sources. *Journal of the Acoustical Society of America,* **34**, 1936–1956.

Williams, R., Bain, D.E., Ford, J.K.B., and Trites, A.W. **2002**. Behavioural responses of male killer whales to a 'leapfrogging' vessel. *Journal of Cetacean Research and Management*, **4**, 305–310.

Yang, W.C., Chou, L.S., Jepson, P.D., Brownell, R.L., Cowan, D., Chang, P.H., Chiou, H.I., Yao, C.J., Yamada, T.K., Chiu, J.T., Wang, P.J., and Fernández, A. **2008**. Unusual cetacean mortality event in Taiwan, possibly linked to naval activities. *Veterinary Record*, **162**, 184–186.

Zimmer, W.M.X., and Tyack, P.L. **2007**. Repetitve shallow dives pose decompression risk in deep-diving beaked whales. *Marine Mammal Science*, **23**, 888–925.

Zirbel, K., Ballint, P., and Parsons, E.C.M. **2011**. Navy sonar, cetaceans and the US Supreme Court: A review of cetacean mitigation and litigation in the US. *Marine pollution Bulletin*, **63**, 40–48.

# Appendix I: CEE_Analyser user's guide

CEE_Analyser is a custom program written in Matlab that allows the user to systematically analyse the sonar pings received on Dtags and towed arrays during the 3S controlled-exposure experiments. The program contains 4 analysis modules that allow one to select consecutively: the start of the sonar ping, a sample of noise preceding the ping, the frequency bandwidth of the ping, and the duration of the ping. In a 5$^{th}$ module, the unweighted and weighted received levels can be calculated using the 4 signal characteristics obtained in the earlier modules. The workings of the program are described in detail below.

## Signal and noise cues

Start-of-ping cues are stored using the module *"*Ping Markers*"*. The module features a matched filter that convolves the received signal with the complex conjugate time-reversed version of the transmitted signal to obtain a zero-lag cross-correlation function (Burdic, 1991). The module automatically selects the highest peak in the cross-correlation function as the signal cue, but also allows the user to choose another point in time. When noise interferes with the beginning of the ping, an "alternative-start" cue can be selected.

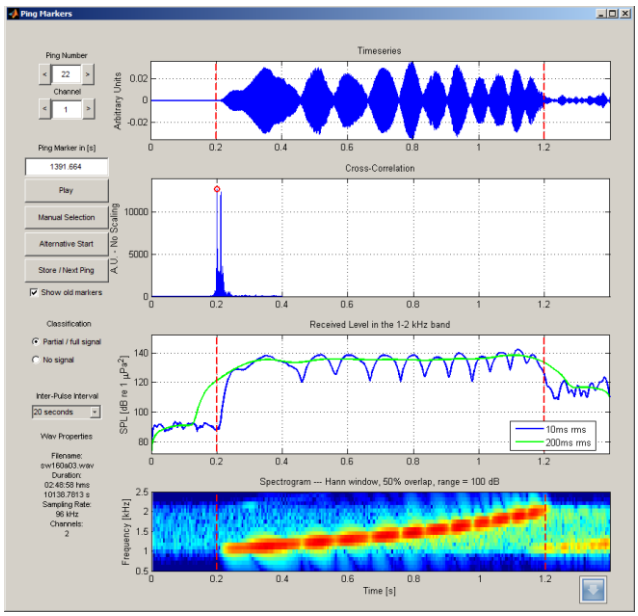


Figure I-1: The graphical interface of the module "Ping Markers" showing a ping that consists of two closely-spaced arrivals, as indicated by the two peaks in the cross-correlation function in the second panel. The first peak is somewhat higher and thus this point in time is selected as the signal cue. The red dashed lines in the other three panels indicate the edges of a 1-s window starting from the signal cue (chosen as one second is the duration of transmitted ping).

The next step of the analysis process involves the analysis module *"*Noise Markers*"*. There a 200-ms window of stationary noise preceding the sonar signal can

be selected for each ping in order to estimate the SNR of the pings in a later stage of analysis. The initially-selected noise window starts at 250 ms before the signal cue, but a different window can be chosen manually to avoid nonstationary noise and transients within the selection. The manual selection can be made by clicking on the new start position in one of the panels. Whenever necessary, the bandwidth and window length of the data chunk that is visible can be adjusted to find the most appropriate noise window.

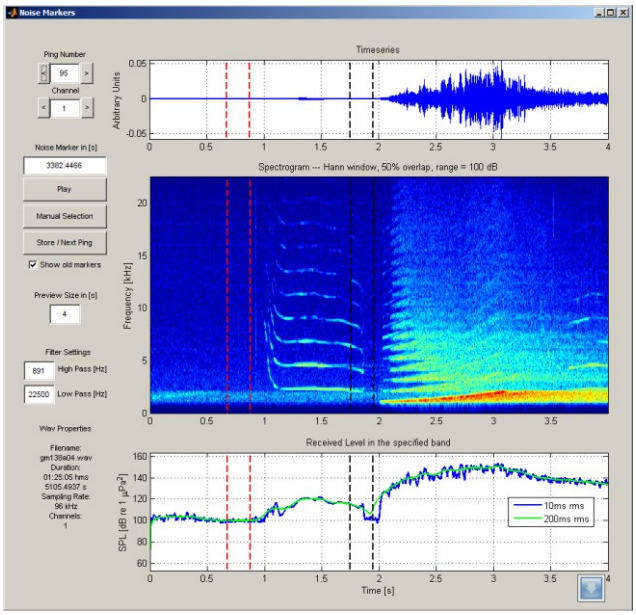


Figure I-2: The graphical interface of the module “Noise Markers” in which the edges of the automatically- and manually-selected windows of stationary noise are indicated with black and red dashed lines, respectively. In this example the noise window is selected manually because a pilot whale vocalised just before the sonar transmitted.

## Band selection and click removal

All the 1/3-octave bands between 1 and 40 kHz centre frequency containing significant signal energy (SNR>10dB) can be selected automatically within the module “Bandwidth”. After this initial selection, 1/3-octave bands for which the slow SPL is influenced by transient noises can also be excluded manually. The toggle buttons which are located below the upper panel (Figure I-3) are used to indicate which 1/3-octave bands are selected and, at the same time, to control for which frequency band the time-weighted SPLs are plotted (lower panel; Figure I-3).

Both the modules “Bandwidth” and “Duration” (next section) include a transient detection and removal algorithm. Clicks can also be selected manually when they are missed by the automatic detector. The algorithm interpolates in the fast SPL data between the minima around each peak, and then recalculates the slow SPL data from the newly-computed mean-square pressures. The locations of the clicks in the recordings are stored so that in the last processing stage click-free received levels will be calculated.

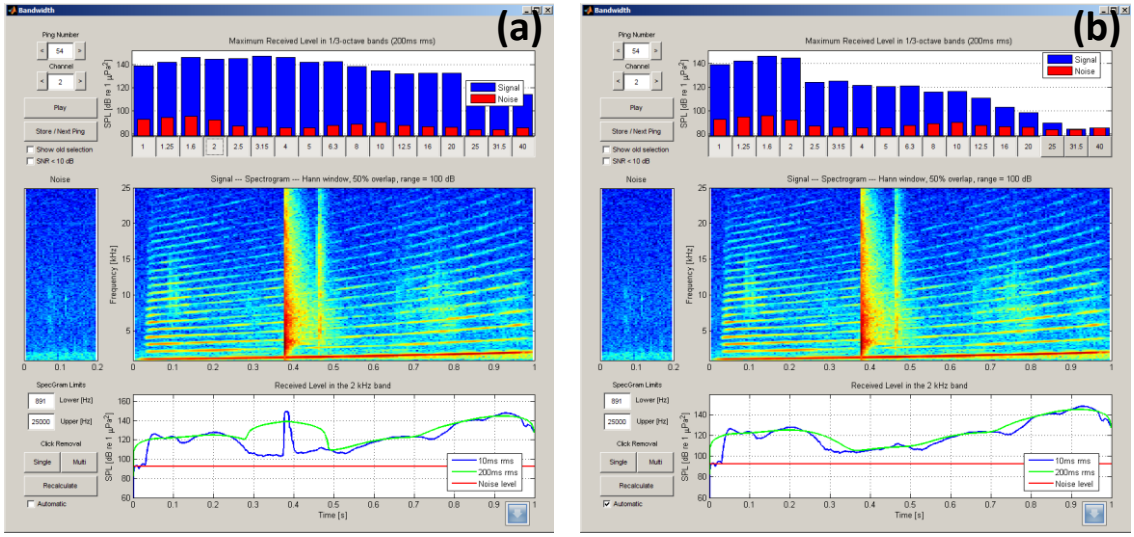


Figure I-3: The graphical interface of the module "Bandwidth" showing the levels of a sonar ping (a) before, and (b) after removal of a sperm whale click. The vertical bars in the upper panel indicate the $SPL_{max}$ and estimated noise level in the 1–40 kHz 1/3-octave bands. Note the drop in $SPL_{max}$ in the 2–40 kHz bands due to the removal of the click.

## Signal duration

Pings can be processed in the module "Duration" to find the signal duration $\tau_{20dB}$ which is defined as the time during which the fast SPL in the sonar band (1-2 kHz or 6-7 kHz) exceeds a 20 dB threshold below the maximum fast SPL. The analysis window length can be altered to ensure that the reverberation level drops below the 20 dB threshold.

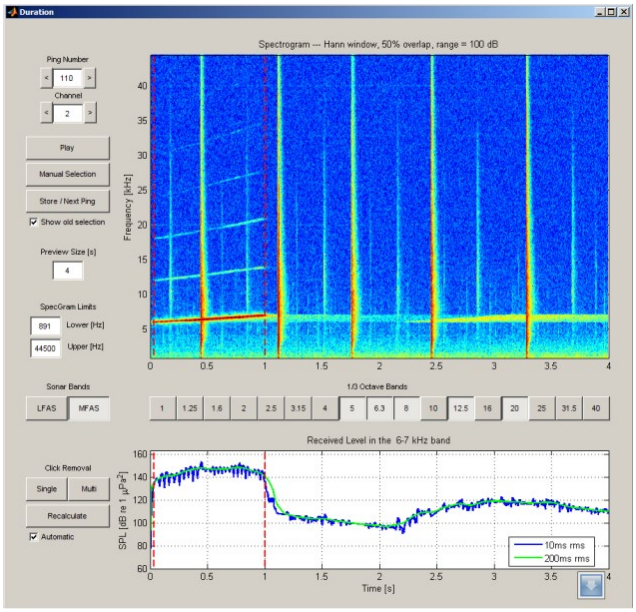


Figure I-4: The graphical interface of the module "Duration" showing a 4-s sample of a ping with a tail of reverberation. In the example echolocation clicks were removed from the time-weighted SPLs. The –20 dB points that mark the start and end of the ping are shown with red dashed lines.

## Data management and advanced processing

The 4 analysis modules and the module for calculating the received levels are accessible from the main window of CEE_Analyser [Figure I-5(a)]. The main window also allows the user to create a new recording, open an existing recording [Figure I-5(b)], and save or delete a loaded recording. Summary information about the loaded exposure recording and the progress of the analysis is shown in the main gui.

All data are stored in a Matlab data structure file. Also, a dedicated excel file can be used to import to and export from the data structure. The ping numbers, ping transmission times, and source levels can be imported from the log file produced by the Socrates source processing.

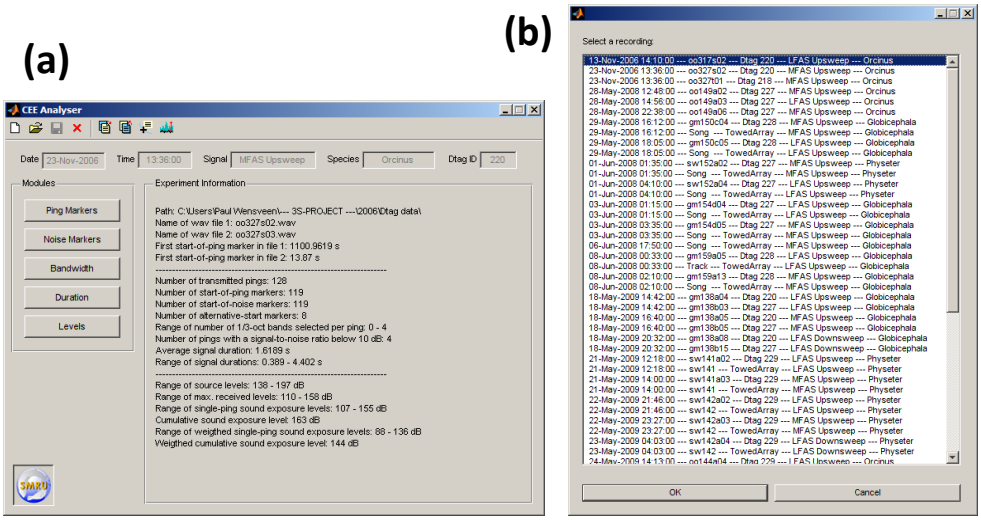


Figure I-5: (a) Main window of CEE_Analyser. (b) Listbox to select the exposure recording.

# Appendix II: Seafloor sediment maps

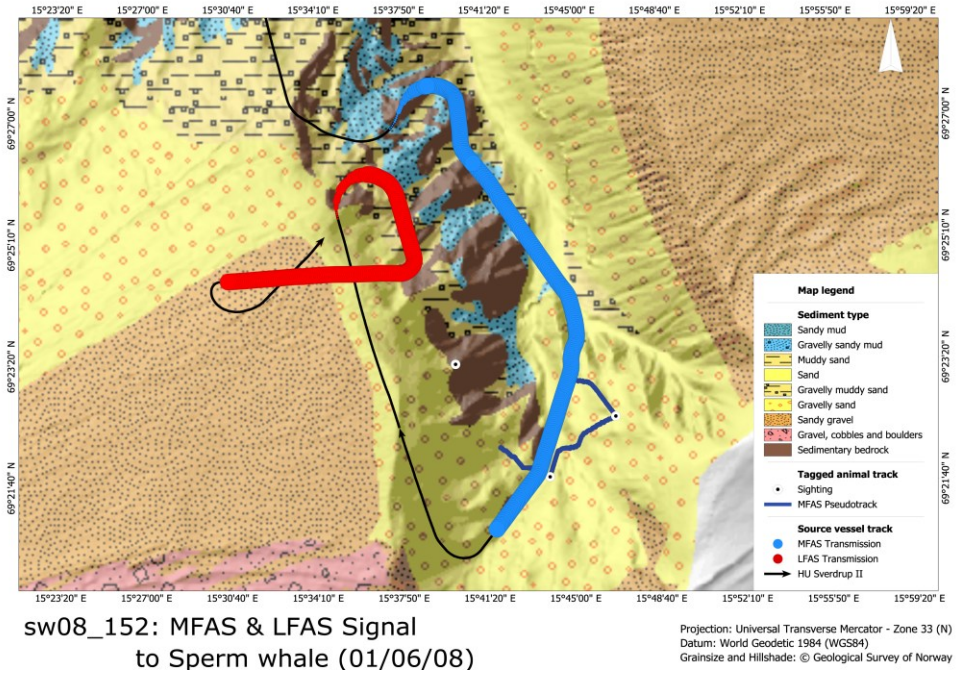


Figure II-1: Map of experimental site for sw08_152 with the seafloor sediment types, the vessel track, and the whale sightings and pseudotrack. The location of the animal during the LFAS CEE is uncertain; the single, most-northern sighting represents a possible location a few mins before exposure.

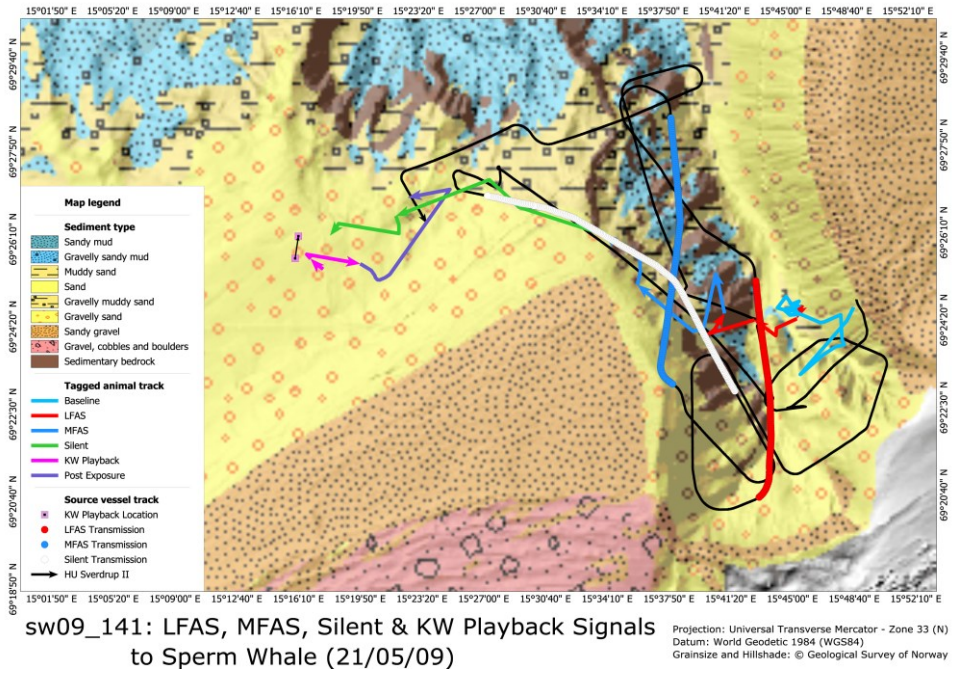


Figure II-2: Map of experimental site for sw09_141 with the seafloor sediment types, the vessel track, and the whale track from the sightings.

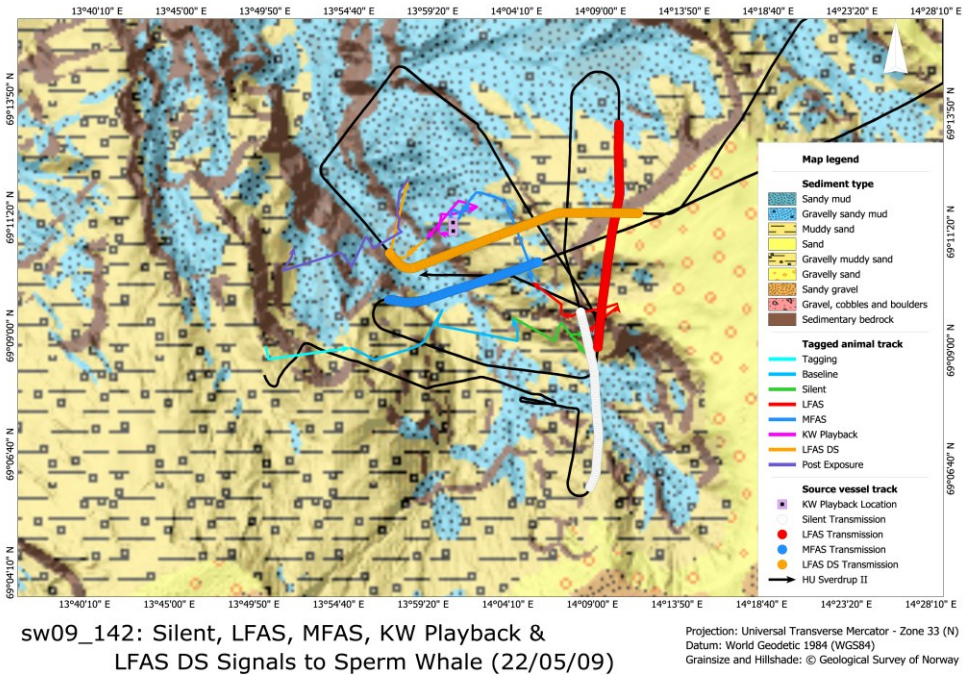


Figure II-3: Map of experimental site for sw09_142 with the seafloor sediment types, the vessel track, and the whale track from the sightings.

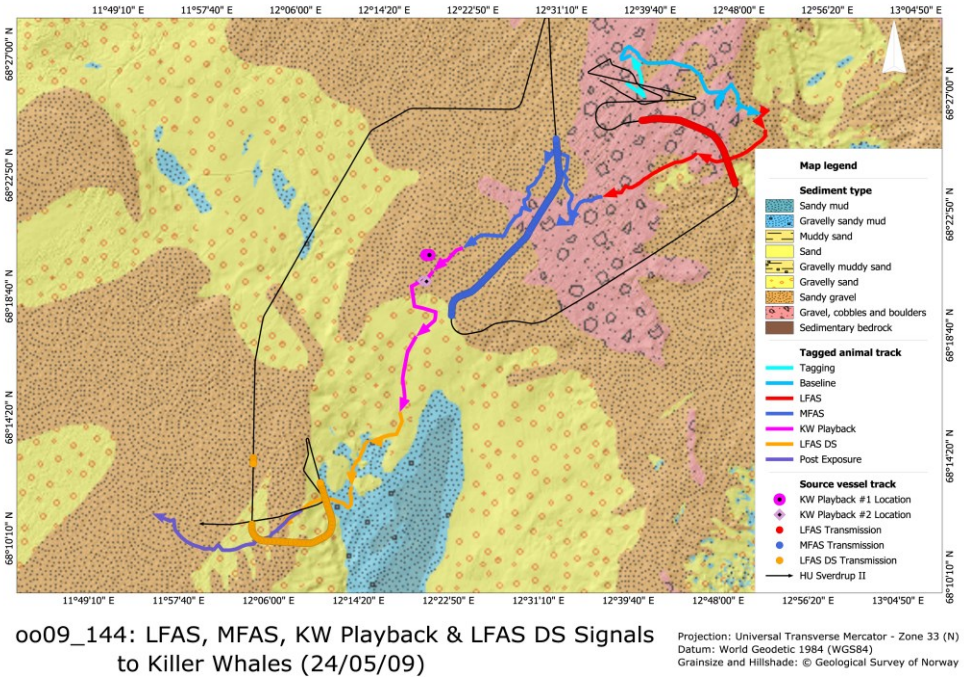


Figure II-4: Map of experimental site for oo09_144 with the seafloor sediment types, the vessel track, and the whale track from the sightings.

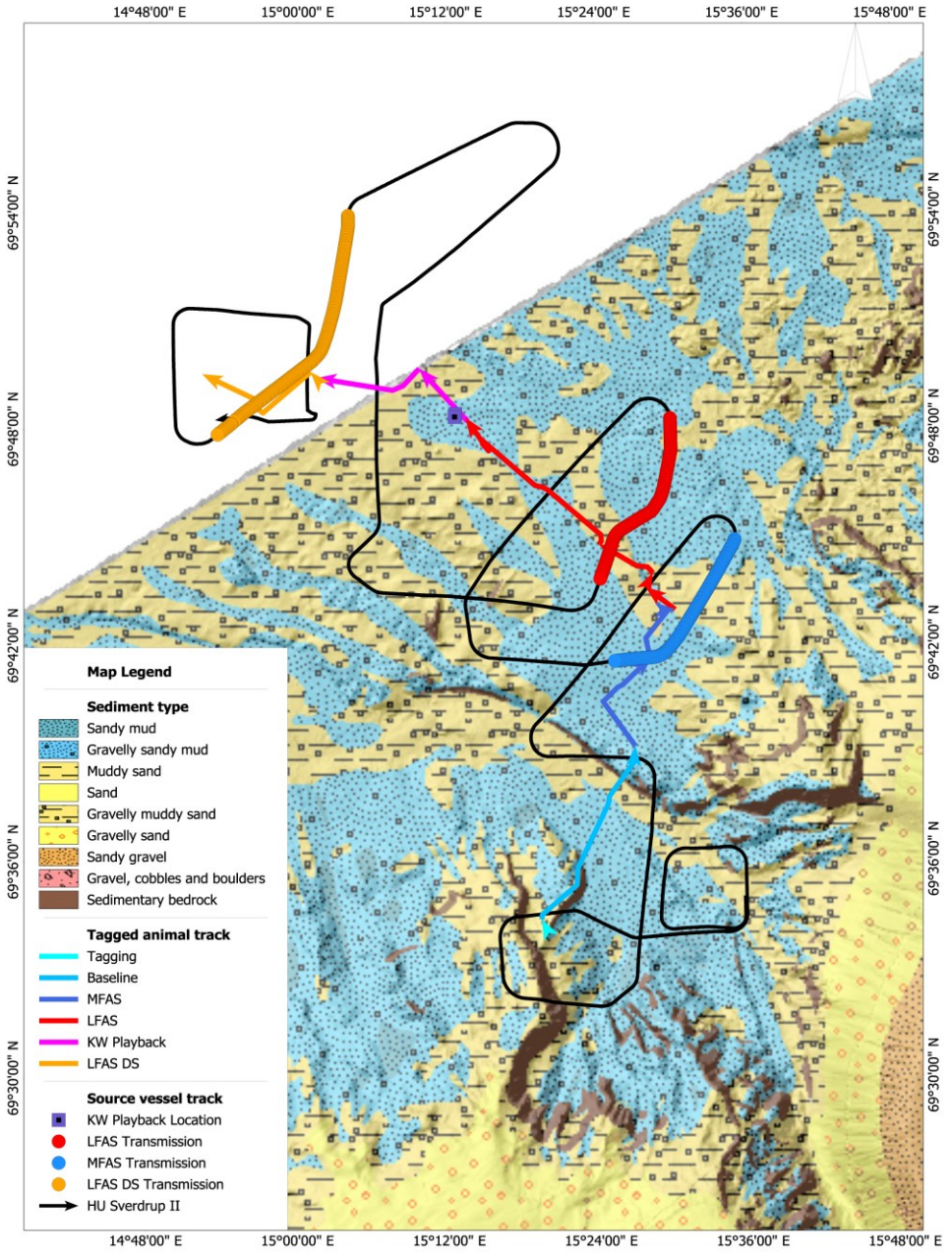


Figure II-5: Map of experimental site for sw09_160 with the seafloor sediment types, the vessel track, and the whale track from the sightings.

## Appendix III: Sediment table

| *Sediment* | *Definition* | *$M_z(\varphi)$* | *Experiment ID* |
|---|---|---|---|
| *Sandy mud* | *Clay:silt ratio from 1:2 to 2:1, silt+clay >50%, sand <50%, gravel <2%* | *6* | *oo06_317*<br>*oo08_149*<br>*gm08_150*<br>*gm08_154*<br>*gm08_158*<br>*gm08_159*<br>*gm09_138*<br>*gm09_156* |
| *Gravelly sandy mud* | *Sand:silt+clay ratio from 1:9 to 1:1, gravel 2-30%* | *5* | *sw09_142 (MFAS)*<br>*sw09_160 (MFAS)*<br>*sw09_160 (LFAS-UP)* |
| *Muddy sand* | *Clay:silt ratio from 1:2 to 2:1, sand >50%, silt+clay <50%, gravel <2%* | *3* | |
| *Sand* | *Sand >90%, silt+clay <10%, gravel <2%* | *1.5* | |
| *Gravelly muddy sand* | *Sand:silt+clay ratio from 1:1 to 9:1, gravel 2-30%* | *1* | *sw09_142 (LFAS-UP)*<br>*sw09_142 (LFAS-DO)*<br>*sw09_160 (LFAS-DO)* |
| *Gravelly sand* | *Sand:silt+clay ratio >9:1, gravel 2-30%* | *0.5* | *sw08_152*<br>*sw09_141*<br>*oo09_144 (LFAS-DO)* |
| *Sandy gravel* | *Sand:silt+clay ratio >9:1, gravel 30-80%* | *-1* | *oo06_327*<br>*oo09_144 (MFAS)* |
| *Gravel, cobbles and boulders* | *Dominant are gravel, cobbles and boulders.* | *…* | *oo09_144 (LFAS-UP)* |

Note: Signal type is given in parentheses for experiments that had different sediment classes among sonar runs.

# Appendix IV: Transmission loss patterns

## Killer whale experiments

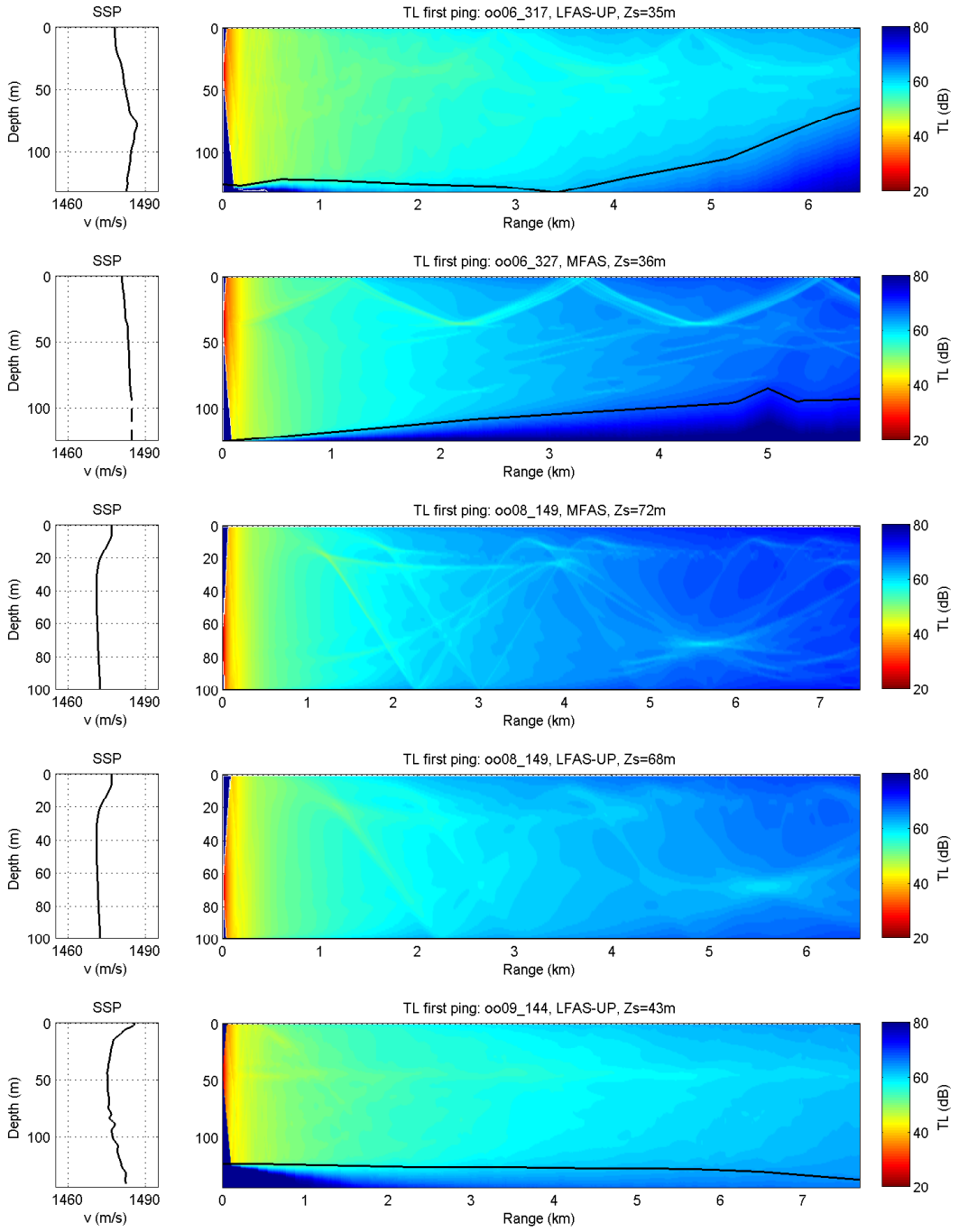

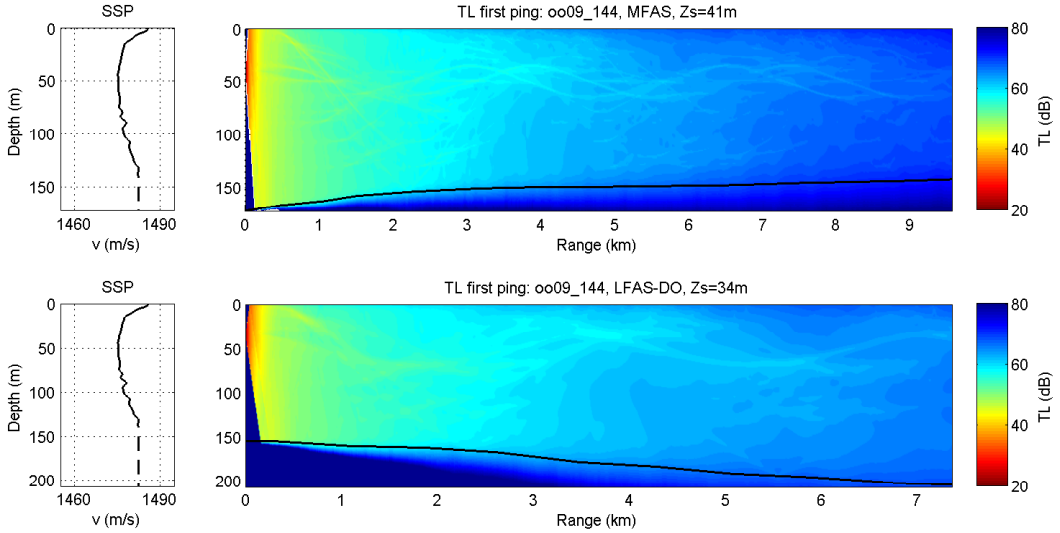


## Pilot whale experiments

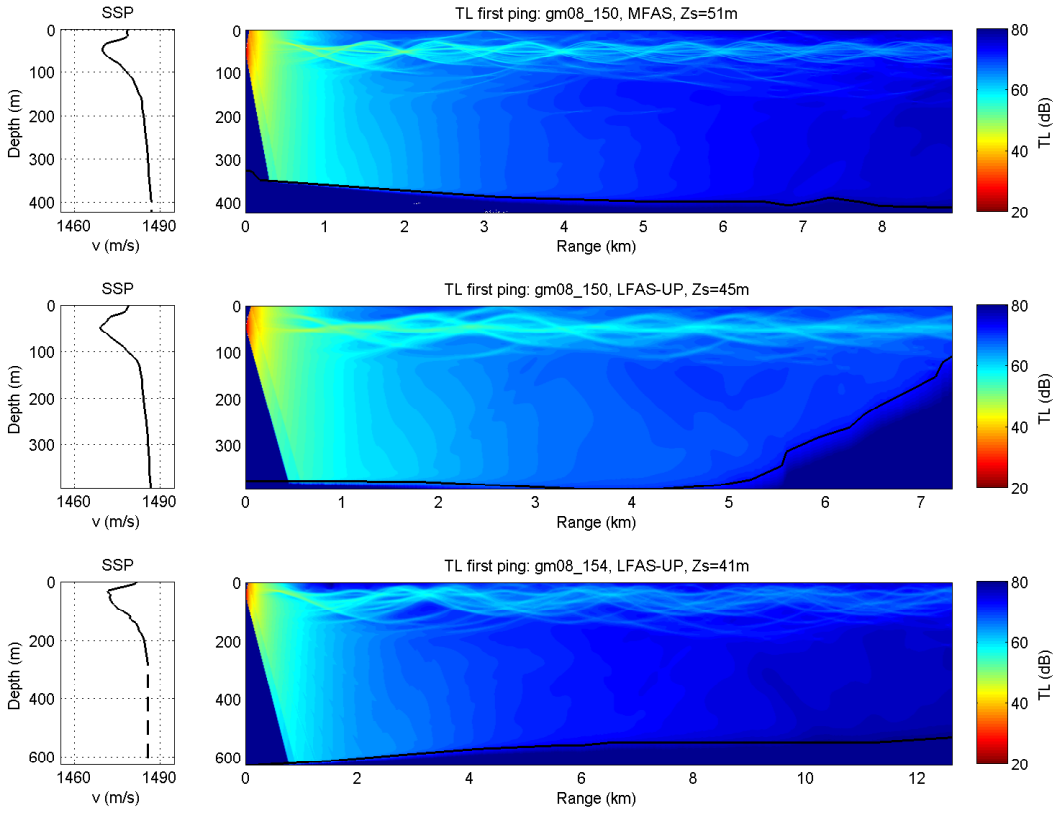

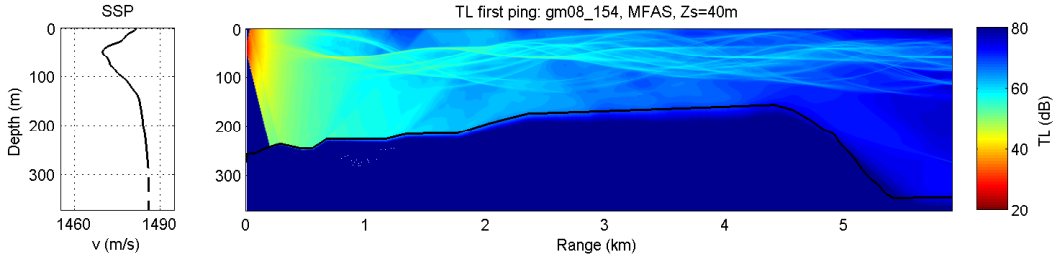
SSP
Depth (m)
v (m/s)
TL first ping: gm08_154, MFAS, Zs=40m
Range (km)
TL (dB)

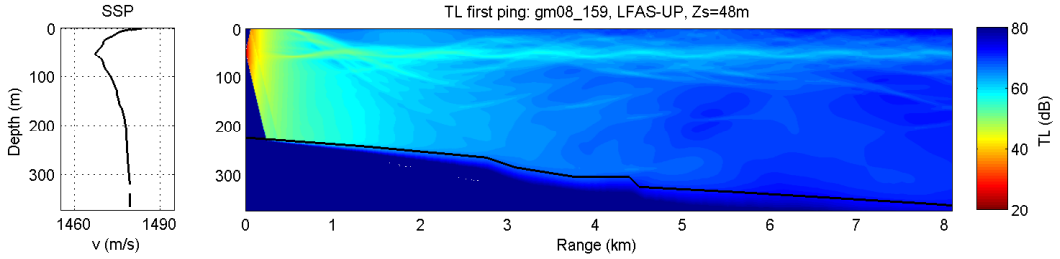
SSP
Depth (m)
v (m/s)
TL first ping: gm08_159, LFAS-UP, Zs=48m
Range (km)
TL (dB)

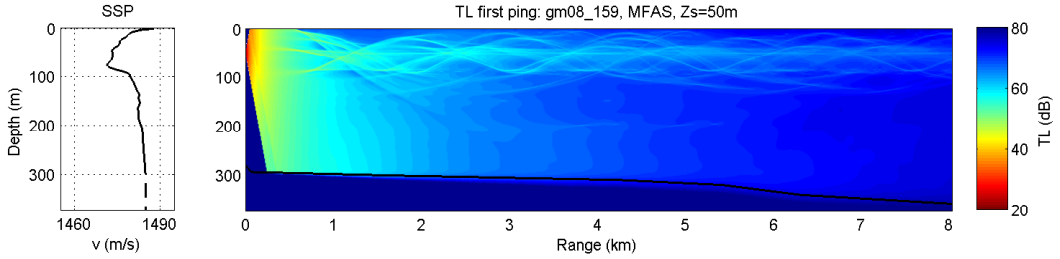
SSP
Depth (m)
v (m/s)
TL first ping: gm08_159, MFAS, Zs=50m
Range (km)
TL (dB)

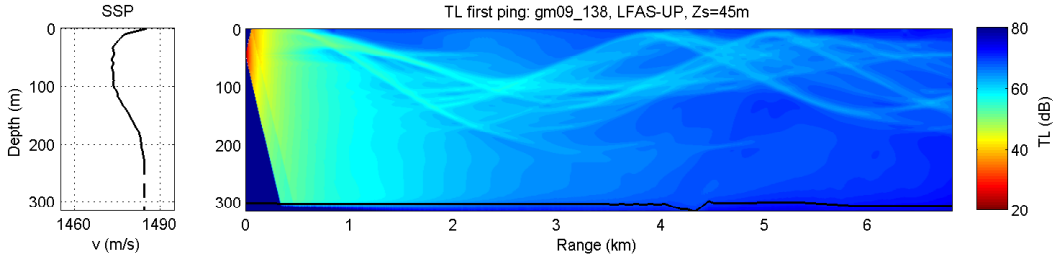
SSP
Depth (m)
v (m/s)
TL first ping: gm09_138, LFAS-UP, Zs=45m
Range (km)
TL (dB)

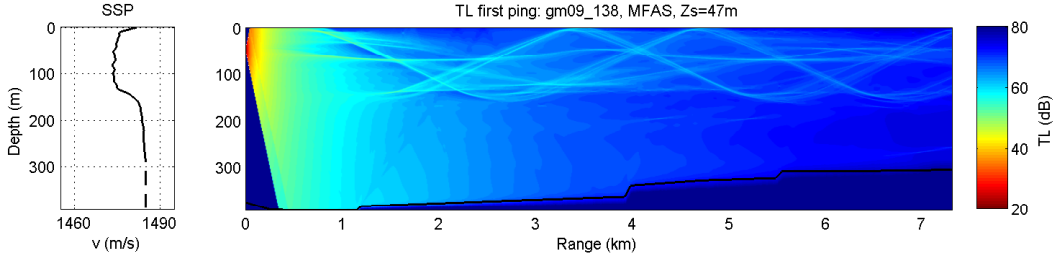
SSP
Depth (m)
v (m/s)
TL first ping: gm09_138, MFAS, Zs=47m
Range (km)
TL (dB)

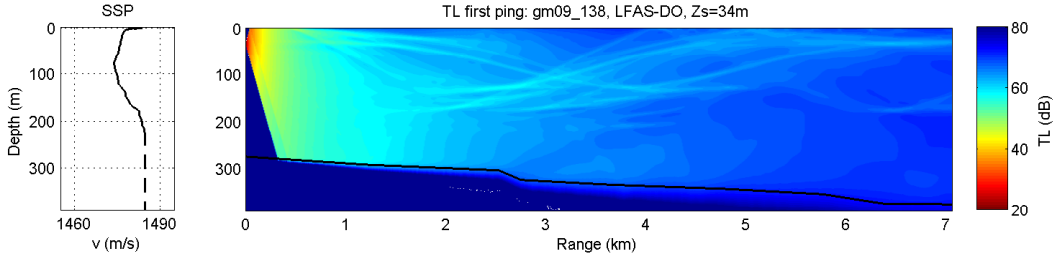
SSP
Depth (m)
v (m/s)
TL first ping: gm09_138, LFAS-DO, Zs=34m
Range (km)
TL (dB)

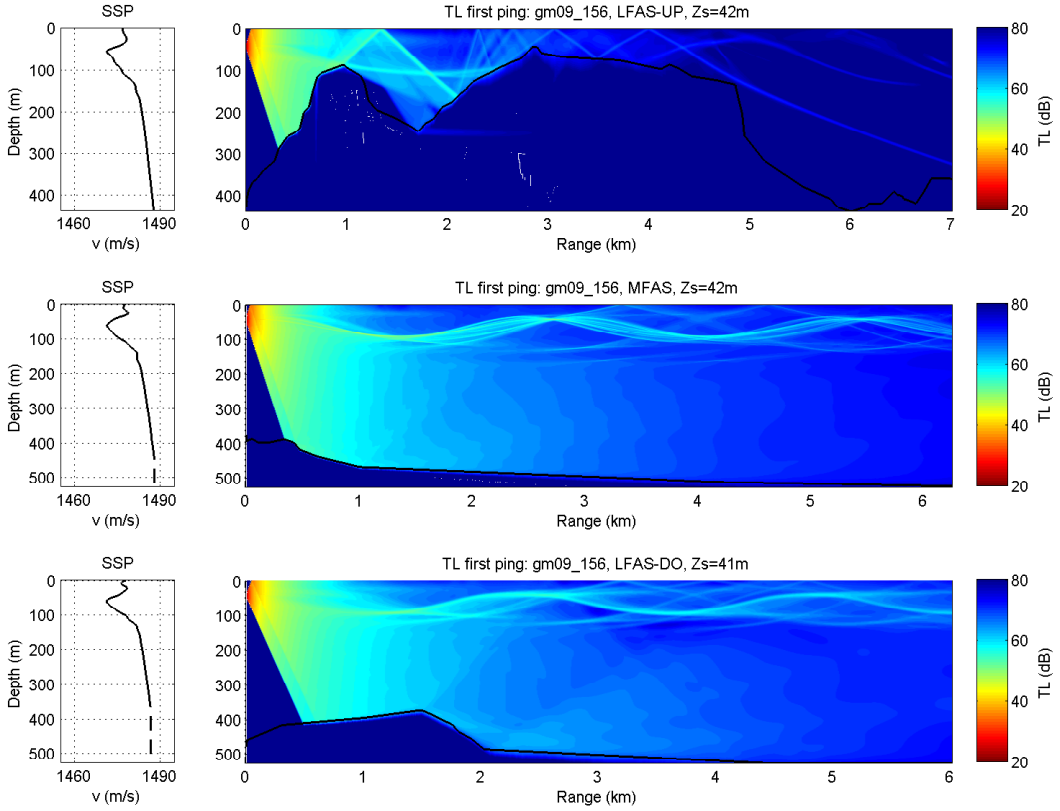


## Sperm whale experiments

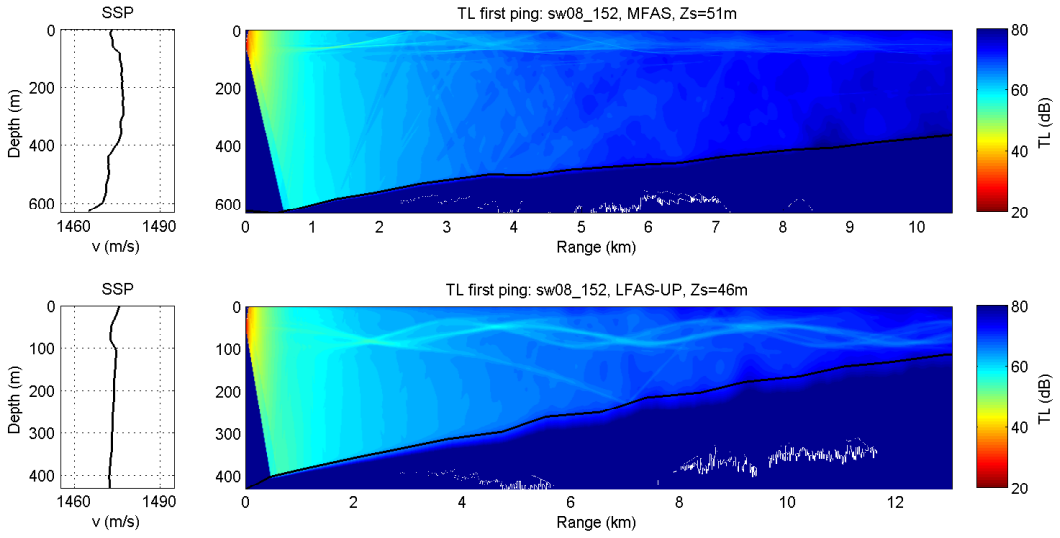

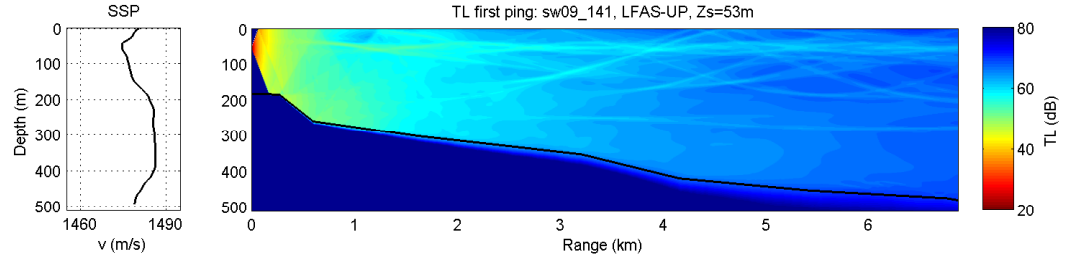
SSP
Depth (m)
v (m/s)
TL first ping: sw09_141, LFAS-UP, Zs=53m
Range (km)
TL (dB)

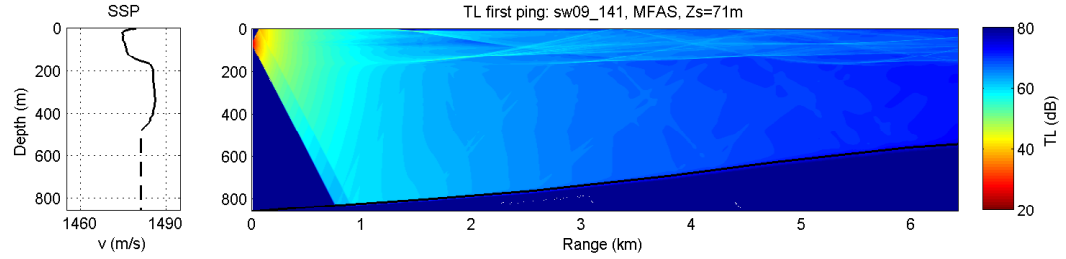
SSP
Depth (m)
v (m/s)
TL first ping: sw09_141, MFAS, Zs=71m
Range (km)
TL (dB)

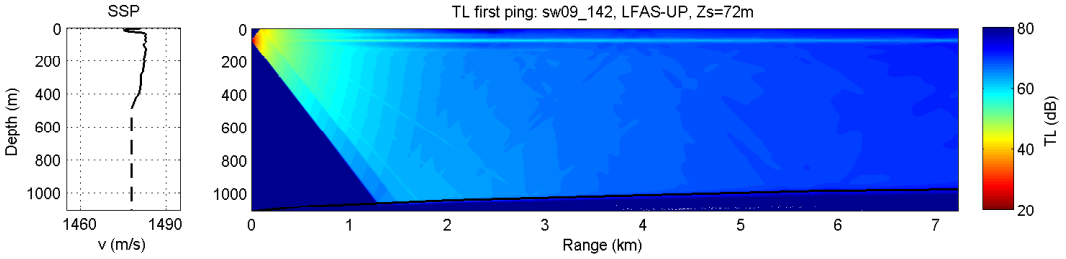
SSP
Depth (m)
v (m/s)
TL first ping: sw09_142, LFAS-UP, Zs=72m
Range (km)
TL (dB)

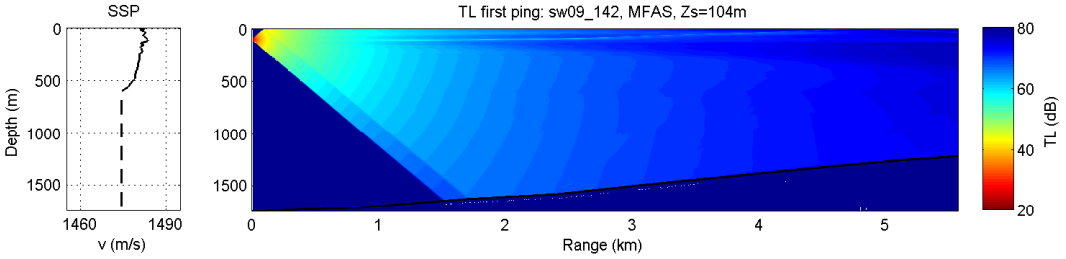
SSP
Depth (m)
v (m/s)
TL first ping: sw09_142, MFAS, Zs=104m
Range (km)
TL (dB)

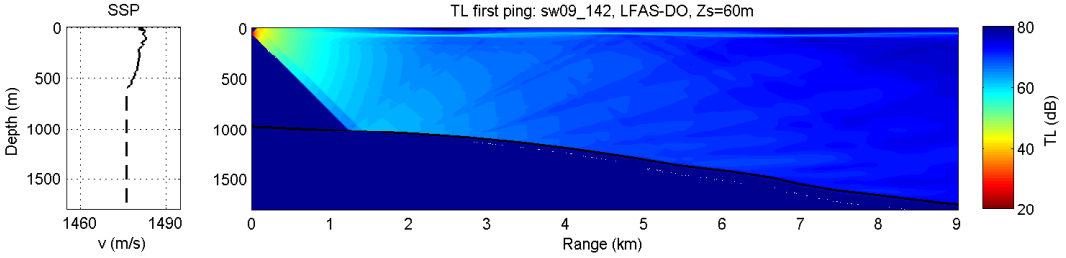
SSP
Depth (m)
v (m/s)
TL first ping: sw09_142, LFAS-DO, Zs=60m
Range (km)
TL (dB)

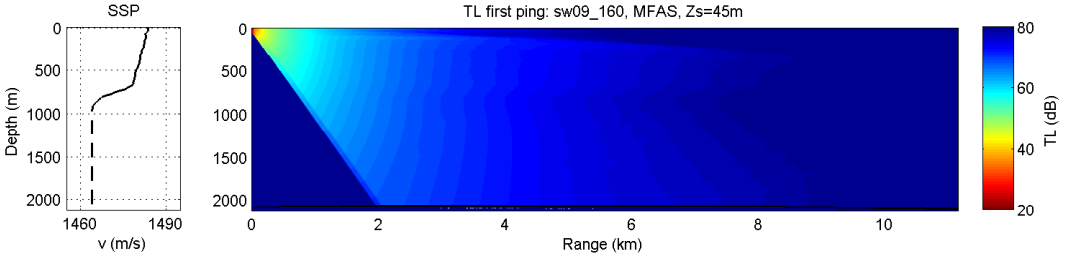
SSP
Depth (m)
v (m/s)
TL first ping: sw09_160, MFAS, Zs=45m
Range (km)
TL (dB)

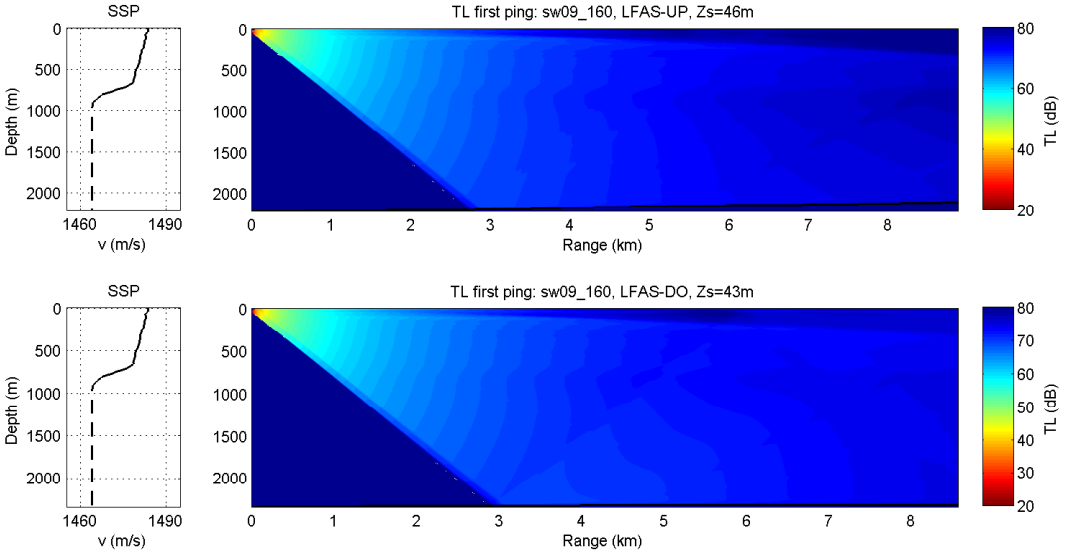
SSP
Depth (m)
v (m/s)
TL first ping: sw09_160, LFAS-UP, Zs=46m
Range (km)
TL (dB)
SSP
Depth (m)
v (m/s)
TL first ping: sw09_160, LFAS-DO, Zs=43m
Range (km)
TL (dB)